The Pennsylvania State University

The Graduate School

Department of Civil and Environmental Engineering

MICROBIAL DISSIMILATORY NITRATE REDUCTION IN BIOELECTROCHEMICAL SYSTEMS WITH ELECTRODE-RESPIRING BIOFILMS AND WASTEWATER TREATMENT PROCESSES

A Dissertation in

Environmental Engineering

by

Hiroyuki Kashima

© 2016 Hiroyuki Kashima

Submitted in Partial Fulfillment
of the Requirements
for the Degree of

Doctor of Philosophy

May 2016

The dissertation of Hiroyuki Kashima was reviewed and approved* by the following:

John M. Regan
Professor of Environmental Engineering
Dissertation Advisor
Chair of Committee

Mary Ann Bruns
Associate Professor of Soil Science/Microbial Ecology

Ming Tien
Professor of Biochemistry

Christopher A. Gorski
Assistant Professor of Civil Engineering

Patrick J. Fox
John A. and Harriette K. Shaw Professor and
Head of the Department of Civil and Environmental Engineering

*Signatures are on file in the Graduate School

ABSTRACT

Some microorganisms dynamically alter their metabolic states in response to changes in the environmental conditions, such as availability of compatible electron donors and acceptors. A prominent example is nitrate, which is the most energetically favorable electron acceptor in the absence of oxygen and often dominantly controls microbial reactions taking place in anoxic systems. Solid electrodes present another substrate that can regulate microbial reactions, serving as an electron donor and/or electron acceptor for microbes capable of extracellular electron transfer (EET). Electrode-mediated microbial metabolisms are central in bioelectrochemical systems (BESs), an emerging technology with a variety of potential applications, including a novel experimental platform to study the dynamic change of microbial metabolisms with real-time monitoring under controlled conditions. A better characterization of microbial reactions associated with such key substrates has important implications to understand microbial reactions in anoxic environments and also developing biological processes that exploit relevant microbial metabolisms. This research investigated the capabilities and constraints of microbial metabolisms at the nexus of electrode- and nitrate-mediated respirations relevant to wastewater treatment processes.

The facultative metabolic shift between anode electrode reduction and nitrate reduction was investigated in anode-reducing biofilms to study the effects of alternative metabolic options on exoelectrogenic biofilms in BESs. This has important implications not only to explain the fundamental ecology and performance of these systems, but also to develop reliable integrated nutrient removal strategies in BESs, which potentially involve

nitrate that can support/induce alternative metabolisms. Using the exoelectrogenic nitrate reducer *Geobacter metallireducens*, the critical conditions controlling those alternative metabolisms were investigated in two-chamber, potentiostatically controlled BESs at various anode potentials, biofilm thicknesses, and nitrate concentrations. Results showed that anode-reducing biofilms preferentially reduced nitrate at all tested anode potentials (-150 to + 900 mV vs Standard Hydrogen Electrode) with a rapid metabolic shift, despite the fact that the biofilms had no prior nitrate exposure. The critical nitrate concentration that triggered a significant decrease in BES performance was a function of anode biofilm thickness but not anode potential. This indicates that these alternative metabolisms were controlled by the availability of nitrate, which is a function of nitrate concentration in the bulk solution and its diffusion into an anode-reducing biofilm. Coulombic recovery decreased as a function of nitrate dose due to electron-acceptor substrate competition, and nitrate-induced suspended biomass growth decreased the effluent quality.

This nitrate-induced metabolic shift of anode-reducing biofilms was further investigated in the context of a shift between two different electrode-mediated metabolisms, electrode reduction and electrode oxidation. The characterization of metabolic shifts among different electrode-mediated reactions such as anode reduction and cathode oxidation is important to understand EETs in natural settings and also to develop stable BESs. This part of the research investigated the capability of anodically-grown *G. metallireducens* biofilms to shift from anode reduction to cathode oxidation. In tests with potentiostatically controlled graphite electrodes, *G. metallireducens* biofilms demonstrated a quick and alternative shift between anode reduction and cathode oxidation as a function

of electrode potential and availability of the co-substrates nitrate and acetate. Cathodic electrode oxidation was coupled with nitrate reduction by metabolically active biofilms with a large cathodic current of ~ 3.68 A/m^2. This metabolic shift from anode reduction to nitrate reduction took place quicker than the metabolic shift from ferric reduction to nitrate reduction. The presence of nitrate-reducing enzyme in the anode-reducing biofilms cells in the absence of nitrate, measured as specific in-vitro nitrate-reducing enzyme activity, was thought to enable such a quick metabolic shift to start nitrate reduction. Cyclic voltammetry and the analysis of its first derivative provided insights into the electron transfer mechanisms of these biofilms.

Finally, the potential occurrence of dissimilatory nitrate reduction to ammonium (DNRA), a microbial nitrate-reducing metabolism that involves the sequential reduction of nitrate to nitrite and then nitrite to ammonium, was investigated in two full-scale wastewater treatment plants. DNRA in biological wastewater treatment systems and BESs is largely unstudied despite its potential impacts on system performance. This part of the research examined differential expression and diversity of *nrfA*, a key marker gene for DNRA, in activated sludge from full-scale domestic wastewater treatment plants with one designed for enhanced biological phosphorus removal (EBPR). Expression of *nrfA*, which encodes the penta-heme nitrite reductase NrfA catalyzing the nitrite ammonification step of DNRA, was observed in anaerobic and anoxic mixed liquor, but not in aerobic mixed liquor samples. The expression of *nrfA* under anaerobic and anoxic conditions suggests an overlooked potential for DNRA activity to occur in biological wastewater treatment systems. Some retrieved *nrfA* sequences were related to sequences associated with a

microbial community with anammox activity, and the *nrfA* diversity in this wastewater treatment system differed from that observed in soil systems. Retrieved *nrfA* sequences both in genomic DNA and transcript samples were dominated by sequences associated with *Actinobacteria*, which are often abundant in EBPR processes. These results suggested potential occurrence of DNRA in wastewater activated sludge and encourage further studies in different types of wastewater treatment systems and with chemical tracer analyses to obtain comprehensive understanding of DNRA in this context.

This research investigated dissimilatory nitrate reduction in electrode-respiring biofilms and full-scale wastewater treatment processes. Elucidating the dynamics of nitrate-dependent reactions of electrode-respiring *G. metallireducens* in the contexts of a competitive reaction to anode reduction and an alternative electrode-mediated reaction have implications for BES development. Moreover, the experimental frameworks that were developed to address those problems would be applicable to study other electrode-mediated microbial metabolisms. Findings of *nrfA* expression and its diversity in full-scale wastewater treatment processes indicated potential occurrences of DNRA in wastewater treatment processes, which would have implications for energy and chemical utilization in these systems, and broadened the representation of diversity in the rather limited *nrfA* database.

TABLE OF CONTENTS

LIST OF FIGURES

LIST OF TABLES

ACKNOWLEDGEMENTS

During my time as a graduate student at Penn State, I have been supported and encouraged by numerous people who had been around the campus as well as who had been in distant parts of the world. I am grateful for all of them.

I especially would like to express my deep gratitude to my advisor Dr. John (Jay) Regan for guiding and supporting me throughout my time at Penn State. Jay was a wonderful mentor, and I have been very fortunate to work with him. He has helped me to develop as a researcher, writer, and speaker, while remaining down-to-earth. I really appreciate Jay's willingness (and patience) to have endless discussions with me over coffee and chocolate.

I would also like to thank Dr. Bruce Logan for his insightful suggestions on my research, as well as on my career development. First hand exposure to his leading research projects and his approach to communicating research findings and related topics with a broad range of people throughout the world enriched my experience as a graduate student. I would also like to offer my special thanks to Dr. Mary Ann Bruns, Dr. Ming Tien, and Dr. Chris Gorski for guiding me as my dissertation committee.

I very much appreciate my fellow researchers in the Regan and the Logan groups, and the unique skills, ideas, and friendships they shared with me. I learned so much that shaped me as a researcher. I would also thank all of my friends in the Environmental Engineering program for sharing times both inside and outside of our home – Sackett.

Thanks to you, I really enjoyed fun times with you all and because of you I could somehow enjoy the difficult times as well. I wish all of you the best in your future.

I would like to thank my family for their unconditional support throughout my life, including my latest years in beautiful Happy Valley. I cannot fully express my gratitude to Izumi Mori for her understanding and warm encouragement, which were essential to completing this dissertation.

Chapter 1

Introduction

Human society is facing a global demand for food, energy, chemicals, clean water, and many other fundamental resources that is increasing rapidly and may exceed the earth's capacity to support. To supply essential commodities while maintaining the associated negative environmental impacts within acceptable levels, current infrastructures must be transformed into more sustainable forms. For example, current wastewater treatment infrastructure involves cost- and energy-intensive designs [1]. Energy consumption in wastewater treatment facilities requires up to 3 % of domestic electricity production in the U.S. [2] due to extremely energy intensive aerobic biological treatment processes. As wastewater contains chemical energy, ~18-29 kJ/gCOD in domestic wastewaters [3], there is a potential to recover/offset the current energy imbalance by developing appropriate technologies to recover such endogenous energy. Bioelectrochemical systems (BESs) offer a potential platform technology to treat wastewaters with low energy inputs while recovering valuable products [4] such as electricity, chemicals, energy careers, freshwater from brines via incorporated desalination processes [5].

The current global nitrogen cycle is a prime example of the serious consequences of anthropogenic activity. Industrial nitrogen fixation via the Haber-Bosch process is used to supply much of the global nitrogen fertilizer demands, and its use increased ~800 %

from 1960 to 2000 [6]. Collectively, human activities are responsible for about 1.9 times greater rate of nitrogen fixation than natural terrestrial nitrogen fixation, and they account for about 45 % of the total nitrogen fixation on the Earth [7]. As a result, significant flow of fixed nitrogen from terrestrial to marine ecosystems, 4.9×10^{12} (mol-N/year), leads to extensive eutrophication of freshwater systems and coastal ocean. We need to mitigate such negative impact by realizing better nitrogen management.

We utilize microbial reactions for various environmental processes, such as wastewater treatment and nitrogen management discussed above, and characterization of these useful microbial metabolisms has implications for bioprocess development. In the context of stable BES development, an existing knowledge gap is the potential shift of microbial metabolisms in response to availabilities of substrates, such as nitrate. This has broader implications for the understanding of microbial reactions in anoxic environments, and also developing biological processes that exploit relevant microbial metabolisms in a more energetically efficient manner.

1.1. Organization of dissertation

My dissertation research investigated the capabilities and constraints of microbial metabolisms at the nexus of electrode- and nitrate-mediated respirations relevant to wastewater treatment processes which have important implications to understand microbial reactions in anoxic environments and also for development of nitrogen management process based on BESs. This PhD dissertation is composed of six chapters includes this Chapter 1 for general introduction, Chapter 2 for a literature review of electron transfer based microbial metabolisms as well as microbial nitrogen, particularly nitrate,

transformation reactions with the emphasis of molecular mechanisms and implications in engineered systems, Chapter 3 to 5 for three different research projects.

In chapter 3, I investigated metabolic shift between anode electrode reduction and nitrate reduction of anode-reducing biofilms to study the effects of alternative metabolic options on exoelectrogenic biofilms in BESs by using exoelectrogenic nitrate reducer, *Geobacter metallireducens.* This has important implications not only to explain the fundamental ecology and performance of these systems, but also to develop reliable integrated nutrient removal strategies in BESs, which potentially involve nitrate that can support/induce alternative metabolisms. Results demonstrated that nitrate reduction acted as a competitive metabolism to electrode reduction which constrained anodic BES performances, and these facultative metabolisms were controlled by availability of nitrate, the preferential electron acceptor, determined by bulk nitrate concentration and its diffusion into a biofilm but not by anode availability determined by anode potential, which was analogous to other facultative metabolisms such as oxygen versus nitrate respirations. Coulombic recovery decreased as a function of nitrate dose due to electron-acceptor substrate competition, and nitrate-induced suspended biomass growth decreased the effluent quality. Materials presented in this chapter has been published as Kashima, H., & Regan, J. M., Facultative nitrate reduction by electrode-respiring *Geobacter metallireducens* biofilms as a competitive reaction to electrode reduction in a bioelectrochemical system. *Environmental science & technology*, **2015**, 49 (5), 3195-3202. I conducted all the experimental work and prepared the first draft of the manuscript.

In chapter 4, I further investigated nitrate-induced metabolic shift of anode-reducing biofilms in the context of a shift between two different electrode-mediated

metabolisms, electrode reduction and electrode oxidation. The characterization of metabolic shifts among different electrode-mediated reactions such as anode reduction and cathode oxidation is important to understand extracellular electron transfer (EET) in natural settings and also to develop stable BESs. This part of the research investigated the capability of anodically-grown *G. metallireducens* biofilms to shift from anode reduction to cathode oxidation. *G. metallireducens* biofilms demonstrated a quick and alternative shift between anode reduction and cathode oxidation as a function of electrode potential and availability of the co-substrates nitrate and acetate. Cathodic electrode oxidation was coupled with nitrate reduction by metabolically active biofilms with a large cathodic current of ~ 3.68 A/m^2. This metabolic shift from anode reduction to nitrate reduction took place quicker than the metabolic shift from ferric reduction to nitrate reduction. The presence of nitrate-reducing enzyme in the anode-reducing biofilms cells in the absence of nitrate, measured as specific in-vitro nitrate-reducing enzyme activity, was thought to enable such a quick metabolic shift to start nitrate reduction. Cyclic voltammetry and the analysis of its first derivative provided insights into the electron transfer mechanisms of these biofilms. I conducted all the experimental work for this project. The manuscript of this project is currently in preparation.

In chapter 5, I surveyed differential expression and diversity of *nrfA*, a key marker gene for DNRA, in activated sludge from full-scale domestic wastewater treatment plants to investigate potential occurrence of dissimilatory nitrate reduction to ammonium (DNRA), a microbial nitrate-reducing metabolism that involves the sequential reduction of nitrate to nitrite and then nitrite to ammonium in wastewater activated sludge processes designed for enhanced biological phosphorus removal (EBPR). Expression of *nrfA*, which

encodes the penta-heme nitrite reductase NrfA catalyzing the nitrite ammonification step of DNRA, was observed in anaerobic and anoxic mixed liquor, but not in aerobic mixed liquor samples. The expression of *nrfA* under anaerobic and anoxic conditions suggests an overlooked potential for DNRA activity to occur in biological wastewater treatment systems. Some retrieved *nrfA* sequences were related to sequences associated with a microbial community with anammox activity, and the *nrfA* diversity in this wastewater treatment system differed from that observed in soil systems. Retrieved *nrfA* sequences both in genomic DNA and transcript samples were dominated by sequences associated with *Actinobacteria*, which are often abundant in EBPR processes. These results suggested potential occurrence of DNRA in wastewater activated sludge and encourage further studies in different types of wastewater treatment systems and with chemical tracer analyses to obtain comprehensive understanding of DNRA in this context. In this project, Illumina MiSeq amplicon sequencing and initial bioinformatics analysis was conducted by Research and Testing Laboratory at Lubbock, Texas. I conducted rest of experimental works as well as data analyses. Part of materials presented in this chapter was submitted as Kashima, H., Bruns, M. A., Regan, J. M., Detection of *nrfA* genes and transcripts, molecular markers of dissimilatory nitrate reduction to ammonium, in wastewater activated sludge. Co-authors of the manuscript, Drs John M Regan and Mary Ann Bruns contributed to construction of *nrfA* survey plan and revisions and final writing of the submitted manuscript.

In addition to the research project that presented in this dissertation, I have contributed following researches as a co-author of papers:

Zhang, L., Zhu, X., **Kashima, H.,** Li, J., Ye, D. D., Liao, Q., & Regan, J. M. (2015). Anolyte Recirculation Effects in Buffered and Unbuffered Single-Chamber Air-Cathode Microbial Fuel Cells. *Bioresource Technology*, 179, 26-34.

Liu, J., Hou, H., Chen, X., Bazan, G., **Kashima, H.,** & Logan, B. E. (2015). Conjugated Oligoelectrolyte Represses Hydrogen Oxidation by *Geobacter sulfurreducens* in Microbial Electrolysis Cells. *Bioelectrochemistry*, 106, 379-382.

Ou, S., **Kashima, H.,** Aaron, D. S., Regan, J. M., & Mench, M. M. Multi-Variable Mathematical Models for the Air-Cathode Microbial Fuel Cell System. *Journal of Power Sources*. Accepted.

1.2. Literature Cited

1. Sedlak, D., *Water 4.0: the past, present, and future of the world's most vital resource*. 2014: Yale University Press.
2. McCarty, P.L., J. Bae, and J. Kim, *Domestic wastewater treatment as a net energy producer--can this be achieved?* Environmental Science & Technology, 2011. **45**(17): p. 7100-6.
3. Heidrich, E.S., T.P. Curtis, and J. Dolfing, *Determination of the internal chemical energy of wastewater.* Environmental Science & Technology, 2011. **45**(2): p. 827-32.
4. Logan, B.E. and K. Rabaey, *Conversion of wastes into bioelectricity and chemicals by using microbial electrochemical technologies.* Science, 2012. **337**(6095): p. 686-690.
5. Mehanna, M., et al., *Using microbial desalination cells to reduce water salinity prior to reverse osmosis.* Energy & Environmental Science, 2010. **3**(8): p. 1114-1120.
6. Fixen, P.E. and F.B. West, *Nitrogen fertilizers: meeting contemporary challenges.* Ambio: a journal of the human environment, 2002. **31**(2): p. 169-176.
7. Canfield, D.E., A.N. Glazer, and P.G. Falkowski, *The evolution and future of Earth's nitrogen cycle.* science, 2010. **330**(6001): p. 192-196.

Chapter 2

Literature review

2.1. Microbial metabolisms associated with solid electrodes

Extracellular electron transfer (EET) is microbial reactions that discharge electrons from a cell to the environment or take in electrons into a cell. Microbial metabolisms based on EET are central in bioelectrochemical systems (BESs) an emerging technological platform with a variety of potential applications [1-3], and recent studies suggested potential contribution of EET-based microbial metabolisms yet to be discovered in the environments [4-8]. The characterization of electrode-mediated microbial EET is not only the foundation for a stable BES development, but also it has implication to understand EET metabolisms in natural settings in which cells exchange electrons to insoluble minerals and other cells as analogous reactions. The following sections review current understandings and challenges of electrode-mediated microbial reactions in the context of BES applications and of natural systems.

2.1.1. Bioelectrochemical systems (BESs) based on electrode mediated microbial reactions

The first demonstration, that I know, of electrochemical activities of living microorganisms was reported over 100 years ago. Potter (1911) showed electrochemical potential generated by two different microbes under the amendment of organic substrates

[9]. After this initial demonstration, various types of BESs have been demonstrated. Examples include microbial fuel cells (MFCs) (Figure 2-1) which produce electrical power with EET-based microbial metabolisms on anodic, or both of anodic and cathodic reactions [10, 11], microbial electrolysis cells (MECs) which produces hydrogen gas on cathode by using electrons derived from EET anodes [1, 12], microbial desalination cells (MDCs) [13] and microbial reverse-electrodialysis cells (MRCs) [14, 15] in which microbial EET metabolisms are exploited as novel efficient electrode reactions for electrochemical-salinity gradient related processes, microbial electrosynthesis which reduce carbon dioxide into reduced hydrocarbons by cathode-derived electrons input into cells via EET [3, 16]. BESs exampled above demonstrated unique features as a microbial-based process in which we could input or output not only chemical compounds but also electrons or electrical potential compared to other bioprocesses most of which take input of chemical compounds and output other chemical compounds.

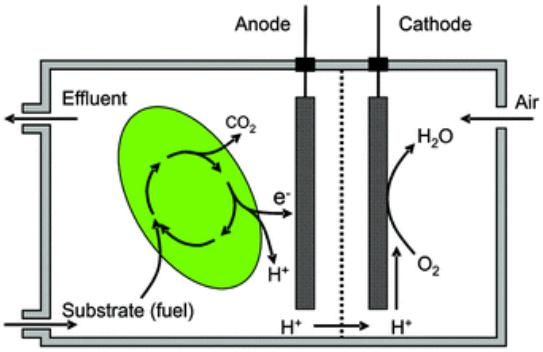

Figure 2-1: Illustration of a microbial fuel cell in which anode reduction is catalyzed by a microbial cell via EET coupled with substrate oxidation and cathode oxidation (oxygen reduction) is abiotically catalyzed. (Source [17])

2.1.2. Extracellular electron transfer (EET) based microbial metabolisms

Discovery of EET based-metabolisms were originated in soluble and insoluble metal reduction by metal reducers *Geobacter* [18-20] and *Shewanella* [21, 22]. Microbial EET mechanisms have been studied in dissimilatory insoluble metal reduction, EET between cells and oxidized insoluble minerals, and in dissimilatory electrode reduction, EET between cells and solid electrodes, with several model organisms such as *Geobacter sulfurreducens* [23] and *Shewanella oneidensis* [21]. Proposed molecular mechanisms of electrode reduction includes direct electron transfer (DET) based on electron transfer through physical contact of cell membrane and insoluble electrode [17], and mediated electron transfer (MET) in which electron transfer between cells and insoluble electrodes are mediated by mobile redox species [17].

For DET, several molecular mechanisms have been reported in above model organisms (Figure 2-2). For example, outer membrane cytochromes such as OmcS [24] and OmcZ [25], and type IV pili such as pilA were shown to play important roles in electrode reduction by *G. sulfurreducens*, and their optimal current production and development of thick electroactive biofilms [26-28]. In addition, findings of locations and roles of these redox-active outer-surface proteins and conductive pili throughout their conductive biofilm matrix [29] [30] have been providing insights into electron transfer to an electrode at the whole biofilm scale [31] [32]. Concerning electrode reduction by *S. oneidensis*, it has been shown that *S. oneidensis* MR-1 uses the Mtr pathway [33] composed of a series of c-type cytochromes located in the cytoplasmic membrane, periplasmic space, and outer membrane. This involves transferring electrons from the quinone pool in the

cytoplasmic membrane to MtrC, located at the outer surface of the outer membrane, to release electrons to extracellular electron acceptors such as insoluble iron and an electrode.

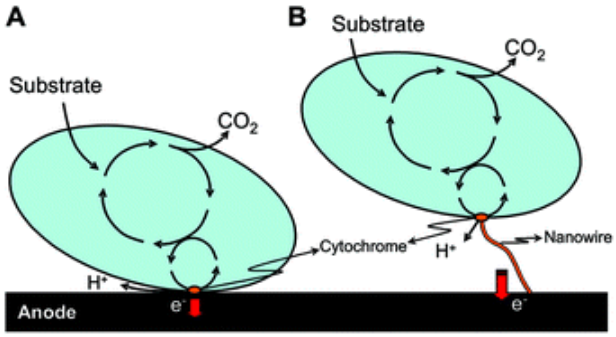

Figure 2-2: Illustration of DET via (A) membrane-bound cytochromes (B) electrically conducting nanowires (conductive pili). (Source [17])

For MET, early MFC studies demonstrated performance enhancement by addition of various exogenous mediators [34, 35], but obtained current densities were much lower than ones obtained by DET in later studies. Requirement of considerable amount of artificial mediator compounds, some of which are hazardous, really limited practical applications of MET based on exogenous mediators. Later studies reported MET processes based on endogenous, self-generating, mediators such as phenazine and pyocyanin excreted by *Pseudomonas aeruginosa* [17, 36, 37] (Figure 2-3). Although MET reactions with those endogenous mediators appeared better for practical applications than earlier exogenous mediator-based ones, impact for large-scale applications is rather limited it is challenging to maintain self-generated mediator compounds in high concentration in an electrolyte.

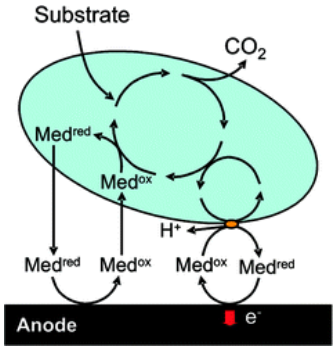

Figure 2-3: Illustration of MET via microbial secondary metabolites. Two possible redox mechanisms: shuttling via outer cell membrane cytochromes and via periplasmic or cytoplasmic redox couples. (Source [17])

2.1.3. Microbial metabolisms coupled with EET

Electrode-mediated respirations couple various redox half-reactions with electrode reduction or oxidation. For example, *Geobacter* spp., which are often dominant taxa in BESs [38-40] and subsurface environments [41, 42], can oxidize organic and inorganic electron donors such as acetate [43], hydrogen [23], lactate [44], ethanol, and aromatic compounds [20] coupled with reduction of an electrode or insoluble iron. Also, *Geobacter* spp. reduce nitrate [45], fumarate [45, 46], and tetrachloroethene [46] with an electrode as the sole electron donor. In addition, studies have reported a wide variety of reactions coupled with electrode reduction and oxidation by various types of microorganisms. Examples include cathode-supported methanogenesis [47-49], acetogenesis [16, 50], uranium (VI) reduction to uranium (IV) [51], oxygen reduction [52], denitrification [53], dechlorination [54], and perchlorate reduction [55]; as well as anode-supported oxidation of organic compounds [1].

2.1.4. Expanding borders of known EET metabolisms in the world

Recent studies have been expanding borders of EET-mediated metabolisms beyond insoluble metal/electrode reduction to various natural and engineered systems. For example, demonstrations of interspecies electron transfer (IET) in various syntrophic systems have been challenging our understanding of microbial syntrophic reactions based on transfer of reduced intermediates such as hydrogen or formate between syntrophic partner cells. Examples include demonstration of IET mediated conductive minerals in a binary culture [5], direct IET within aggregates of syntrophic bacterial co-culture [56] and syntrophic bacterium-archaeon co-culture [57], indications of direct IET in methanogenic wastewater digester aggregates [58, 59], indication of IET between methane oxidizing archaea and sulfate reducing bacteria in aggregates conducting sulfate-reducing anaerobic methane oxidation [6-8]. In particular, a study by McGlynn et al. suggested IET in methane oxidizing consortia based on analysis of intra-aggregate cell distribution and detection of cytochromes within the consortia [6], and its follow-up report demonstrated decoupling of archaeal methane oxidation from bacterial sulfate reduction by amending artificial electron acceptors [8]. These researches, particularly the first research, addressed a fundamental nature of diffusive transport based reactions versus reactions not limited by diffusive transport.

Models based on diffusive transport of syntrophic intermediates such as hydrogen and formate between syntrophic partners described well the benefit of microbial aggregates with densely packed syntrophs over spatially distributed system such as suspended culture containing syntrophs without forming aggregates. For example, the flux of hydrogen between the hydrogen-forming fermenter and the hydrogen-consuming methanogen is

inversely proportional to the distance between both cell types [60]. Also, studies of methanogenic-syntrophic consortia, interspecies hydrogen and formate transfer were facilitated by co-aggregation of syntrophic partners due to favorable metabolite transfer by diffusion [61].

Spatial distribution of syntrophic partner cells within an aggregate also has significant effects on the overall reaction. Alperin and Hoehler [62] discussed effects of morphology of syntrophic microbial aggregates on their overall reaction rates and energy yields of the aggregates of archaea and sulfate reducing bacteria conducting anaerobic methane oxidation coupled with sulfate reduction by using spherical diffusion-reaction model. The model suggested that homogeneous mix of bacterial and archaeal cells results in higher overall reaction rate relative to ones composed of large chunks of the same cell type [62]. Another study discussed that the efficiency of metabolite transfer within an aggregate will decrease with age of the aggregates unless there are ways of internal mixing of the aggregates [60] based on the assumption that syntrophs in an aggregate will be spatially segregated as the adjacent space surrounding a cell would be filled with its offspring cells. This discussion also speculated that growth and internal structure development of syntrophic aggregates are limited by metabolite diffusion kinetics and the sulfate-reducing methane oxidizing aggregates with largely segregated syntrophic partner distribution within aggregates such as reported in [63] probably represents a terminal growth stage of syntrophic aggregates [60].

However, the study by McGlynn et al. showed very different results from above assumptions. They analyzed their empirical data with diffusive transport based models as discussed above, but (1) the degree of mixing between cell types did not influence the

average biosynthetic activity of the entire consortium, and (2) the cells located at syntrophic interfaces were not significantly more active than those surrounded by the same cell type, indicating that closely-located partner cells did not significantly improve activity of each cell as well as entire consortia. Next, they analyzed empirical data with another generalized model that captures basic features of IET based on electric conductivity in which electrons can freely flow across the entire aggregate with a dependence on electric potential difference generated within the aggregate. This model indicated higher levels of activity in more segregated consortia as such spatial segregation increase polar charge separation. The study concluded that their electric conductivity model best fit their empirical data [6]. This study is insightful to think fundamental features of electron-transfer based reactions relative to reactions based on diffusive transport of molecules.

In addition to the significance of EET for syntrophic reactions, EET could also couple distantly isolated reactions in natural settings by wiring them electrically. Report of filamentous bacteria that is suggested to couple sulphide oxidation in oxygen-free layers in marine sediment to oxygen reduction in oxic-layers by electrical current as living electrical cables [4] indicated potential EET-based metabolisms yet to be discovered in various environments.

2.1.5. Metabolic options of electrode-associated microbes

In contrast to variety of known electrode-mediated metabolisms, considerably less research has addressed questions about how electrode-associated biofilms select or shift their metabolisms among their options. Microbes often dynamically change their metabolic pathways among options in response to changes in conditions such as availabilities of

substrates in natural systems and also mixed-culture engineered systems (Figure 2-4) on which most BESs are based, and thus it is hypothesized to be important to study metabolic shift of electrode-associated microbes.

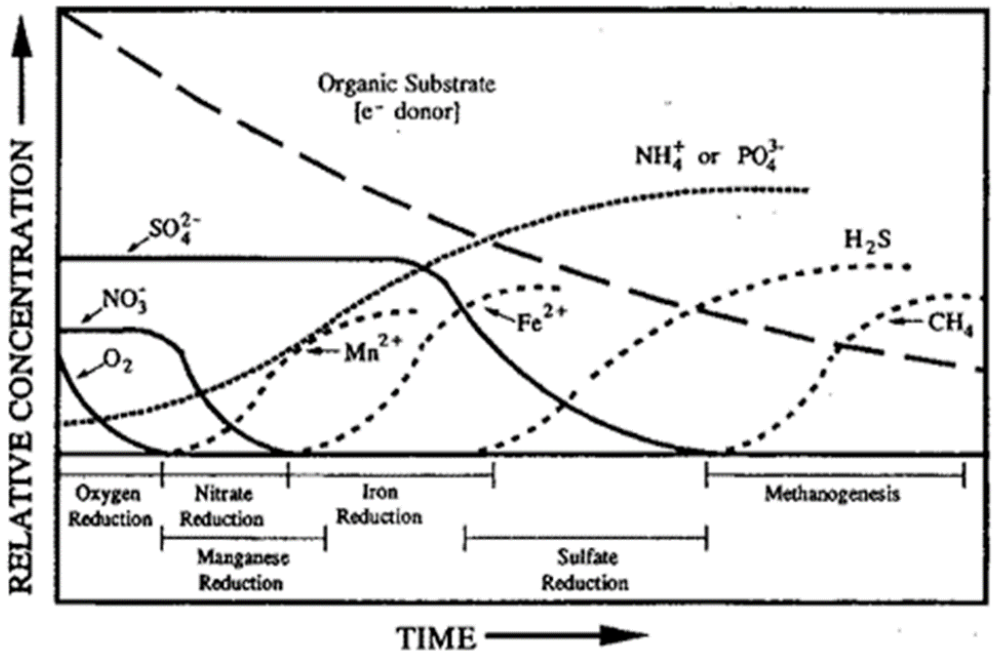

Figure 2-4: Shift of redox reactions based on availability of electron acceptors in a subsurface system. Groundwater with a source of organic carbon or other electron donors shows a sequence of distinct redox zones along flowpaths.
(Source: http://md.water.usgs.gov/posters/nutrientsRedox/)

BES researches have addressed several different issues of undesirable alternative microbial activities that compete with targeted processes. For example, studies addressed decreased coulombic efficiency in single-chamber MFCs by aerobic organic degradation supported by oxygen crossover through the air cathode [64-67], and decreased hydrogen recovery in MECs by methanogenic activity [68-70] yielded better engineering strategies

to overcome those problems. Although above examples investigated contributions of non-electrode respiring microbes residing in systems, metabolic shift of microbes conducting electrode-mediated metabolisms could have impacts on BES performances.

The potential metabolic shift from electrode reduction to nitrate reduction is of particular interest because some anode-reducing bacteria such as *G. metallireducens* [20], *S. oneidensis* [71], *Comamonas denitrificans* [72], *Geoalkalibacter subterraneus* [73, 74], and *Calditerrivibrio nitroreducens* [75] are capable of reducing nitrate, the most energetically favorable electron acceptor in anoxic conditions that often dominantly controls anoxic microbial reactions. Although some mixed culture studies reported decreased anodic performance by nitrate addition [76, 77], contribution of metabolic shift of anode-reducing cells is unknown. Metabolic shifts among different electrode-mediated reactions, such as electrode reduction and oxidation, are also of interest to develop stable BES processes. For example, alternating anodic-cathodic operation of an electrode catalyzed by mixed-culture biofilms mitigated the pH imbalance often encountered in anodic or cathodic biofilms [78-80]. Also, conversion of an anode biofilm into a cathode biofilm was reported as a strategy to accelerate the start-up of biocathode processes [81].

2.2. Microbial nitrogen transformation

2.2.1. Significance of nitrogen cycle on the earth today

We are in a situation of imbalanced global nitrogen cycle derived from modern human activity. For example, the use of nitrogen fertilizers increased by ~800 % from 1960 to 2000 [82]. Current anthropogenic nitrogen fixation composed of Haber-Bosch process, nitrogen fixation in agricultural activity, and fossil fuel combustion responsible about 1.9 times greater than rate of natural terrestrial nitrogen fixation and that is accounted as about 45 % of the total nitrogen fixation on the Earth (Figure 2-5) [83]. Significant, 4.9×10^{12} (mol-N/year), flow of nitrogen from terrestrial to marine results in extensive eutrophication of freshwater systems and coastal ocean. Also, N_2O, the 300 times stronger greenhouse effect relative to carbon dioxide and it also destroys ozone in the stratosphere [84] as an intermediate in denitrification and nitrification [85]. Modern agricultural systems are responsible for about 25 % of global N_2O emission [86]. It should be noted that the performance of reactive nitrogen removal process in a wastewater treatment facility results in rather limited contribution for nitrogen fate in such global scale, but it has fatal consequences in local aquatic ecosystems. With such outstanding anthropogenic activity, nitrogen management imposes high economic and environmental costs on human society with both in industrial nitrogen fixation consuming a considerable percentage of the world's natural gas production, and in mitigation of negative impacts of anthropogenic reactive nitrogen compounds discharged to the environment [87]. It is clear that realization of better nitrogen management is one of the grand challenges for human beings.

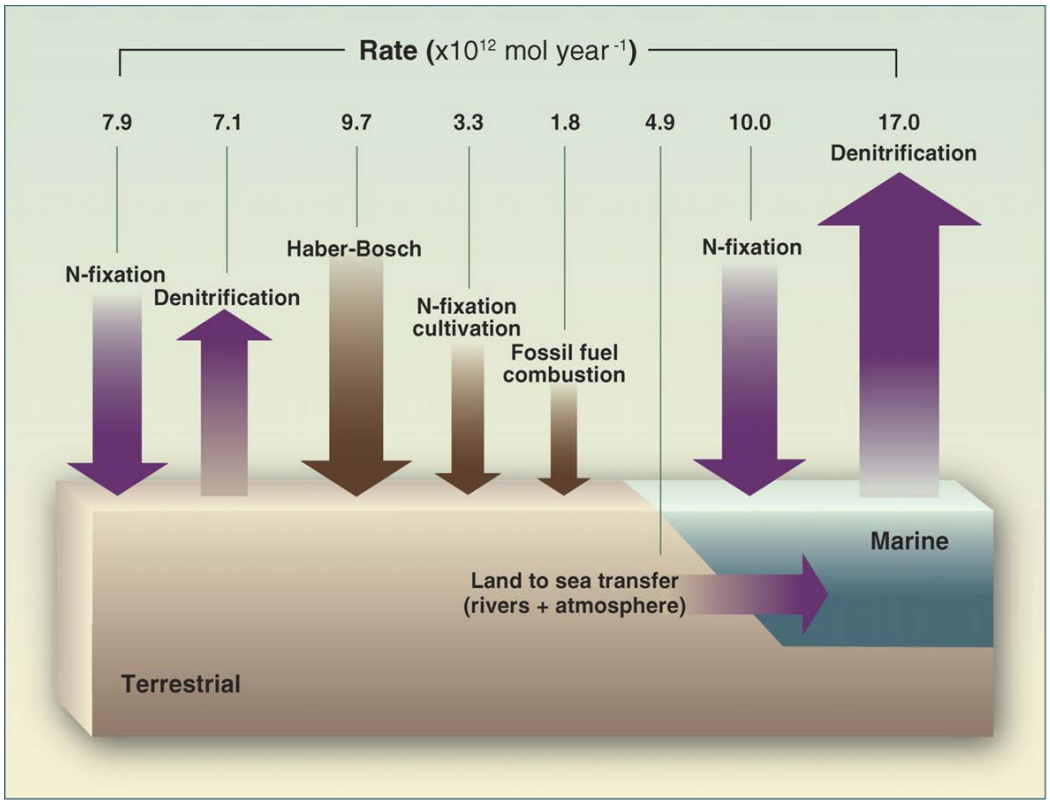

Figure 2-5: Rates of nitrogen flux in the modern nitrogen cycle depend on the efficiency of the transformations between reservoirs. Arrow size reflects relative size of the flux. The dark brown arrows represent anthropogenic inputs. (Source [83])

2.2.2. Discoveries of novel microbial nitrogen transformations have changed our understanding of nitrogen cycle

For past few decades, our understanding of global nitrogen cycle have greatly changed by discoveries of novel microbial nitrogen transformation reactions. Anaerobic ammonia oxidation (anammox), microbial anaerobic ammonia oxidation coupled with nitrite reduction was discovered in 1990s [88, 89]. Researchers took fairly long time to discover the reaction and to isolate slow-growing bacteria responsible for this reaction although potential occurrence of such microbial reaction was expected by

thermodynamics, but now we appreciate significant contribution of this reaction. For instance, anammox reaction is estimated to be responsible for about 50% of all nitrogen gas released into the atmosphere [90]. Other examples of recently discovered microbial nitrogen transformation reaction include ammonia oxidation by ammonia oxidizing archaea (AOA) [91], denitrification by nitrifier [92], nitrate reduction coupled with ferrous [93, 94] or solid extracellular electrode [53]. Recent report of complete nitrification by a single microorganism [95, 96] was surprising not only with its significance in our understanding of life and nitrogen cycle, but also due to the fact that it was discovered in a group of bacteria that have been the most extensively studied for nitrification over decades. This illustrates wide spectrum of potential microbial reactions yet to be discovered even in the area in which we have heavily investigated. Our expanded understanding of microbial nitrogen transformation reactions would lead to improved predictive models and management processes for nitrogen and the associated carbon cycles.

2.2.3. Biological machineries for transformation of nitrate and nitrite

Other than anthropogenic nitrogen fixation with Haber-Bosch process and fossil fuel combustion, the biogeochemistry of nitrogen of the biosphere on the Earth is almost entirely dependent on microbially-mediated redox reactions [83, 97]. Enzymes, biological machineries, responsible for major nitrogen transformation reactions include nitrogenase, **Nif**, that fix dinitrogen gas into ammonium with the energy from ATP consumption, ammonium monooxygenase, **Amo**, that oxidize ammonium to hydroxylamine by using molecular oxygen as the electron acceptor, hydroxylamine oxidoreductase, **Hao**, that oxidize hydroxylamine into nitrite, nitrite oxidoreductase, **Nxr**, that oxidize nitrite into

nitrate, various types of nitrate reductases such as cytoplasmic assimilatory **Nas**, membrane-bound dissimilatory **Nar**, periplasmic dissimilatory **Nap**, nitric oxide forming nitrite reductase such as **NirS** and **NirK**, nitrous oxide forming nitric oxide reductase **Nor**, dinitrogen forming nitrous oxide reductase **Nos**, ammonium forming nitrite reductase, **Nrf**, for DNRA, and hydrazine hydrolase, **Hh**, associated ammonia oxidation in anammox. Major biological nitrogen transformations and genes encoding enzymes responsible these reactions are shown in (Figure 2-6) [83]. Following sections summarize machineries for dissimilatory nitrate/nitrite reduction reactions: denitrification and DNRA.

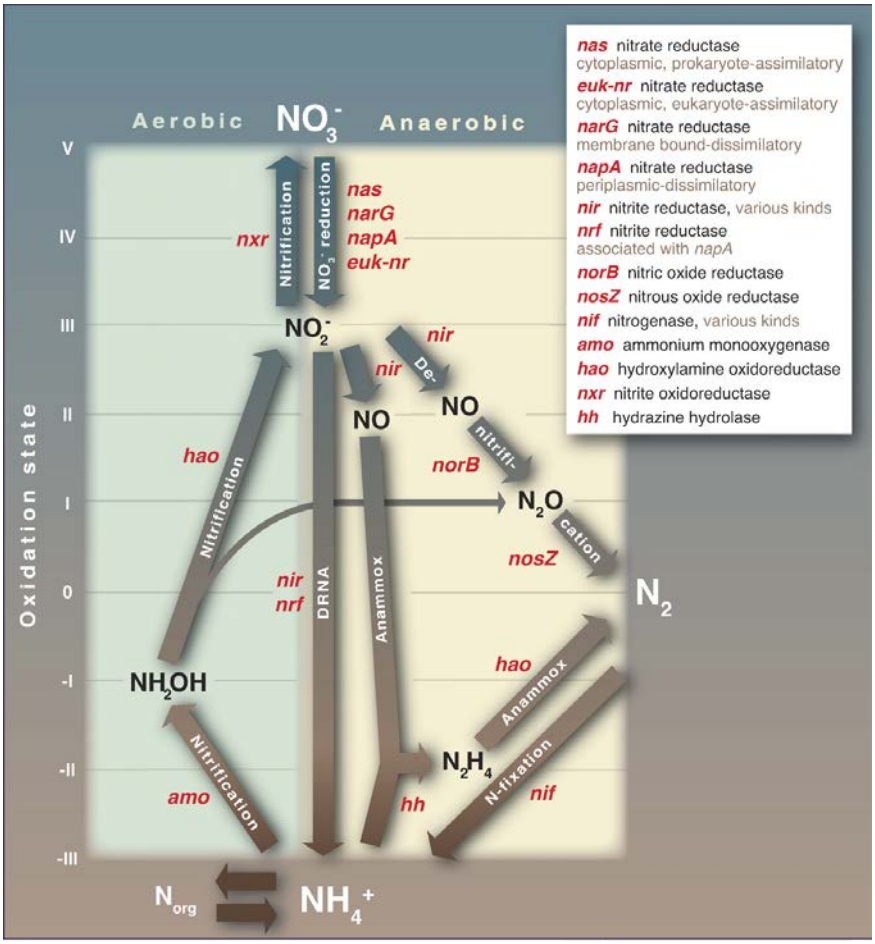

Figure 2-6: The major biological nitrogen transformation pathways are linked by their associated enzymes. (Source [83])

2.2.3.1. Nitrate reductase

Reduction of nitrate to nitrite is the first reduction step of both dissimilatory nitrate reduction reactions, denitrification and DNRA. Dissimilatory nitrate reduction is catalyzed by the membrane bound nitrate reductase Nar, or periplasmic nitrate reductase Nap. In both types of enzymes, subunits that reduce nitrate, NarG or NapA, produce nitrite in an energetically favorable reaction using quinol as electron donor [98].

Membrane bound Nar enzyme forms the trimeric complex NarGHI belongs to the family of molybdopterine oxidoreductases (Figure 2-7). Subunit NarI anchors the enzyme to the membrane and receives electrons from quinone pool in the membrane. Electrons are transferred from NarI to NarG in which nitrate reaction occurs through NarH via its four Fe-S clusters. NarG, the subunit facing the cytoplasm, reduce nitrate to nitrite by using received electrons at the active site: the molybdenum cofactor or Mo-bis-MGD factor [99-103]. Two protons are consumed in the cytoplasm to form H_2O in the reduction of a nitrate. To maintain charge balance in the quinone pool, protons are released from the quinone pool to periplasm as the quinone pool donates electrons to NarI [99], which generates proton motive force.

Some bacteria conduct nitrate reduction by periplasmic Nap enzyme which forms NapAB complex (Figure 2-7). The subunit conducts nitrate reduction to nitrite, NapA, contains the molybdenum cofactor and a [4Fe–4S] center. The NapB subunit is a c-type cytochrome transfers electrons to NapA. The NapAB complex receives electrons from membrane bound quinol-oxidizing enzymes such as NapC or NapGH complex. NapC is a tetraheme cytochrome c enzyme in the NapC/NrfH family, and NapGH is composed of membrane bound quinol dehydrogenese NapH and periplasmic electron transfer adapter protein NapG [98].

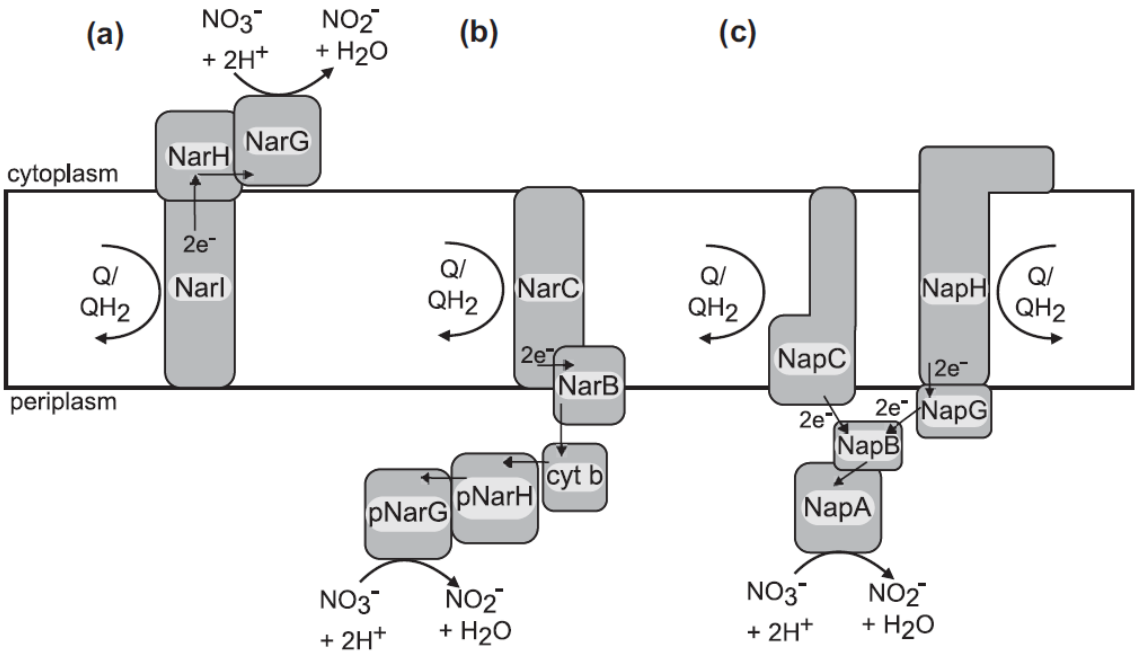

Figure 2-7: Structures of prokaryotic dissimilatory nitrate reductases. (a) Bacterial membrane-bound nitrate reductase (Nar). (b) Model of archaeal form of membrane-bound nitrate reductase (c) Periplasmic nitrate reductase (Nap) and membrane bound electron donors. (Source [99])

2.2.3.2. Nitrite reductase

In denitrification, nitrite is reduced to nitric oxide by two isofunctional periplasmic nitrite reductases NirK and NirS, which are evolutionary unrelated. NirK is a homotrimeric enzyme that is composed of three identical units each monomer contains two copper centers (Figure 2-8) [99]. NirS is a homodimeric enzyme composed of two identical units each monomer binds two prosthetic heme groups, heme c and heme d1. Electrons are transferred from heme c to heme d1 in which bound nitrite is reduced to nitric oxide (Figure 2-8) [99]. Generated nitric oxide is stepwisely reduced to dinitrogen in denitrification. Namely, nitric oxide that is produced by NirK or NirS is reduced to nitrous oxide via

membrane bound NorBC complex, and nitrous oxide is further reduced to dinitrogen via multi copper containing periplasmic Nos enzyme (Figure 2-8) [98, 99].

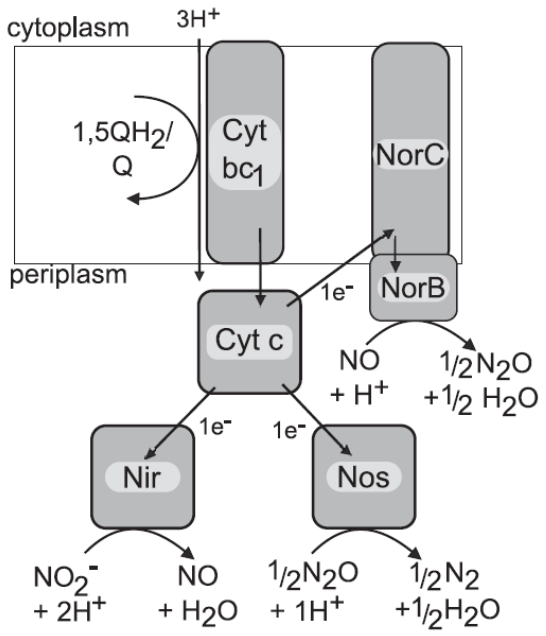

Figure 2-8: Respiratory chain in bacterial denitrification. Cyt bc1: cytochrome bc1 complex, cyt c: cytochrome c, nir: nitrite reductase, Nor: nitric oxide reductase, Nos: nitrous oxide reductase, Q: co-enzyme Q. (Source [99])

In DNRA, nitrite ammonification, transformation of nitrite into ammonium is catalyzed by a periplasmic pentaheme cytochrome c nitrite reductase, NrfA, without the formation of intermediate product [104, 105]. NrfA was reported as the soluble periplasmic protein (e.g. Gammaproteobacteria *Escherichia coli* and *S. oneidensis*) or as a subunit of membrane bound menaquinol-reactive NrfHA complex which is composed of NrfA and NrfH, a tetraheme cytochrome c that mediate electron transport from menaquinones to NrfA and anchors NrfHA complex to the membrane (e.g. Epsilonproteobacteria *Wolinella succinogenes*) (Figure 2-9) [98, 99]. Both of NrfA and NrfH are encoded by the *nrfHAIJ*

operon. This pentaheme nitrite reductase, NrfA, was reported to have a phylogenetic link to octaheme cytochrome octaheme cytochrome c hydroxylamine oxidoreductase responsible for the aerobic ammonium oxidation and hydrazine oxidoreductase in anammox [106] with recently discovered octaheme cytochrome c nitrite reductase [107].

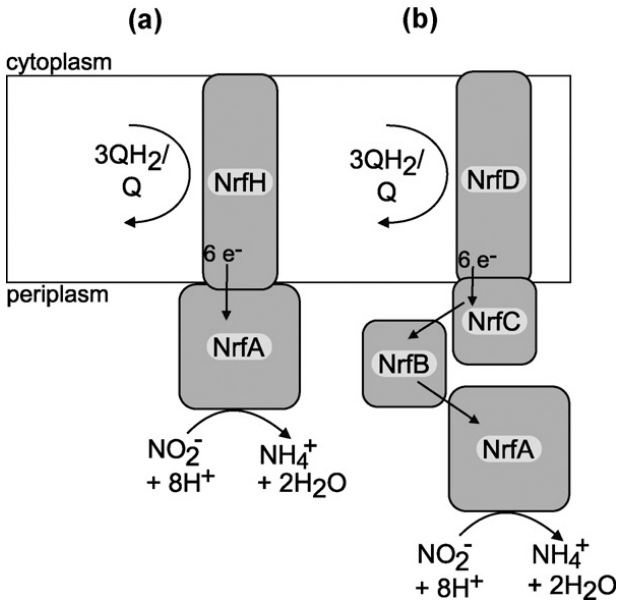

Figure 2-9: Respiratory chain in DNRA. (a) NrfHA complex. (b) NrfABCD complex. (Source [99])

2.2.3.3. Regulation of nitrate/nitrite-reducing enzyme synthesis

Expression of genes encoding enzymes for dissimilatory reduction of nitrate and nitrite is regulated by availability of oxygen as well as availability of nitrate/nitrite. In *Enterobacteriaceae*, which includes model organisms intensively studied for nitrate/nitrite reduction mechanisms, synthesis of dissimilatory nitrate/nitrite-reducing enzymes are induced by anaerobiosis, absence of oxygen, via Fumarate and Nitrate reductase Regulatory (FNR) system [108-110]. Under the absence of oxygen, expression of those genes is induced by nitrate and nitrite [111, 112]. Specifically, two-component regulatory

system composed of NarX which is nitrate/nitrite sensor that respond to both of nitrate and nitrite, and NarL which is the DNA-binding regulator that control gene expression [113]. A homologous two component system with nitrate/nitrite sensor, NarQ, and transcription regulator, NarP, works similarly [111]. For example, *G. metallireducens* GS-15, a model electrode-respiring bacterium that is capable of DNRA two operons encoding Nar enzyme complexes on genome [114] of which *narG*-1 operon, which encodes all of *narGHIJ* as well as nitrate/nitrite transporters, was reported to be expressed in cells growing nitrate as the electron acceptor while expression of *narG*-2, which only encodes *narGHI*, *nirD* and unknown cytochrome C gene, was not detected [114] (Figure 2-10).

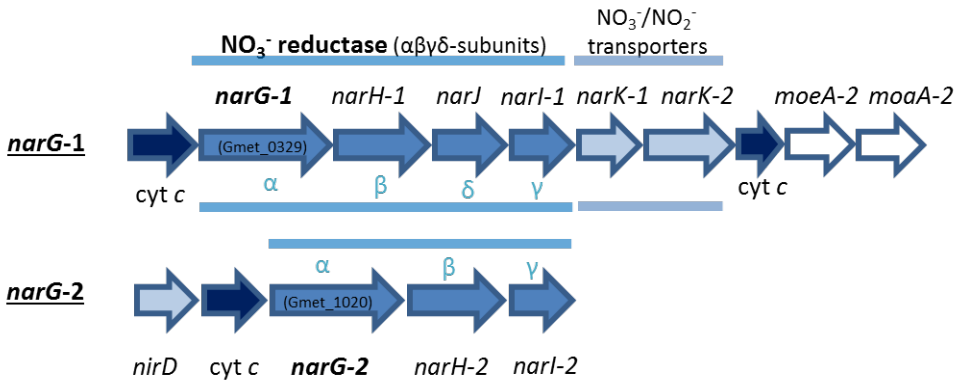

Figure 2-10: The respiratory Nar operons of *G. metallireducens*. The figure was made based on [114].

Such regulation of synthesis of dissimilatory nitrate/nitrite-reducing enzymes are distinctive from the ones of assimilatory nitrate-reducing enzyme, Nas. Synthesis of assimilatory nitrate reducing enzyme is induced by limitation of ammonia availability by nitrogen regulatory protein C (NTRC) [115], but it is not controlled by availability of oxygen (Table 2-1) [111].

Table 2-1: Functions and regulation of nitrate/nitrite-reducing enzymes in Enterobacteria. Table was adapted from [111].

	Enzymes			
	Nar	Nrf	Nir	Nas
Function	NO_3^- reduction	NO_2^- reduction	NO_2^- reduction	NO_3^- reduction
	Dissimilation			Assimilation
FNR control (O_2)	Yes	Yes	Yes	No
NarL/NarP control (NO_3^-/NO_2^-)	Yes	Yes	Yes	No
NTRC control (NH_4^+)	No	No	No	Yes

2.2.4. Nitrogen transformation in wastewater treatment context: removal and/or recovery

In wastewater treatment processes, reactive nitrogen species are removed from water body to avoid negative impacts of discharged treated wastewater, such as eutrophication, on the environment. Conventional activated sludge-based nutrient removal processes that are employed most centralized wastewater treatment facilities in the world employ nitrification process followed by denitrification process to remove reactive nitrogen species from water body [116]. Specifically, ammonia which is the abundant reactive nitrogen species in most wastewaters is oxidized by nitrification process which is composed of aerobic oxidation of ammonia to nitrite by ammonia-oxidizing bacteria (AOB) such as *Nitrosomonas* or ammonia-oxidizing archaea (AOA) such as *Thaumarchaeota* [91, 117], followed by nitrite oxidation to nitrate by nitrite-oxidizing bacteria (NOB) such as *Nitrospira*. Although above two oxidation reactions were thought

to be conducted by independent microbial groups, AOB/AOA and NOB, recent studies that reported single microorganism that conducted both reactions challenged such presumption [95, 96]. Supplying the oxygen, which is usually done by pumping air into wastewater, for nitrification as well as organic degradation in wastewater treatment processes is responsible for significant fraction of energy consumption in wastewater treatment which takes up to 3 % of domestic electricity production in the U.S. [87]. The water body that contains oxidized nitrogen species is subjected to anoxic condition under the presence of electron donor such as BOD in wastewater or supplemental electron donors to promote microbial dissimilatory nitrate reduction to dinitrogen gas, denitrification, to remove reactive nitrogen compounds from aqueous phase into gaseous phase. Wide variety of bacteria are involved in the all steps or partial steps of this sequential reductions of nitrate to nitrite, nitric oxide (NO), nitrous oxide (N_2O), and dinitrogen gas.

To liberate nitrogen removal processes from such massive oxygen supply and extra electron donor supply that burdens processes with demand in energy and cost, we have attempted to better exploit microbial nitrogen transformation reactions. For example, the Single Reactor High Activity Ammonia Removal Over Nitrite (SHARON) process demonstrated significant cost and energy reduction by stopping nitrification process in nitrite, not further oxidize it to nitrate. Specifically, the SHARON process successfully inhibited second process of nitrification reaction, nitrite oxidation to nitrate, by inhibiting NOB activity relative to AOB with the process operation in short solid retention time and elevated temperature [118]. This saved cost and energy input required for oxygen supply to further oxidize nitrite to nitrate in conventional nitrification process. Nitrite generated in such processes has been demonstrated to be reduced to dinitrogen gas either by stepwise

denitrification, or by incorporated anammox reaction to further reduce oxygen supply and supplemental electron donor for heterotrophic denitrification. In addition, alternative electron donors for nitrate/nitrite reduction also been intensively studied. For example, autotrophic denitrification on biocathode in BESs [53, 119-122], and anaerobic methane oxidation [123-125] demonstrated potential of alternative nitrate/nitrite reduction reactions as nitrogen removal process.

In addition to nitrogen removal, processes to recover nitrogen from wastewaters have been studied. Anaerobic digestion sludge and slurry that retain nitrogen in ammonium form and also in the form of assimilated biomass have applied in agricultural systems as fertilizer [126-128]. Also, studies have addressed to separate ammonia from wastewater body by heat [129-131] to recover it for agricultural and industrial applications. Recent study proposed electrochemical ammonium separation in a BES demonstrated 57-79 % of total nitrogen recovery (Figure 2-11) [132]. To better manage global nitrogen cycle, it would be ideal to recover the nitrogen into agricultural or industrial applications, which would reduce industrial nitrogen fixation, rather than removing nitrogen as dinitrogen gas into the atmosphere with cost/energy input, but further effort is needed to realize nitrogen recovery processes in the scale of current centralized wastewater treatment infrastructures.

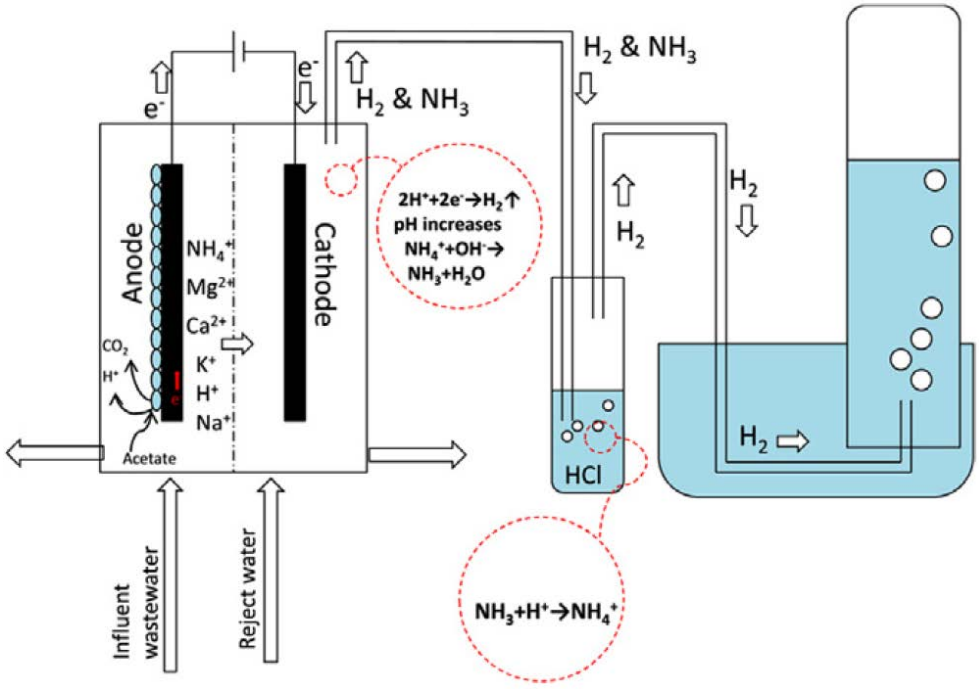

Figure 2-11: Ammonia recovery with simultaneous hydrogen production based on electrochemical ammonium ion separation proposed by Wu and Modin [132].

2.2.5. Dissimilatory nitrate reduction to ammonium (DNRA)

A relatively less understood microbial nitrogen transformation is dissimilatory nitrate reduction to ammonium (DNRA) [133]. DNRA is the two-step sequential reduction of nitrate into ammonium, in which nitrate is first reduced to nitrite by nitrate reductase, a reaction that also occurs during denitrification. The second step, respiratory nitrite ammonification, is distinct from other nitrate transformation reactions such as denitrification or anammox, because it produces ammonium rather than gaseous end products.

2.2.5.1. DNRA in natural and agricultural systems

DNRA has been conventionally presumed to have a minor contribution to nitrate transformation relative to denitrification in anoxic environments [134]. However, recent studies indicate a greater role of DNRA in the nitrogen cycle of various anoxic systems such as soil [135], sediment [136], estuary [137, 138], and ocean [139]. For example, recent studies measured nitrogen transformation reactions in forest soils [140, 141] and agriculturally used soils [142] with stable isotope-labeled nitrogen compounds as tracers detected DNRA activity. Such recent studies overcame assumptions of earlier studies concluded DNRA was likely not important in temporary oxic soils [133, 143]. In addition, a laboratory study demonstrating comparable or an even higher actual energy yield of DNRA to denitrification [144] challenged our presumption of superior energy conservation of denitrification over DNRA based on thermodynamic estimation. The results of growth yields measurements in pure culture experiments indicated that ATP synthesis in denitrification is far lower than expected from the free energy changes and even lower than in nitrate ammonification for some cases [144]. The *nrfA* encoding pentaheme cytochrome C nitrite reductase NrfA, which catalyzes respiratory nitrite ammonification, was reported to be a useful molecular marker to assess diversity and activity of microbial populations associated with DNRA [138, 145-147]. Further study is encouraged to understand DNRA in various anoxic systems. Combined use of isotope labeled tracers and molecular marker would be a promising approach to characterize DNRA in complex systems.

2.2.5.2. DNRA in wastewater treatment context: current understandings and potential contributions

In contrast to studies investigated DNRA in natural systems as discussed above, DNRA has been largely overlooked in wastewater treatment systems, even though many systems remove nitrate through biological denitrification processes under conditions permissible for DNRA. For example, the data from a metatranscriptomic analysis of activated sludge showed expression of a DNRA-related gene at levels comparable to nitrification and denitrification genes, but no mention of DNRA was made in the text [148]. The occurrence of DNRA during biological wastewater treatment would have impacts on system performance. For example, DNRA (8 electron transfer reaction) requires 60 % more reducing equivalents than denitrification (5 electron transfer reaction), which would be provided by the oxidation of biochemical oxygen demand (BOD) in wastewater or supplemental electron donors. Also, whereas denitrification removes aqueous nitrogen to the gas phase as dinitrogen, the formation of ammonium by DNRA would result in additional oxygen demand for nitrification or elevated effluent ammonia concentrations. In addition, DNRA could impact emissions of nitrous oxide, a strong greenhouse gas [83] associated with denitrification processes as DNRA does not produce nitrous oxide. Some studies suggested a potential contribution of DNRA to explain increased ammonium levels in denitrifying reactors [149, 150], biofilters [151, 152], and a bioelectrochemical system (BES) [153], but none of these studies investigated direct evidence of DNRA activity. The investigation of DNRA through chemical monitoring is confounded by interconnected nitrogen transformations (e.g., ammonium release associated with biomass decay). Although the use of isotope-labeled nitrogen compounds would resolve this problem, this

is not feasible in full-scale wastewater treatment systems. Thus, incorporation of molecular markers such as *nrfA* is thought to be useful to characterize DNRA in wastewater treatment systems.

2.2.5.3. Nitrogen transformation in BESs and potential contribution of DNRA

As wastewater treatment processes, BESs have primarily focused on removal of organics, or BOD, but they are beginning to be designed for integrated nitrogen removal. After the demonstration of biological cathodic denitrification in a MFC in 2007 [53], various studies have addressed cathodic denitrification as novel autotrophic denitrification processes with lower input of energy and supplemental electron donors, as well as lower sludge production relative to conventional heterotrophic denitrification processes [119-121, 154, 155]. These studies were intended to convert nitrate in cathode chamber under autotrophic conditions via denitrification but none of those studies intentionally examined contribution of other biological nitrate reduction reactions such as DNRA. Also, process designs of simultaneous nitrification and denitrification with single-chamber air-cathode MFCs [156, 157], two-chamber MFC with denitrifying biocathode with an anion exchange membrane to avoid ammonia crossover [155], and BES-driven in-situ groundwater nitrate removal systems [158, 159] have brought nitrate into anodic BES system. Potential for nitrate reduction by anode-reducing communities is poorly understood as discussed in 2.1.5., and pathways of their nitrate reduction are also unknown.

Contribution of DNRA in nitrate/nitrite reduction in anodic and cathodic BESs could be important because as many metal/sulfate-reducing bacteria with electrogenic or electrotrophic activity such as *Geobacter metallireducens* [160], *Shewanella oneidensis*

[71], and *Desulfobulbaceae* [4, 161] have potential to conduct DNRA. Namely, those bacteria or their relatives have proven to conduct DNRA, and/or possess *nrfA* catalyzing DNRA but not *nirS/nirK* catalyzing denitrification. Studies of cathodic nitrogen removal in BESs [121, 122] have been primarily focused on denitrification as the nitrate reduction mechanism, but the potential contribution of DNRA has not been investigated. In addition, DNRA could act as a competitive side reaction to desired BES processes. For example, facultative DNRA could disrupt anode reduction as discussed in 2.1.5. Alternatively, cathode-derived electrons could be directed to DNRA instead of reductive dechlorination with bacteria capable of DNRA such as *Anaeromyxobacter dehalogenans* [162, 163]. A study investigated effect of C/N ratio on nitrogen removal in a BES detected ammonia formation and discussed potential contribution of DNRA for measured ammonia production [153]. This study infers potential contribution of DNRA but further study is needed to understand nitrogen transformation mechanisms in BESs and contribution of DNRA.

2.3. Literature Cited

1. Logan, B.E. and K. Rabaey, *Conversion of wastes into bioelectricity and chemicals by using microbial electrochemical technologies.* Science, 2012. **337**(6095): p. 686-690.
2. Angenent, L.T., et al., *Production of bioenergy and biochemicals from industrial and agricultural wastewater.* Trends in biotechnology, 2004. **22**(9): p. 477-85.
3. Rabaey, K. and R.A. Rozendal, *Microbial electrosynthesis — revisiting the electrical route for microbial production.* Nature Reviews Microbiology, 2010. **8**(10): p. 706-716.
4. Pfeffer, C., et al., *Filamentous bacteria transport electrons over centimetre distances.* Nature, 2012. **491**(7423): p. 218-221.
5. Kato, S., K. Hashimoto, and K. Watanabe, *Microbial interspecies electron transfer via electric currents through conductive minerals.* Proceedings of the National Academy of Sciences, 2012. **109**(25): p. 10042-10046.
6. McGlynn, S.E., et al., *Single cell activity reveals direct electron transfer in methanotrophic consortia.* Nature, 2015. **526**(7574): p. 531-5.
7. Wegener, G., et al., *Intercellular wiring enables electron transfer between methanotrophic archaea and bacteria.* Nature, 2015. **526**(7574): p. 587-90.
8. Scheller, S., et al., *Artificial electron acceptors decouple archaeal methane oxidation from sulfate reduction.* Science, 2016. **351**(6274): p. 703-707.
9. Potter, M.C., *Electrical effects accompanying the decomposition of organic compounds.* Proceedings of the Royal Society of London. Series B, Containing Papers of a Biological Character, 1911. **84**(571): p. 260-276.

10. Kim, H.J., et al., *A mediator-less microbial fuel cell using a metal reducing bacterium, Shewanella putrefaciens.* Enzyme and Microbial Technology, 2002. **30**(2): p. 145-152.

11. Logan, B.E., et al., *Microbial fuel cells: methodology and technology.* Environmental Science & Technology, 2006. **40**(17): p. 5181-5192.

12. Liu, H., S. Grot, and B.E. Logan, *Electrochemically assisted microbial production of hydrogen from acetate.* Environmental Science & Technology, 2005. **39**(11): p. 4317-4320.

13. Mehanna, M., et al., *Using microbial desalination cells to reduce water salinity prior to reverse osmosis.* Energy & Environmental Science, 2010. **3**(8): p. 1114-1120.

14. Kim, Y. and B.E. Logan, *Hydrogen production from inexhaustible supplies of fresh and salt water using microbial reverse-electrodialysis electrolysis cells.* Proceedings of the National Academy of Sciences, 2011. **108**(39): p. 16176-16181.

15. Cusick, R.D., Y. Kim, and B.E. Logan, *Energy capture from thermolytic solutions in microbial reverse-electrodialysis cells.* Science, 2012. **335**(6075): p. 1474-1477.

16. Nevin, K.P., et al., *Microbial electrosynthesis: feeding microbes electricity to convert carbon dioxide and water to multicarbon extracellular organic compounds.* MBio, 2010. **1**(2).

17. Schröder, U., *Anodic electron transfer mechanisms in microbial fuel cells and their energy efficiency.* Physical Chemistry Chemical Physics, 2007. **9**(21): p. 2619-2629.

18. Lovley, D.R. and E.J. Phillips, *Availability of ferric iron for microbial reduction in bottom sediments of the freshwater tidal Potomac River*. Applied and Environmental Microbiology, 1986. **52**(4): p. 751-757.

19. Lovley, D.R. and E.J. Phillips, *Novel mode of microbial energy metabolism: organic carbon oxidation coupled to dissimilatory reduction of iron or manganese.* Applied and Environmental Microbiology, 1988. **54**(6): p. 1472-1480.

20. Lovley, D.R., et al., *Geobacter metallireducens gen. nov. sp. nov., a microorganism capable of coupling the complete oxidation of organic compounds to the reduction of iron and other metals.* Archives of microbiology, 1993. **159**(4): p. 336-344.

21. Myers, C.R. and K.H. Nealson, *Bacterial manganese reduction and growth with manganese oxide as the sole electron acceptor.* Science, 1988. **240**.

22. Krause, B. and K.H. Nealson, *Physiology and enzymology involved in denitrification by Shewanella putrefaciens.* Applied and Environmental Microbiology, 1997. **63**(7): p. 2613-2618.

23. Caccavo, F., et al., *Geobacter sulfurreducens sp. nov., a hydrogen-and acetate-oxidizing dissimilatory metal-reducing microorganism.* Applied and Environmental Microbiology, 1994. **60**(10): p. 3752-3759.

24. Holmes, D.E., et al., *Microarray and genetic analysis of electron transfer to electrodes in Geobacter sulfurreducens.* Environmental Microbiology, 2006. **8**(10): p. 1805-15.

25. Nevin, K.P., et al., *Anode biofilm transcriptomics reveals outer surface components essential for high density current production in Geobacter sulfurreducens fuel cells.* Plos One, 2009. **4**(5): p. e5628.

26. Reguera, G., et al., *Extracellular electron transfer via microbial nanowires.* Nature, 2005. **435**(7045): p. 1098-1101.

27. Reguera, G., et al., *Biofilm and nanowire production leads to increased current in Geobacter sulfurreducens fuel cells.* Applied and Environmental Microbiology, 2006. **72**(11): p. 7345-7348.

28. Reguera, G., et al., *Possible nonconductive role of Geobacter sulfurreducens pilus nanowires in biofilm formation.* Journal of Bacteriology, 2007. **189**(5): p. 2125-2127.

29. Inoue, K., et al., *Specific localization of the c-type cytochrome OmcZ at the anode surface in current-producing biofilms of Geobacter sulfurreducens.* Environmental microbiology reports, 2011. **3**(2): p. 211-7.

30. Leang, C., et al., *Alignment of the c-type cytochrome OmcS along pili of Geobacter sulfurreducens.* Applied and Environmental Microbiology, 2010. **76**(12): p. 4080-4.

31. Nikhil S. Malvankar, M.V., Kelly P. Nevin, Ashley E. Franks, Ching Leang,, K.I. Byoung-Chan Kim, Tu¨nde Mester, Sean F. Covalla, Jessica P. Johnson,, and M.T.T.a.D.R.L. Vincent M. Rotello, *Tunable metallic-like conductivity in microbial nanowire networks.* NATURE NANOTECHNOLOGY, 2011.

32. Strycharz-Glaven, S.M., et al., *On the electrical conductivity of microbial nanowires and biofilms.* Energy & Environmental Science, 2011. **4**(11): p. 4366.

33. Shi, L., et al., *Respiration of metal (hydr)oxides by Shewanella and Geobacter: a key role for multihaem c-type cytochromes.* Molecular microbiology, 2007. **65**(1): p. 12-20.

34. Roller, S.D., et al., *Electron ‐ transfer coupling in microbial fuel cells: 1. comparison of redox ‐ mediator reduction rates and respiratory rates of bacteria.* Journal of Chemical Technology and Biotechnology. Biotechnology, 1984. **34**(1): p. 3-12.

35. Delaney, G.M., et al., *Electron ‐ transfer coupling in microbial fuel cells. 2. performance of fuel cells containing selected microorganism—mediator—substrate combinations.* Journal of chemical technology and biotechnology. Biotechnology, 1984. **34**(1): p. 13-27.

36. Rabaey, K., et al., *Biofuel cells select for microbial consortia that self-mediate electron transfer.* Applied and environmental microbiology, 2004. **70**(9): p. 5373-5382.

37. Rabaey, K., et al., *Microbial phenazine production enhances electron transfer in biofuel cells.* Environmental science & technology, 2005. **39**(9): p. 3401-3408.

38. Kiely, P.D., et al., *Anode microbial communities produced by changing from microbial fuel cell to microbial electrolysis cell operation using two different wastewaters.* Bioresour Technol, 2011. **102**(1): p. 388-94.

39. Yates, M.D., et al., *Convergent development of anodic bacterial communities in microbial fuel cells.* ISME J, 2012. **6**(11): p. 2002-13.

40. Vargas, I.T., I.U. Albert, and J.M. Regan, *Spatial distribution of bacterial communities on volumetric and planar anodes in single ‐ chamber air ‐ cathode microbial fuel cells.* Biotechnology and Bioengineering, 2013. **110**(11): p. 3059-3062.

41. Holmes, D.E., et al., *Enrichment of members of the family Geobacteraceae associated with stimulation of dissimilatory metal reduction in uranium-contaminated aquifer sediments.* Applied and Environmental Microbiology, 2002. **68**(5): p. 2300-2306.

42. Anderson, R.T., et al., *Stimulating the in situ activity of Geobacter species to remove uranium from the groundwater of a uranium-contaminated aquifer.* Applied and environmental microbiology, 2003. **69**(10): p. 5884-5891.

43. Bond, D.R. and D.R. Lovley, *Electricity Production by Geobacter sulfurreducens Attached to Electrodes.* Applied and Environmental Microbiology, 2003. **69**(3): p. 1548-1555.

44. Call, D.F. and B.E. Logan, *Lactate oxidation coupled to iron or electrode reduction by Geobacter sulfurreducens PCA.* Appl Environ Microbiol, 2011. **77**(24): p. 8791-4.

45. Gregory, K.B., D.R. Bond, and D.R. Lovley, *Biocathode Geobacter nitrate reduction. Graphite electrodes as electron donors for anaerobic respiration.* Environmental Microbiology, 2004. **6**(6): p. 596-604.

46. Strycharz, S.M., et al., *Graphite electrode as a sole electron donor for reductive dechlorination of tetrachlorethene by Geobacter lovleyi.* Applied and Environmental Microbiology, 2008. **74**(19): p. 5943-7.

47. Cheng, S., et al., *Direct biological conversion of electrical current into methane by electromethanogenesis.* Environmental Science & Technology, 2009. **43**(10): p. 3953-3958.

48. Siegert, M., et al., *The presence of hydrogenotrophic methanogens in the inoculum improves methane gas production in microbial electrolysis cells.* Frontiers in Microbiology, 2015. **5**.

49. Siegert, M., et al., *MethanobacteriumDominates Biocathodic Archaeal Communities in Methanogenic Microbial Electrolysis Cells.* ACS Sustainable Chemistry & Engineering, 2015. **3**(7): p. 1668-1676.

50. Patil, S.A., et al., *Selective Enrichment Establishes a Stable Performing Community for Microbial Electrosynthesis of Acetate from CO2.* Environ Sci Technol, 2015. **49**(14): p. 8833-43.

51. Gregory, K.B. and D.R. Lovley, *Remediation and recovery of uranium from contaminated subsurface environments with electrodes.* Environmental Science & Technology, 2005. **39**(22): p. 8943-8947.

52. Cournet, A., et al., *Electrochemical reduction of oxygen catalyzed by a wide range of bacteria including Gram-positive.* Electrochemistry Communications, 2010. **12**(4): p. 505-508.

53. Clauwaert, P., et al., *Biological denitrification in microbial fuel cells.* Environmental Science & Technology, 2007. **41**(9): p. 3354-3360.

54. Aulenta, F., et al., *Characterization of an electro-active biocathode capable of dechlorinating trichloroethene and cis-dichloroethene to ethene.* Biosens Bioelectron, 2010. **25**(7): p. 1796-802.

55. Thrash, J.C., et al., *Electrochemical stimulation of microbial perchlorate reduction.* Environmental science & technology, 2007. **41**(5): p. 1740-1746.

56. Summers, Z.M., et al., *Direct exchange of electrons within aggregates of an evolved syntrophic coculture of anaerobic bacteria.* Science, 2010. **330**(6009): p. 1413-5.

57. Rotaru, A.-E., et al., *Direct interspecies electron transfer between Geobacter metallireducens and Methanosarcina barkeri.* Applied and environmental microbiology, 2014. **80**(15): p. 4599-4605.

58. Morita, M., et al., *Potential for direct interspecies electron transfer in methanogenic wastewater digester aggregates.* MBio, 2011. **2**(4): p. e00159-11.

59. Rotaru, A.-E., et al., *A new model for electron flow during anaerobic digestion: direct interspecies electron transfer to Methanosaeta for the reduction of carbon dioxide to methane.* Energy Environ. Sci., 2014. **7**(1): p. 408-415.

60. Schink, B. and A.J. Stams, *Syntrophism among prokaryotes*. 2013: Springer.

61. Ishii, S., et al., *Coaggregation facilitates interspecies hydrogen transfer between Pelotomaculum thermopropionicum and Methanothermobacter thermautotrophicus.* Appl Environ Microbiol, 2005. **71**(12): p. 7838-45.

62. Alperin, M.J. and T.M. Hoehler, *Anaerobic methane oxidation by archaea/sulfate-reducing bacteria aggregates: 1. Thermodynamic and physical constraints.* American Journal of Science, 2009. **309**(10): p. 869-957.

63. Boetius, A., et al., *A marine microbial consortium apparently mediating anaerobic oxidation of methane.* Nature, 2000. **407**(6804): p. 623-626.

64. Cheng, S., H. Liu, and B.E. Logan, *Increased performance of single-chamber microbial fuel cells using an improved cathode structure.* Electrochemistry Communications, 2006. **8**(3): p. 489-494.

65. Watson, V.J., et al., *Polymer coatings as separator layers for microbial fuel cell cathodes.* Journal of Power Sources, 2011. **196**(6): p. 3009-3014.

66. Ahn, Y. and B.E. Logan, *A multi-electrode continuous flow microbial fuel cell with separator electrode assembly design.* Appl Microbiol Biotechnol, 2012. **93**(5): p. 2241-8.

67. Ren, L., et al., *High current densities enable exoelectrogens to outcompete aerobic heterotrophs for substrate.* Biotechnol Bioeng, 2014. **111**(11): p. 2163-9.

68. Clauwaert, P. and W. Verstraete, *Methanogenesis in membraneless microbial electrolysis cells.* Appl Microbiol Biotechnol, 2009. **82**(5): p. 829-36.

69. Lee, H.-S., et al., *Fate of H2 in an upflow single-chamber microbial electrolysis cell using a metal-catalyst-free cathode.* Environ. Sci. Technol., 2009. **43**(20): p. 7971-7976.

70. Cusick, R.D., et al., *Performance of a pilot-scale continuous flow microbial electrolysis cell fed winery wastewater.* Applied microbiology and biotechnology, 2011. **89**(6): p. 2053-63.

71. Cruz-Garcia, C., et al., *Respiratory nitrate ammonification by Shewanella oneidensis MR-1.* Journal of Bacteriology, 2007. **189**(2): p. 656-62.

72. Xing, D., et al., *Isolation of the exoelectrogenic denitrifying bacterium Comamonas denitrificans based on dilution to extinction.* Applied microbiology and biotechnology, 2010. **85**(5): p. 1575-87.

73. Greene, A.C., B.K. Patel, and S. Yacob, *Geoalkalibacter subterraneus sp. nov., an anaerobic Fe(III)- and Mn(IV)-reducing bacterium from a petroleum reservoir,*

and emended descriptions of the family Desulfuromonadaceae and the genus Geoalkalibacter. Int. J. Syst. Evol. Microbiol., 2009. **59**(Pt 4): p. 781-5.

74. Badalamenti, J.P., R. Krajmalnik-Brown, and C.I. Torres, *Generation of high current densities by pure cultures of anode-respiring Geoalkalibacter spp. under alkaline and saline conditions in microbial electrochemical cells.* MBio, 2013. **4**(3): p. e00144-13.

75. Fu, Q., et al., *A thermophilic gram-negative nitrate-reducing bacterium, Calditerrivibrio nitroreducens, exhibiting electricity generation capability.* Environ. Sci. Technol., 2013. **47**(21): p. 12583-90.

76. Sukkasem, C., et al., *Effect of nitrate on the performance of single chamber air cathode microbial fuel cells.* Water Research, 2008. **42**(19): p. 4743-4750.

77. Kim, B., et al., *Enrichment of microbial community generating electricity using a fuel-cell-type electrochemical cell.* Applied microbiology and biotechnology, 2004. **63**(6): p. 672-681.

78. Cheng, K.Y., G. Ho, and R. Cord-Ruwisch, *Anodophilic biofilm catalyzes cathodic oxygen reduction.* Environmental science & technology, 2010. **44**(1): p. 518-525.

79. Cheng, K.Y., M.P. Ginige, and A.H. Kaksonen, *Ano-cathodophilic biofilm catalyzes both anodic carbon oxidation and cathodic denitrification.* Environ Sci Technol, 2012. **46**(18): p. 10372-8.

80. Blanchet, E., et al., *Protons accumulation during anodic phase turned to advantage for oxygen reduction during cathodic phase in reversible bioelectrodes.* Bioresour Technol, 2014. **173**: p. 224-30.

81. Pisciotta, J.M., et al., *Enrichment of microbial electrolysis cell biocathodes from sediment microbial fuel cell bioanodes.* Appl Environ Microbiol, 2012. **78**(15): p. 5212-9.

82. Fixen, P.E. and F.B. West, *Nitrogen fertilizers: meeting contemporary challenges.* Ambio: a journal of the human environment, 2002. **31**(2): p. 169-176.

83. Canfield, D.E., A.N. Glazer, and P.G. Falkowski, *The evolution and future of Earth's nitrogen cycle.* science, 2010. **330**(6001): p. 192-196.

84. Ravishankara, A., J.S. Daniel, and R.W. Portmann, *Nitrous oxide (N2O): the dominant ozone-depleting substance emitted in the 21st century.* science, 2009. **326**(5949): p. 123-125.

85. Ishii, S., et al., *Identification of key nitrous oxide production pathways in aerobic partial nitrifying granules.* Environ Microbiol, 2014. **16**(10): p. 3168-80.

86. Mosier, A., et al., *Assessing and mitigating N2O emissions from agricultural soils.* Climatic change, 1998. **40**(1): p. 7-38.

87. McCarty, P.L., J. Bae, and J. Kim, *Domestic wastewater treatment as a net energy producer--can this be achieved?* Environmental Science & Technology, 2011. **45**(17): p. 7100-6.

88. Strous, M., et al., *Missing lithotroph identified as new planctomycete.* Nature, 1999. **400**(6743): p. 446-449.

89. Jetten, M.S., et al., *The anaerobic oxidation of ammonium.* FEMS Microbiology reviews, 1998. **22**(5): p. 421-437.

90. Kartal, B., et al., *How to make a living from anaerobic ammonium oxidation.* FEMS Microbiol Rev, 2013. **37**(3): p. 428-61.

91. Park, H.D., et al., *Occurrence of ammonia-oxidizing archaea in wastewater treatment plant bioreactors.* Appl Environ Microbiol, 2006. **72**(8): p. 5643-7.

92. Wrage, N., et al., *Role of nitrifier denitrification in the production of nitrous oxide.* Soil Biology and Biochemistry, 2001. **33**(12): p. 1723-1732.

93. Finneran, K.T., M.E. Housewright, and D.R. Lovley, *Multiple influences of nitrate on uranium solubility during bioremediation of uranium ‐ contaminated subsurface sediments.* Environmental Microbiology, 2002. **4**(9): p. 510-516.

94. Straub, K.L., et al., *Diversity of Ferrous Iron-Oxidizing, Nitrate-Reducing Bacteria and their Involvement in Oxygen-Independent Iron Cycling.* Geomicrobiology Journal, 2004. **21**(6): p. 371-378.

95. van Kessel, M.A., et al., *Complete nitrification by a single microorganism.* Nature, 2015. **528**(7583): p. 555-9.

96. Daims, H., et al., *Complete nitrification by Nitrospira bacteria.* Nature, 2015. **528**(7583): p. 504-9.

97. Falkowski, P.G., *Evolution of the nitrogen cycle and its influence on the biological sequestration of CO 2 in the ocean.* Nature, 1997. **387**(6630): p. 272-275.

98. Simon, J. and M.G. Klotz, *Diversity and evolution of bioenergetic systems involved in microbial nitrogen compound transformations.* Biochimica et biophysica acta, 2013. **1827**(2): p. 114-35.

99. Kraft, B., M. Strous, and H.E. Tegetmeyer, *Microbial nitrate respiration--genes, enzymes and environmental distribution.* Journal of Biotechnology, 2011. **155**(1): p. 104-17.

100. Hille, R., *The mononuclear molybdenum enzymes.* Chemical Reviews, 1996. **96**(7): p. 2757-2816.

101. Jormakka, M., et al., *Architecture of NarGH reveals a structural classification of Mo-bisMGD enzymes.* Structure, 2004. **12**(1): p. 95-104.

102. Lalucat, J., et al., *Biology of Pseudomonas stutzeri.* Microbiology and Molecular Biology Reviews, 2006. **70**(2): p. 510-547.

103. Richardson, D., et al., *Functional, biochemical and genetic diversity of prokaryotic nitrate reductases.* Cellular and Molecular Life Sciences CMLS, 2001. **58**(2): p. 165-178.

104. Einsle, O., et al., *Structure of cytochrome c nitrite reductase.* Nature, 1999. **400**(6743): p. 476-480.

105. Einsle, O., et al., *Mechanism of the six-electron reduction of nitrite to ammonia by cytochrome c nitrite reductase.* Journal of the American Chemical Society, 2002. **124**(39): p. 11737-11745.

106. Klotz, M.G., et al., *Evolution of an octahaem cytochrome c protein family that is key to aerobic and anaerobic ammonia oxidation by bacteria.* Environ Microbiol, 2008. **10**(11): p. 3150-63.

107. Atkinson, S.J., et al., *An octaheme c‐type cytochrome from Shewanella oneidensis can reduce nitrite and hydroxylamine.* FEBS letters, 2007. **581**(20): p. 3805-3808.

108. Unden, G., et al., *Oxygen regulated gene expression in facultatively anaerobic bacteria.* Antonie Van Leeuwenhoek, 1994. **66**(1-3): p. 3-22.

109. Unden, G., et al., *O2-sensing and O2-dependent gene regulation in facultatively anaerobic bacteria.* Archives of microbiology, 1995. **164**(2): p. 81-90.

110. Unden, G. and J. Schirawski, *The oxygen ‐ responsive transcriptional regulator FNR of Escherichia coli: the search for signals and reactions.* Molecular microbiology, 1997. **25**(2): p. 205-210.

111. Stewart, V., *Regulation of nitrate and nitrite reductase synthesis in enterobacteria.* Antonie van Leeuwenhoek, 1994. **66**(1-3): p. 37-45.

112. Moreno-Vivián, C., et al., *Prokaryotic nitrate reduction: molecular properties and functional distinction among bacterial nitrate reductases.* Journal of bacteriology, 1999. **181**(21): p. 6573-6584.

113. Nohno, T., et al., *The narX and narL genes encoding the nitrate-sensing regulators of Escherichia coli are homologous to a family of prokaryotic two-component regulatory genes.* Nucleic acids research, 1989. **17**(8): p. 2947-2957.

114. Aklujkar, M., et al., *The genome sequence of Geobacter metallireducens: features of metabolism, physiology and regulation common and dissimilar to Geobacter sulfurreducens.* BMC microbiology, 2009. **9**: p. 109.

115. Cali, B.M., J.L. Micca, and V. Stewart, *Genetic regulation of nitrate assimilation in Klebsiella pneumoniae M5al.* Journal of bacteriology, 1989. **171**(5): p. 2666-2672.

116. Grady Jr, C.L., et al., *Biological wastewater treatment*. 2011: CRC Press.

117. Stahl, D.A. and J.R. de la Torre, *Physiology and diversity of ammonia-oxidizing archaea.* Annu Rev Microbiol, 2012. **66**: p. 83-101.

118. Jetten, M.S., et al., *Microbiology and application of the anaerobic ammonium oxidation ('anammox') process.* Current opinion in biotechnology, 2001. **12**(3): p. 283-288.

119. Virdis, B., et al., *Microbial fuel cells for simultaneous carbon and nitrogen removal.* Water Research, 2008. **42**(12): p. 3013-3024.

120. Virdis, B., et al., *Electron fluxes in a microbial fuel cell performing carbon and nitrogen removal.* Environmental Science & Technology, 2009. **43**(13): p. 5144-5149.

121. Virdis, B., et al., *Simultaneous nitrification, denitrification and carbon removal in microbial fuel cells.* Water Research, 2010. **44**(9): p. 2970-80.

122. Kelly, P.T. and Z. He, *Nutrients removal and recovery in bioelectrochemical systems: a review*. Bioresource Technology, 2014. **153**: p. 351-60.

123. Cai, C., et al., *Nitrate reduction by denitrifying anaerobic methane oxidizing microorganisms can reach a practically useful rate.* Water Res, 2015. **87**: p. 211-7.

124. Hu, S., et al., *Enrichment of denitrifying anaerobic methane oxidizing microorganisms.* Environmental microbiology reports, 2009. **1**(5): p. 377-84.

125. Hu, B., et al., *Cultivation of nitrite-dependent anaerobic methane-oxidizing bacteria: impact of reactor configuration.* Appl Microbiol Biotechnol, 2014. **98**(18): p. 7983-91.

126. Hospido, A., et al., *Environmental assessment of anaerobically digested sludge reuse in agriculture: Potential impacts of emerging micropollutants.* water research, 2010. **44**(10): p. 3225-3233.

127. Sunaga, K., et al., *Impacts of heavy application of anaerobically digested slurry to whole crop rice cultivation in paddy environment on water, air and soil qualities.* Japanese Journal of Soil Science and Plant Nutrition, 2009. **80**(6): p. 596-605.

128. Chen, D., et al., *Nitrogen dynamics of anaerobically digested slurry used to fertilize paddy fields.* Biology and Fertility of Soils, 2012. **49**(6): p. 647-659.

129. Abouelenien, F., et al., *Dry anaerobic ammonia-methane production from chicken manure.* Appl Microbiol Biotechnol, 2009. **82**(4): p. 757-64.

130. Saracco, G. and G. Genon, *High temperature ammonia stripping and recovery from process liquid wastes.* Journal of hazardous materials, 1994. **37**(1): p. 191-206.

131. Katehis, D., V. Diyamandoglu, and J. Fillos, *Stripping and recovery of ammonia from centrate of anaerobically digested biosolids at elevated temperatures.* Water Environment Research, 1998. **70**(2): p. 231-240.

132. Wu, X. and O. Modin, *Ammonium recovery from reject water combined with hydrogen production in a bioelectrochemical reactor.* Bioresource Technology, 2013. **146**: p. 530-6.

133. Tiedje, J.M., *Ecology of denitrification and dissimilatory nitrate reduction to ammonium.* Biology of anaerobic microorganisms, 1988. **717**: p. 179-244.

134. Cole, J., *Physiology, biochemistry and genetics of nitrate dissimilation to ammonia*, in *Denitrification in soil and sediment*. 1990, Springer. p. 57-76.

135. Rutting, T., et al., *Assessment of the importance of dissimilatory nitrate reduction to ammonium for the terrestrial nitrogen cycle.* Biogeosciences, 2011. **8**(7): p. 1779-1791.

136. Nizzoli, D., et al., *Effect of organic enrichment and thermal regime on denitrification and dissimilatory nitrate reduction to ammonium (DNRA) in hypolimnetic sediments of two lowland lakes.* Water Research, 2010. **44**(9): p. 2715-2724.

137. Smith, C.J., et al., *Seasonal variation in denitrification and dissimilatory nitrate reduction to ammonia process rates and corresponding key functional genes along an estuarine nitrate gradient.* Front Microbiol, 2015. **6**: p. 542.

138. Decleyre, H., et al., *Dissimilatory nitrogen reduction in intertidal sediments of a temperate estuary: small scale heterogeneity and novel nitrate-to-ammonium reducers.* Front Microbiol, 2015. **6**: p. 1124.

139. Lam, P., et al., *Revising the nitrogen cycle in the Peruvian oxygen minimum zone.* Proceedings of the National Academy of Sciences, 2009. **106**(12): p. 4752-4757.

140. Templer, P.H., et al., *PLANT AND MICROBIAL CONTROLS ON NITROGEN RETENTION AND LOSS IN A HUMID TROPICAL FOREST.* Ecology, 2008. **89**(11): p. 3030-3040.

141. Silver, W.L., D.J. Herman, and M.K. Firestone, *Dissimilatory nitrate reduction to ammonium in upland tropical forest soils.* Ecology, 2001. **82**(9): p. 2410-2416.

142. Wan, Y., et al., *Gross nitrogen transformations and related nitrous oxide emissions in an intensively used calcareous soil.* Soil Science Society of America Journal, 2009. **73**(1): p. 102-112.

143. Buresh, R. and W. Patrick, *Nitrate reduction to ammonium in anaerobic soil.* Soil Science Society of America Journal, 1978. **42**(6): p. 913-918.

144. Strohm, T.O., et al., *Growth yields in bacterial denitrification and nitrate ammonification.* Appl Environ Microbiol, 2007. **73**(5): p. 1420-4.

145. Mohan, S.B., et al., *Detection and widespread distribution of the nrfA gene encoding nitrite reduction to ammonia, a short circuit in the biological nitrogen*

cycle that competes with denitrification. Fems Microbiology Ecology, 2004. **49**(3): p. 433-43.

146. Smith, C.J., et al., *Diversity and abundance of nitrate reductase genes (narG and napA), nitrite reductase genes (nirS and nrfA), and their transcripts in estuarine sediments.* Applied and Environmental Microbiology, 2007. **73**(11): p. 3612-22.

147. Welsh, A., et al., *Refined NrfA phylogeny improves PCR-based nrfA gene detection.* Applied and Environmental Microbiology, 2014.

148. Yu, K. and T. Zhang, *Metagenomic and metatranscriptomic analysis of microbial community structure and gene expression of activated sludge.* PLoS One, 2012. **7**(5): p. e38183.

149. Shen, Z., Y. Zhou, and J. Wang, *Comparison of denitrification performance and microbial diversity using starch/polylactic acid blends and ethanol as electron donor for nitrate removal.* Bioresource Technology, 2013. **131**: p. 33-39.

150. Wu, W., F. Yang, and L. Yang, *Biological denitrification with a novel biodegradable polymer as carbon source and biofilm carrier.* Bioresource technology, 2012. **118**: p. 136-140.

151. McCarthy, M.J. and W.S. Gardner, *An application of membrane inlet mass spectrometry to measure denitrification in a recirculating mariculture system.* Aquaculture, 2003. **218**(1): p. 341-355.

152. Rodriguez-Caballero, A., et al., *Treatment of high ethanol concentration wastewater by biological sand filters: enhanced COD removal and bacterial community dynamics.* Journal of environmental management, 2012. **109**: p. 54-60.

153. Huang, B., et al., *The effect of C/N ratio on nitrogen removal in a bioelectrochemical system.* Bioresource technology, 2013. **132**: p. 91-98.

154. Clauwaert, P., et al., *Open air biocathode enables effective electricity generation with microbial fuel cells.* Environmental Science & Technology, 2007. **41**(21): p. 7564-7569.

155. Zhang, F. and Z. He, *Integrated organic and nitrogen removal with electricity generation in a tubular dual-cathode microbial fuel cell.* Process Biochemistry, 2012. **47**(12): p. 2146-2151.

156. Yan, H., T. Saito, and J.M. Regan, *Nitrogen removal in a single-chamber microbial fuel cell with nitrifying biofilm enriched at the air cathode.* Water Research, 2012. **46**(7): p. 2215-24.

157. Yan, H. and J.M. Regan, *Enhanced nitrogen removal in single‐chamber microbial fuel cells with increased gas diffusion areas.* Biotechnology and Bioengineering, 2013. **110**(3): p. 785-791.

158. Zhang, Y. and I. Angelidaki, *A new method for in situ nitrate removal from groundwater using submerged microbial desalination-denitrification cell (SMDDC).* Water Res, 2013. **47**(5): p. 1827-36.

159. Tong, Y. and Z. He, *Current-driven nitrate migration out of groundwater by using a bioelectrochemical system.* RSC Advances, 2014. **4**(20): p. 10290.

160. Aklujkar, M., et al., *The genome sequence of Geobacter metallireducens: features of metabolism, physiology and regulation common and dissimilar to Geobacter sulfurreducens.* BMC Microbiol., 2009. **9**: p. 109.

161. Ishii, S., et al., *A novel metatranscriptomic approach to identify gene expression dynamics during extracellular electron transfer.* Nature communications, 2013. **4**: p. 1601.

162. Strycharz, S.M., et al., *Reductive dechlorination of 2-chlorophenol by Anaeromyxobacter dehalogenans with an electrode serving as the electron donor.* Environ Microbiol Rep, 2010. **2**(2): p. 289-94.

163. Sanford, R.A., J.R. Cole, and J.M. Tiedje, *Characterization and description of Anaeromyxobacter dehalogenans gen. nov., sp. nov., an aryl-halorespiring facultative anaerobic myxobacterium.* Applied and Environmental Microbiology, 2002. **68**(2): p. 893-900.

Chapter 3

Facultative Nitrate Reduction by Electrode-Respiring *Geobacter metallireducens* Biofilms as a Competitive Reaction to Electrode Reduction in a Bioelectrochemical System

Abstract

Alternative metabolic options of exoelectrogenic biofilms in bioelectrochemical systems (BESs) are important not only to explain the fundamental ecology and performance of these systems but also to develop reliable integrated nutrient removal strategies in BESs, which potentially involve substrates or intermediates that support/induce those alternative metabolisms. This research focused on dissimilatory nitrate reduction as an alternative metabolism to dissimilatory anode reduction. Using the exoelectrogenic nitrate reducer *Geobacter metallireducens*, the critical conditions controlling those alternative metabolisms were investigated in two-chamber, potentiostatically controlled BESs at various anode potentials and biofilm thicknesses and challenged over a range of nitrate concentrations. Results showed that anode-reducing biofilms facultatively reduced nitrate at all tested anode potentials (-150 to + 900 mV vs Standard Hydrogen Electrode) with a rapid metabolic shift. The critical nitrate concentration that triggered a significant decrease in BES performance was a function of anode biofilm thickness but not anode potential. This indicates that these alternative

metabolisms were controlled by the availability of nitrate, which is a function of nitrate concentration in bulk solution and its diffusion into an anode-reducing biofilm. Coulombic recovery decreased as a function of nitrate dose due to electron-acceptor substrate competition, and nitrate-induced suspended biomass growth decreased the effluent quality.

This chapter was adapted from the following publication:

Kashima, H., & Regan, J. M., Facultative nitrate reduction by electrode-respiring *Geobacter metallireducens* biofilms as a competitive reaction to electrode reduction in a bioelectrochemical system. *Environmental science & technology*, **2015**, 49 (5), 3195-3202.

3.1 Introduction

Electrode reduction by exoelectrogenic biofilms is central to anodic bioelectrical system (BES) performance [1]. These systems have potential applications in mixed-culture bioprocesses, such as wastewater treatment or bioremediation, that often harbor undesirable alternative microbial activities with the potential to compete with the desired bioelectrochemical process. For example, aerobic organic degradation supported by oxygen crossover at the air cathode decreases the coulombic efficiency of single-chamber microbial fuel cells (MFCs) [2-5], and methanogenic activity decreases hydrogen yields in microbial electrolysis cells (MECs) [6-8]. While these alternative metabolisms involve non-electrode respiring microbes residing in a system, some exoelectrogens have alternative metabolisms to electrode reduction, such as ferric, nitrate, or sulfate reduction. BESs offer a unique experimental platform for studying these alternative electron-acceptor metabolisms relative to electrode reduction to help us better understand dissimilatory

electrode reduction. In addition, this understanding would be useful for the development and operation of BESs in applications that include these alternative electron acceptors, such as integrated nutrient removal from wastewater [9] and groundwater treatment [10]. Several studies have reported the negative effects of these alternative electron acceptors on mixed-culture BES anode performance [11, 12], but fundamental research is needed to understand these alternative metabolisms specifically on the exoelectrogenic populations in the biofilms.

The effect of nitrate on electrode reduction is of particular interest because some exoelectrogens such as *Geobacter metallireducens* [13], *Shewanella oneidensis* [14], *Comamonas denitrificans* [15], *Geoalkalibacter subterraneus* [16, 17], and *Calditerrivibrio nitroreducens* [18] conduct this energetically favorable dissimilatory metabolism in anoxic natural and engineered systems, and it is a key factor for the development of nitrogen removal technologies in BESs from wastewater [19-23] and groundwater [10, 24]. Recent designs involving simultaneous nitrification and denitrification with single-chamber air-cathode MFCs [23, 25], denitrifying biocathode MFCs with an anion exchange membrane to avoid ammonia crossover [22], and BES-driven in-situ groundwater nitrate removal systems [10, 24] have brought us new anode systems under the influence of nitrate. Thus it is critical to understand the effects of nitrate on exoelectrogens to develop effective and reliable nitrogen-removal strategies in BESs. Sukkasem et al. examined the effects of nitrate on performance of mixed-culture single-chamber MFCs [12]. The study reported decreased coulombic recovery and maximum voltage output in the presence of nitrate under high current conditions, and attributed these negative effects to competition for electrons between anode reduction and denitrification

[12]. Also, other studies reported heterotrophic nitrate reduction activity in the anode compartments of nitrogen-removal BESs [22, 24]. Given the mixed-culture conditions in these studies, it is unknown whether such negative nitrate effects were just a minor coulombic loss by non-exoelectrogenic denitrifiers, or nitrate led to a striking deterioration in BES performance due to a metabolic shift of anode reducers to nitrate reduction.

To address the above questions, it is important to understand the critical conditions that control the facultative metabolisms of anode and nitrate reduction in dissimilatory nitrate-reducing exoelectrogens. As an analogous system, the facultative metabolic shift between aerobic respiration and nitrate respiration by facultative denitrifiers is controlled by dissolved oxygen (D.O.), with D.O. above a critical level inhibiting nitrate reductase activity [26] and also its gene expression [27]. This understanding of critical D.O. conditions has been used as a fundamental engineering parameter to design anoxic denitrification processes. Unlike the well-studied case of D.O. effects on the facultative metabolic shift between aerobic respiration and nitrate respiration, the conditions that determine anode versus nitrate reduction are unknown. With respect to the anode conditions, while its availability cannot be described in terms of concentration, it can be described with electrode potential according to the Nernst equation. An anode with a higher electrode potential is a thermodynamically better electron acceptor due to its larger possible metabolic energy gain determined by the redox couple of electron donor and electron acceptor (anode) [28].

This research is focused on understanding the dynamics of nitrate reduction and anode reduction for the exoelectrogenic nitrate-reducing bacterium *G. metallireducens* to determine the critical conditions controlling these possibly competitive metabolisms and

the effects on anode performance. *Geobacter* species are often the dominant taxon in various mixed-culture bioanode systems [29-32], and 16S rRNA gene clones closely related to *G. metallureducens* were found in different mixed-culture BESs [29, 33]. This bacterium is also known to reduce nitrate coupled with the oxidation of organics [13], ferrous [34], and graphite electrode [35] as an electron donor. We hypothesized that graphite anode-reducing *G. metallireducens* biofilms facultatively reduce nitrate and its negative effect on current production would be a function of nitrate concentration, anode potential, and biofilm thickness.

3.2 Materials and Methods

3.2.1 Microbial source and culture condition

G. metallireducens GS-15 (ATCC 53774) stored at – 80 ^{O}C was cultured in the dark at 30°C using sterile, anaerobic ATCC medium 1768 with modified concentrations of the following components: ferric citrate (40 mM), acetate (20 mM), and NaH_2PO_4 (1.67 mM). Stationary phase culture was transferred (10 % in volume) into the same medium and cultured again to obtain more robust growth. This second stationary phase culture was anaerobically centrifuged (3500 ×g, 20 min, 4^{O}C) and cell pellets were resuspended in the anaerobic medium described above but omitting ferric citrate and acetate. A 2-mL aliquot of these cell suspensions ($O.D._{600}$ = 0.23 - 0.28) was transferred into the working electrode chamber of each electrochemical cell as inoculum.

3.2.2 Electrochemical cell configuration and biofilm acclimatization on graphite anode

Dual chamber, H-type electrochemical cells (Glasstron Inc., Vineland, NJ) with Nafion 117 cation exchange membrane separating the working electrode chamber and the counter electrode chamber were used for the tests. Graphite plate blocks (Isomolded Graphite Plate, GM-10 grade, Graphitestore) cut into 1.0 cm × 3.0 cm × 0.3 cm were sanded with 400 and 1500 grit sandpaper, sonicated to remove graphite particles, and then polished with aluminum oxide as described elsewhere [36]. Graphite plates were then soaked in 1 M HCl overnight for three times to remove metal contaminants. Cleaned graphite plates were connected to titanium wire and used as working electrodes. The same graphite plate blocks cut into 1.0 cm × 6.0 cm × 0.3 cm and prepared in the same way were used as counter electrodes. Reference electrodes (Ag/AgCl, 3 M NaCl, +0.211 V vs Standard Hydrogen Electrode (SHE)) were inserted into the working electrode chambers. The electrode chambers (approximately 180 ml of working volume) were filled with 120 mL of growth media described above but without ferric citrate and vitamins solution in the working electrode and without acetate in the counter electrode. All electrochemical cells and media were sterilized and sparged with CO_2:N_2 (20 %: 80 %) gas to keep the system anaerobic prior to inoculation.

Working electrodes were poised at potentials of -150 mV, 0 mV, +400 mV, +650 mV, or +900 mV vs. SHE with a potentiostat (Uniscan model PG580, Buxton, United Kingdom) to acclimatize biofilms. The BESs were operated in batch mode in a 30 ^{O}C temperature-controlled chamber without stirring. Abiotic controls were run under the same conditions but without inoculation. An aluminum gas collection bag was connected to each

chamber through sterile 0.2-μm mesh filters to release any pressure imbalance between the two chambers during operation. To acclimatize anode biofilms of different thicknesses, acclimatization schemes included one acclimatization batch cycle with 0.5 mM acetate, one acclimatization cycle with 10 mM acetate, or two sequential acclimatization cycles with 10 mM acetate. Each acclimatization batch cycle was ended once current production decreased below 100 μA. Acclimatized biofilms were then tested in a subsequent nitrate spike batch cycle.

3.2.3 Nitrate spike tests

After biofilm acclimatization, media in the electrochemical cell chambers were replaced anaerobically with new media containing 10 mM acetate for the working electrode chamber and without acetate for the counter electrode chamber. The working electrode was poised at the same potential as the acclimatization cycle by a potentiostat (VMP3, Bio-Logic USA, TN), and working electrode chambers were stirred at ~180 rpm. After observing stable current (approximately 2.5 hours), a defined amount of nitrate was spiked every 30 minutes into the working electrode chamber to gradually increase the nitrate concentration. Current production was recorded by the potentiostat during the tests, and the working chamber medium was sampled at each spike. The nitrate concentration at which the current decreased without recovery within 30 minutes after a nitrate spike was defined as the critical nitrate concentration (i.e., significantly hampers current production) at that working electrode potential and biofilm thickness. In each experimental condition with a specific anode potential and biofilm thickness, duplicate anodes were tested with gradual nitrate spikes, as well as a control anode with gradual sodium chloride spikes of equivalent concentration, and duplicate anodes for biofilm protein concentration

measurement that were sacrificed at the time of the first nitrate spike. Gradual nitrate spikes were stopped after passing the critical nitrate concentration, and then the test batch cycle was continued until current production increased once again.

In addition to the gradual nitrate spike tests, biofilms acclimatized at 0 mV were subjected to a single nitrate spike to see the effects of nitrate at different levels. Two sets of biofilms were acclimatized, one with a single acclimatization cycle in 0.5 mM acetate medium to form thin biofilms, and the other with two sequential acclimatization cycles in 10 mM acetate medium to form thick biofilms.

3.2.4 Analytical methods

Nitrate, nitrite, and acetate concentrations in anode media were measured with ion chromatography (ICS-1100 with AS-25 anion separation column, Dionex, CA). Ammonia concentration in anode and cathode media was measured with the Salicylate method (Nitrogen-Ammonia Reagent Set, TNT, AmVer (Salicylate), Hach, CO). Cells in biofilms and suspension were solubilized by sodium hydroxide [37], and the resultant solubilized protein was measured by the modified Lowry method with DC Protein Assay Kit (Bio-Rad, CA). Bovine serum albumin fraction V was used to prepare protein standards.

3.3 Results and Discussion

3.3.1 Anode-reducing *G. metallireducens* biofilms preferentially reduced nitrate

G. metallireducens biofilms reducing graphite anodes poised over a potential range of -150 to +900 mV facultatively reduced nitrate as an alternative electron acceptor. For thin biofilms (acclimated with 0.5 mM acetate as electron donor), current production fluctuated in response to each incremental nitrate spike and then continuously decreased

once the nitrate concentration in the chamber exceeded a critical level. Thick biofilms (acclimatized with one or two consecutive cycles of 10 mM acetate) showed little perturbation in current with initial incremental nitrate additions until an abrupt drop in current once reaching a critical nitrate concentration. For example, thin biofilms acclimatized on graphite electrodes poised at 0 mV (0.09 mg-protein/cm^2) showed a critical nitrate concentration of approximately 1.5 mM (Figure 3-1). Nitrite accumulation in bulk solution was observed in most nitrate-spiked anode biofilms during significant current decrease, but nitrite did not accumulate for some thick biofilms even though the current showed an appreciable drop (Figure A-1). Nitrate was sequentially reduced to nitrite and ammonia via dissimilatory nitrate reduction to ammonia (DNRA) [26], which *G. metallireducens* has been shown to conduct in suspended culture coupled with acetate oxidation [13, 38]. Current production recovered once both the nitrate and nitrite concentrations in the chamber decreased. Current production did not recover even after the nitrate concentration dropped below the critical level, suggesting that nitrite formed with nitrate reduction was preferentially reduced over the anode and/or nitrite inhibited the anode reduction reaction. Stable anodic performance of sodium chloride-spiked biofilms showed that the impaired current production observed in nitrate-spiked biofilms was not due to multiple spikes and samplings that might introduce trace amounts of oxygen into an anode chamber and inhibit activity of *G. metallireducens*, an obligate anaerobe (Figure 3-1). In addition, the solution redox potential remained constant throughout the nitrate spikes (Figure A-2) and an abiotic nitrate-spike test showed no current, indicating that the nitrate effect was not indirect or abiotic. Furthermore, there were no measurable negative effects of nitrate on current production by *G. sulfurreducens*, an anode reducer that cannot use

nitrate as an electron acceptor (Figure A-3), providing further evidence that the negative nitrate effects on anode reduction by *G. metallireducens* were attributed to its role as a competitive electron acceptor to the anode.

3.3.2 The availability of nitrate controlled facultative anode and nitrate metabolisms

The critical nitrate concentration that triggered a significant current decrease in anode-reducing *G. metallireducens* biofilms was a function of the biofilm protein concentration (Figure 2). Assuming the biofilms had uniform protein concentrations throughout their thickness, the critical concentration increased with biofilm thickness, which correlates with the diffusion barrier that controls nitrate penetration into the biofilm matrix [39]. Consistent with the findings reported for *G. sulfurreducens* biofilms that peak current increased with biofilm thickness up to 40 μm, above which the peak current was generally lower [40], the maximum current produced by chloride-spiked control anode biofilms in this study were lower for thick biofilms (Figure A-1) than thin biofilms (Figure 3-1). This inverse relationship between peak current and protein concentration suggests the presence of mass transport limitations in the thicker biofilm systems. (There was no correlation between critical nitrate concentration and peak current.) Because the current measurements represent the composite biofilm activity, the contributions of each part of the anode biofilm (i.e., the outer layers near the bulk solution or inner layer immediately next to the anode surface) to current production are not known. Some studies showed that *G. sulfurreducens* anode biofilm had relatively low differences in transcript abundance throughout a biofilm [41] with similar activity [42], while other studies reported spatially heterogeneous metabolic activity throughout thick (> 100 μm) anode-reducing *G. sulfurreducens* biofilms [43, 44]. There is a discrepancy in the reported nature of this

heterogenous activity, with a suggestion of higher activity near the anode [43] versus higher activity at the outside of the biofilm due to acetate depletion within highly conductive biofilms [44]. However, it is possible in our experiments with surplus electron donor that nitrate reduction by cells in the outer layer of a thick anode biofilm did not appreciably decrease current production because these cells that were most distant from the anode surface may have had a slight contribution to the current. This inference is further supported by the current responses in an experiment in which mixing was briefly paused; current production resumed in nitrate-spiked systems, showing an increased nitrate diffusion barrier relative to the high acetate diffusion rate promoted by excess acetate concentrations (Figure A-4).

Anode potential had no significant impact on critical nitrate concentration (Figure 3-2). These facultative reactions were strictly determined by the availability of nitrate as the preferred electron acceptor and not the availability of the anode, similar to the facultative preference of oxygen over nitrate for facultative denitrifiers [26]. Different anode potentials resulted in different current production in the absence of nitrate (Figure A-5), especially the -150 mV anodes versus the 0 and +400 mV anodes, which is expected based on a thermodynamic perspective and previous reports. However, this variable anode availability did not result in different critical nitrate concentrations. This was even the case at the positive extreme of +900 mV, which is essentially the highest technically feasible electrode potential due to the emergence of significant abiotic anode reduction from anode corrosion or water splitting for graphite anodes at higher potentials (Figure A-6), and represents the most thermodynamically favorable anode as an electron acceptor.

The preferential use of nitrate over an anode cannot be explained by a simple thermodynamic perspective of available energy. Biofilms respiring anodes poised at +900 mV, which provide greater available energy than nitrate respiration (Figure A-7), still facultatively reduced nitrate with a critical nitrate concentration comparable to anodes with lower potentials. This is likely because the real biological energy gain of each biofilm was less than the available energy due to the inability of the respiratory machinery to capture all of the available energy. For example, *G. sulfurreducens* reportedly had higher biomass yield with the reduction of an anode poised at 0 mV vs SHE over an anode at -160 mV, but the biomass yield at +400 mV was not higher than 0 mV, illustrating that *G. sulfurreducens* obtained larger energy to support biomass growth from a more positive anode between -160 mV and 0 mV but they could not obtain additional energy from 0 to +400 mV [28]. In anode-reducing *G. sulfurreducens* cells, outer membrane cytochromes (OMCs) have been proposed as terminal electron donors (TEDs) that donate electrons to an anode and potentially constrain actual energy gain if the anode potential is higher than the TED working in the system. Electrochemical analyses such as cyclic voltammetry (CV) and differential pulse voltammetry have identified redox-active components in BES anodes [36, 45, 46] with similar potential ranges and midpoint potentials of purified OMCs such as OmcB (-190 mV) [47], OmcS (-360~-40 mV, -212 mV vs SHE) [48], and OmcZ (-420~-60 mV, -220 mV vs SHE) [49]. Although the electron transfer components of *G. metallireducens* for electrode reduction have not yet been fully determined, no visible oxidation peak that was unique to biofilms acclimatized at high anode potential, +650 and 900 mV, was found in CVs (data not shown), suggesting *G. metallireducens* cannot capture thermodynamic energy from such high anode potentials.

In fact, the anodes with high potentials of +650 mV or +900 mV seemed to be less favorable electron acceptors for *G. metallireducens* cells. It was difficult to acclimatize stable biofilms at 900 mV and it required a medium with higher acetate dose (1.7 mM) than the lower anode potentials, which showed stable current and biomass production with 0.5 mM acetate. Also, the +650 mV and +900 mV anodes showed lower peak current relative to 0 mV and +400 mV in the second batch (Figure A-5), perhaps indicating decreased biological activity due to oxidative stress with these high anode potentials that may cause unfavorable effects such as degradation of electron-transfer proteins at the electrode surface [50]. Another study reported a similar decrease in anode reduction rate with *G. sulfurreducens*-dominated mixed culture biofilms grown at 0.81 V vs SHE relative to anodes with lower potentials (-0.09, 0.21, and 0.51 V vs SHE) in single-chamber MECs [32].

It is also possible that *G. metallireducens* preferentially used nitrate as electron acceptor based on criteria other than actual energy gain, as *G. sulfurreducens* preferentially reduces Fe(III) over fumarate even though it provides significantly less energy to support cell growth [51]. For example, perhaps soluble electron acceptors are preferentially used over insoluble electrodes. Further research is needed to understand the mechanisms that govern these facultative metabolisms.

3.3.3 Nitrate above critical level resulted in significant BES performance decrease

To further investigate abrupt nitrate influences on anode-reducing biofilms, a set of thick anode-reducing biofilms was subjected to nitrate spikes at different levels, higher and lower than the estimated critical nitrate level. The critical nitrate concentration for these biofilms was estimated to be 3.87 mM based on the protein concentrations of two sacrificed

biofilms (0.49 ± 0.03 mg-protein/cm^2) and the linear regression of critical nitrate concentrations (Figure 3-2). With this estimate, four different levels of nitrate were spiked into duplicate anodes: 1.5 mM (low), 4.0 mM (critical), 10.0 mM (high), and 0 mM control with a 1.5 mM sodium chloride spike. Current production showed that bulk nitrate concentrations above the critical level resulted in a significant decrease of current down to the abiotic control level (Figure A-6), whereas anode biofilms subjected to nitrate below the critical level did not show significant current decrease (Figure 3-3). Another set of anodes acclimatized with thin biofilms (0.08 mg-protein/cm^2) at 0 mV and subjected to low or high levels of nitrate showed similar results (Figure A-8). As seen in the gradual nitrate spike tests, nitrate was facultatively reduced to ammonia and the anode biofilms returned to anode reduction once nitrate and nitrite were used up except under high nitrate concentration (10 mM), which resulted in substantial intermediate nitrite accumulation in the system. These high nitrite concentrations seemed to result in inhibition of anode biofilm cells by accumulated nitrite, or free nitrous acid (FNA) that may have accumulated at the base of the biofilms near the electrode-biofilm interface, at which the pH would be expected to be lower than bulk solution [52] (Figure 3).

Time-series electron distribution profiles also show preferential nitrate reduction over anode reduction by biofilms (Figure 3-4). In the presence of nitrate below the critical level, anodes and nitrate were simultaneously reduced in concert with acetate oxidation, while sequential nitrate reduction followed by anode reduction was observed in biofilms subjected to nitrate over the critical level. Greater acetate oxidation and a slight increase of circuit charge recovery was observed in 1.5 mM nitrate-spiked anodes relative to the no-nitrate control anodes over the course of a batch (Figure 3-4). This is possibly due to the

DNRA reaction (Equation 1) mitigating acidification associated with anode reduction [53] (Equation 2), since the final averaged pHs in bulk anode media were 5.63 in the 1.5 mM nitrate anodes and 5.30 in the no nitrate anodes.

$$CH_3COO^- + NO_3^- + 2H^+ = NH_4^+ + CO_2 + HCO_3^- \quad \text{(Eq. 1)}$$

$$CH_3COO^- + 3H_2O = CO_2 + HCO_3^- + 8e^- + 8H^+ \quad \text{(Eq. 2)}$$

Intermediate nitrite was detected only in anodes spiked with nitrate higher than the critical level (Figure 3-3) (Figure A-8). This is possibly because *G. metallireducens* cells preferentially conducted nitrate reduction to nitrite over nitrite reduction to ammonia. DNRA is a sequential two-step reduction of nitrate to ammonia with nitrite as intermediate, and it is thought that energy generation is mostly from the first step, whereas the second step is used to dump excess electrons and degrade toxic nitrite [26].

Previous mixed-culture studies demonstrated decreased BES kinetics performance and cell voltage due to nitrate addition to the anode, and attributed such performance decreases to electron donor competition between strict anode reducers, facultative anode reducers, and non-anode reducing nitrate reducers [9, 12]. By using pure-culture anode-reducing biofilms to exclude the activities of non-anode reducing nitrate reducers, at least in the thin-biofilm systems that would not have had inactive cells at the outer biofilm surface, this study showed that significant BES performance impairment can be caused by a metabolic shift of exoelectrogens from anode reduction to nitrate reduction. The BES performance decrease due to the presence of nitrate concentrations higher than a critical level can occur in mixed-culture BES anodes composed of exoelectrogenic nitrate reducers such as *G. metallireducens* and *C. denitrificans*, and it is important to keep the nitrate level

below this biofilm thickness-dependent critical level to secure stable BES performance. While the findings of this study cannot be directly compared to previous mixed-culture reports due to significant differences in systems and conditions, we expect that the critical nitrate levels for mixed-culture anode biofilms would be higher than those reported here for two reasons: non-exoelectrogenic nitrate reducers could contribute to lowering the nitrate concentration in the biofilm, and the anode-reducing activity of non-nitrate reducing exoelectrogens would not decrease due to nitrate as long as there is surplus electron donor. The anode-reducing activity of non-nitrate reducing exoelectrogens can also be decreased due to inhibition by nitrite/FNA that might be formed by nitrate reduction, and critical nitrite concentration rather than critical nitrate concentration would be a better measure to describe nitrite/FNA inhibition on non-nitrate reducing exoelectrogens.

3.3.4 Decreased anode reduction with metabolic shift from anode to nitrate and nitrite/FNA inhibition

The observed bulk shift from current production to nitrate reduction may be a composite of several different nitrate-induced effects such as a metabolic shift of anode-reducing cells to nitrate/nitrite reduction, nitrite/FNA inhibition of cell metabolisms, and a contribution from previously inactive cells to nitrate reduction. The extent of contribution from these different alternatives depended on the biofilm thickness and the nitrate concentration. For thin biofilms (protein concentration ca. 0.08-0.09 mg/cm^2), which were estimated to be only a few cell layers thick based on an areal protein density of 0.02-0.03 mg/cm^2 for monolayers of *G. sulfurreducens* [54], the biofilm was presumed to be composed almost entirely of active anode-reducing cells without stratification of activities or biochemical conditions across the biofilm cross section. Therefore, the shift from current

production to nitrate reduction in these thin-biofilm systems was due to a change in metabolism from anode to nitrate reduction.

The interpretation of the systems with thick biofilms is more complicated due to the possibility of stratification in activity and conditions. As mentioned above, the thick biofilms had lower peak currents than the thin biofilms, suggesting there were mass transport constraints through the thick biofilms. Prior to nitrate addition, these biofilms may have had cells in the outer layers that were inactive due to electron acceptor limitation. The sudden current drop coupled with nitrate reduction by thick biofilms may have involved nitrate reduction at the outer surface by these previously inactive cells that had not been contributing to current production. This would not be expected in the thin biofilms, in which there would not be an accumulation of inactive cells. A second possible contributing factor in thick-biofilm systems was inhibition by nitrite and/or FNA. Biofilms subjected to nitrate concentrations significantly higher than the critical concentration resulted in a high level of nitrite accumulation, and did not resume anode reduction or reduce the accumulated nitrite even in the presence of excess electron donor (ca. 2.60 mM of acetate). Nitrite inhibition may have contributed to the response of these systems. Moreover, in these thick-biofilm cases where pH gradients would be expected to establish [55], FNA inhibition may also explain the decreased current since the pH at the anode-biofilm interface might be low enough to form FNA at a level sufficient to inhibit cell metabolism [56]. During the current drop coinciding with nitrate addition, active anode-reducing cells around the low-pH anode-biofilm interface could be selectively inhibited by FNA, while the outer part of the biofilm with neutral pH could conduct nitrate reduction without FNA inhibition. However, this FNA inhibition was unlikely in thin biofilms, which

would lack a significant pH gradient. Thin biofilms may have been inhibited by accumulated nitrite, but since nitrate reduction was always observed, if nitrite inhibition occurred it was only partial inhibition of microbial activity. Additional discussion about decreased anode reduction rate in response to nitrate addition was summarized in Appendix A-9.

3.3.5 Concurrent reduction of anode and nitrate and quick metabolic shift from anode to nitrate

The concurrent reduction of both the anode and nitrate was observed in several tests. Anode biofilms exposed to nitrate concentrations less than the critical level reduced nitrate while also producing current (Figure 3-3). Electron distribution analysis showed that almost 50 % of the electrons extracted from acetate oxidation were used for nitrate reduction while the remaining 50 % was used for anode reduction in the initial 5 hours after the nitrate spike, and concurrent electron flow to these two metabolisms was observed until the nitrate in the system was used up (Figure 3-4). This concurrent reduction of two electron acceptors may have been due to a functionally stratified biofilm. The outer parts of the biofilm would be exposed to higher nitrate concentrations and might have switched to nitrate reduction, while the inner biofilm may have continued anode reduction because of lower nitrate concentrations in the interior of the biofilm.

The facultative metabolic shift between anode reduction and nitrate reduction as bulk biofilm level occurred within a short time, on the order of minutes to an hour. For thin biofilms, the anode reduction rate decreased immediately (less than in a minute) in response to nitrate spikes, and reduction of nitrate started less than an hour after the spike (Figure 3-3). This bulk metabolic shift was very rapid, and distinct from previously

reported results for this bacterium under different conditions. Specifically, Finneran et al. (2002) reported that soluble Fe (III) citrate grown *G. metallireducens* suspended cells did not reduce nitrate, and nitrate grown cells continued to reduce nitrate following Fe(III) citrate addition [34]. The metabolic shift from anode reduction to nitrate reduction as bulk biofilm reaction within a short amount of time may be due to the insoluble anode-reducing growth condition or due to heterogeneous metabolic status such as stratified biofilm composed of active anode-reducing cells and inactive cells which had potential to quickly initiate nitrate reduction. Further study is needed to address this question.

3.3.6 Nitrate in the anode chamber lowered coulombic recovery and increased suspended biomass growth

An electron balance analysis showed that electron recovery to the circuit decreased with increased nitrate concentration in the system (Figure 3-5). Almost all of the nitrate spiked in the anode chamber was reduced, resulting in fewer available electrons for anode reduction. The addition of nitrate induced suspended biomass growth (Figure 3-5), as previously reported in mixed-culture MFCs [12]. Cells with an anode as the sole electron acceptor cannot respire independently from the anode, and thus suspended biomass production in an anode chamber without nitrate was due solely to biofilm detachment. However, once nitrate was introduced into the anode chamber, detached cells can grow independently from the anode by using nitrate as the electron acceptor. Detached cells and cells growing in suspension can reduce nitrate and result in lower coulombic recovery, though they do not decrease the anode reduction rate under non-electron donor limited conditions. However, once the biofilm cells actively reducing the anode shift their metabolism to nitrate reduction, there was a significant performance drop due to decreased

anode reduction rate. From a wastewater treatment perspective, suspended growth induced by nitrate would yield high suspended solids in the effluent, and additional processes such as clarification or coagulation might be required to remove suspended solids from the treated water body.

3.4. Acknowledgement

This study was supported by U.S. Army Research Office (W911NF-11-1-0531) and graduate fellowship program from Japan Student Services Organization (L10126050001).

3.5. Supporting Information

Supporting Information for this chapter is found in Appendix A.

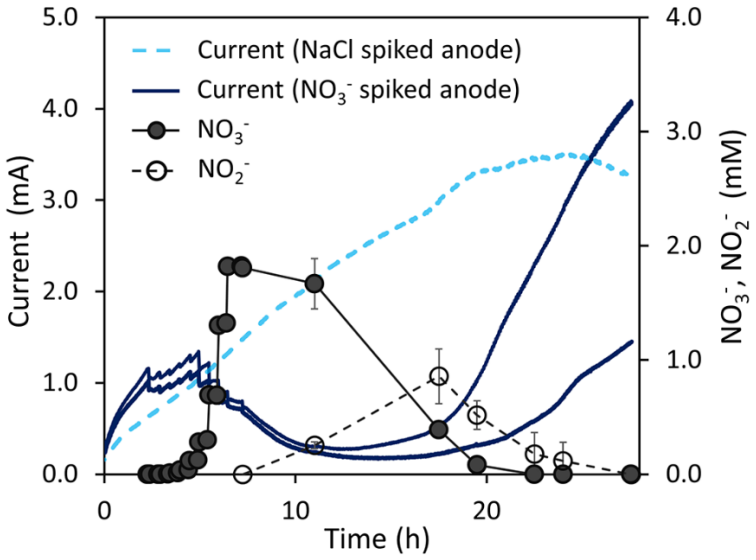

Figure 3-1: Current, nitrate, and nitrite profiles in a gradual nitrate spike test of *G. metallireducens* biofilms acclimatized on anodes poised at 0 mV with 0.5 mM acetate. Nitrate and nitrite data points are means of duplicate. Error bars designate one standard deviation.

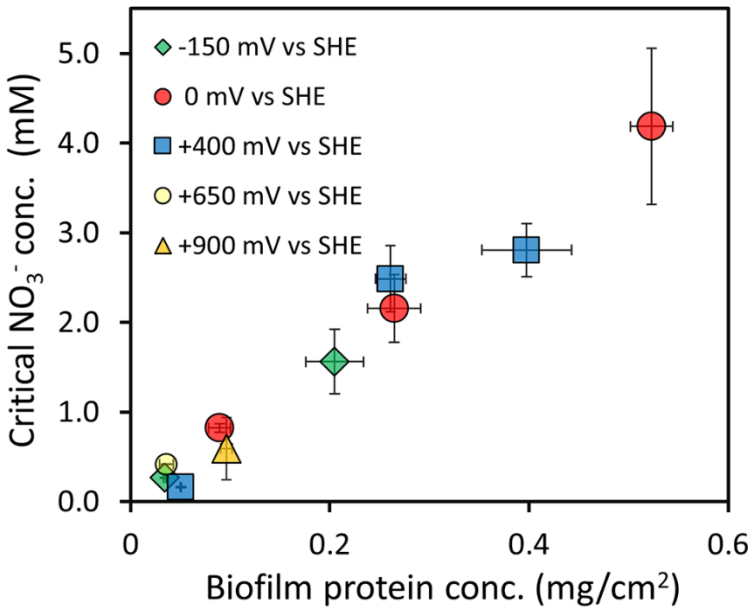

Figure 3-2: Critical nitrate concentrations of anode biofilms with different biofilm protein concentrations at different anode potentials. For each data point, biofilm protein concentration was obtained from two anodes sacrificed for protein analysis at the first nitrate spike (mean, ±S.D.), and critical nitrate concentration was obtained by two anodes (mean, ±S.D.) in a gradual nitrate spike test. Linear regression equation of all averaged data points was as follows: Critical NO_3^- concentration (mM) = 7.901 × biofilm protein concentration (mg/cm^2) - 0.002 (R^2 = 0.974)

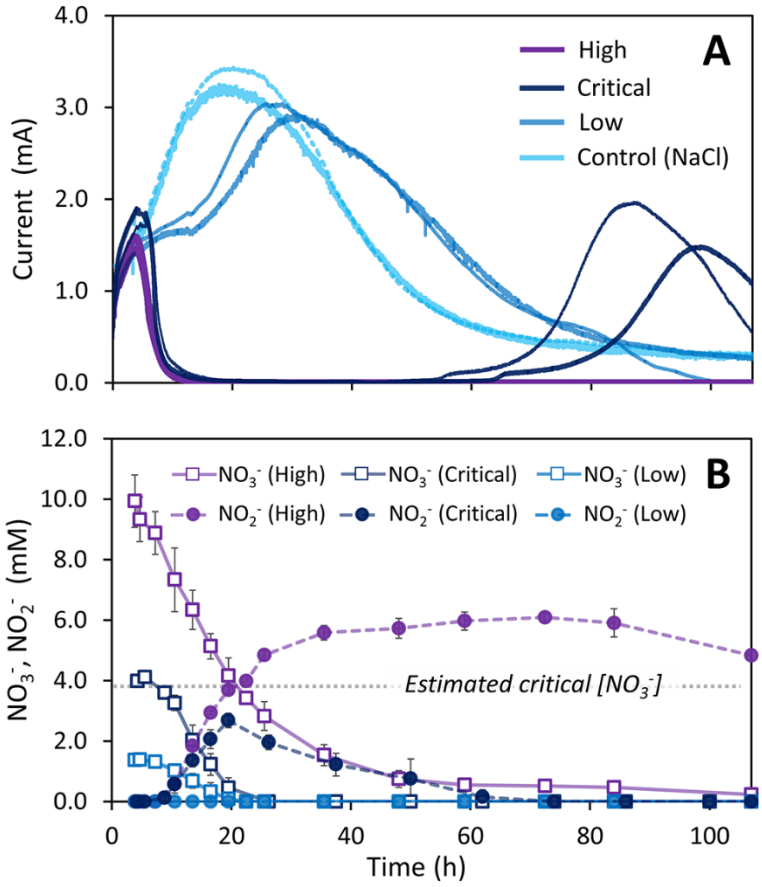

Figure 3-3: Current, nitrate and nitrite profiles of anode reducing biofilms in response to exposure to various levels of nitrate. Biofilms acclimatized on anodes poised at 0 mV (protein concentration: 0.49 (mg-protein/cm^2), estimated critical nitrate concentration: 3.87 mM) were subjected to various levels of nitrate: High condition (10 mM, more than two times higher than the critical level), Critical condition (target 4 mM, approximately the same as the critical level), Low condition (1.5 mM), and No nitrate control (target 1.5 mM sodium chloride). Each condition was tested in duplicate.

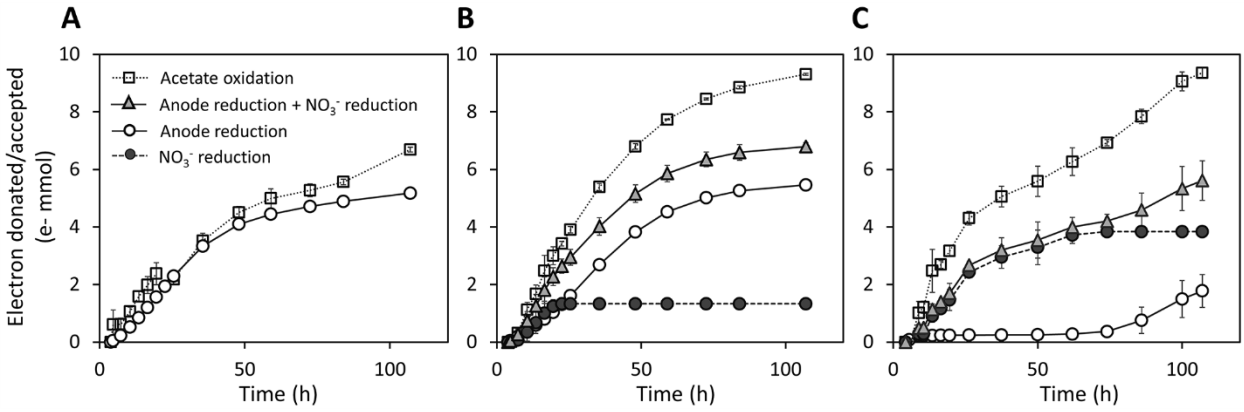

Figure 3-4: Time-series electron distribution profile of an anode biofilms under the presence of various levels of nitrate. Panel A, B, and C shows time-series electron distribution profiles of duplicate anodes of Control, Low, and Critical nitrate conditions shown in Figure 3-3. Error bars designate one standard deviation. Electrons donated by acetate oxidation, electrons used for anode reduction and electrons used for nitrate reduction were calculated based on decrease of acetate, decrease of nitrate and presence of nitrite, and circuit recovered charge. Electrons consumed by nitrate reduction was calculated by assuming dissimilatory nitrate reduction to ammonia as the electron sink for the loss of nitrate as well as nitrate reduction to nitrite for the accumulated nitrite.

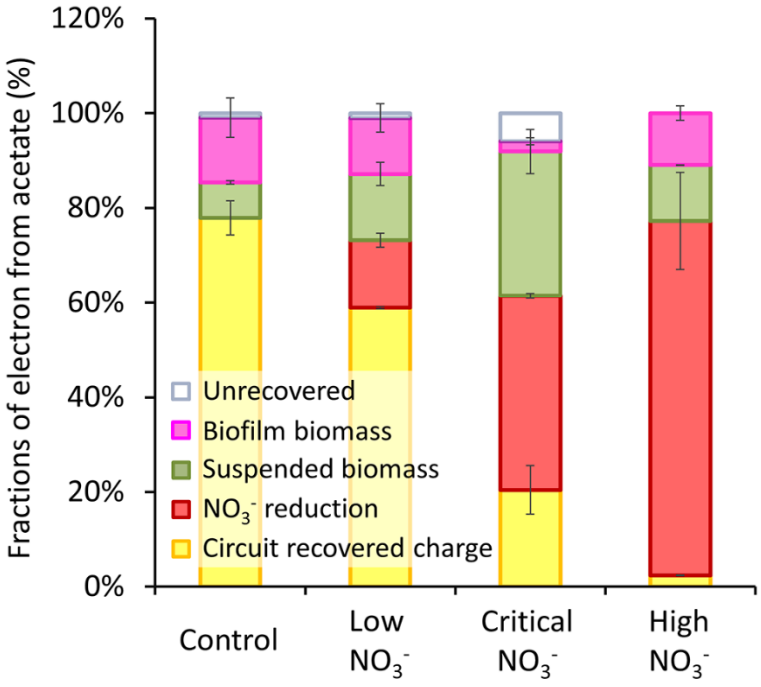

Figure 3-5: Electron balance of anode chambers in the presence of nitrate in different levels. This figure describes anodes with 4 different levels of nitrate described in Figure 3-3. Each data point shows mean of duplicate and bars designate one standard deviation. Electrons consumed by nitrate reduction was calculated by assuming dissimilatory nitrate reduction to ammonia as the electron sink for the loss of nitrate as well as nitrate reduction to nitrite for the accumulated nitrite. Electrons used for biomass synthesis was calculated from protein concentration data by assuming proteins account for 50 % in mass of the biomass composed of $C_5H_7O_2N$.

3.6 Literature Cited

1. Logan, B.E. and K. Rabaey, *Conversion of wastes into bioelectricity and chemicals by using microbial electrochemical technologies.* Science, 2012. **337**(6095): p. 686-690.
2. Cheng, S., H. Liu, and B.E. Logan, *Increased performance of single-chamber microbial fuel cells using an improved cathode structure.* Electrochemistry Communications, 2006. **8**(3): p. 489-494.
3. Watson, V.J., et al., *Polymer coatings as separator layers for microbial fuel cell cathodes.* Journal of Power Sources, 2011. **196**(6): p. 3009-3014.
4. Ahn, Y. and B.E. Logan, *A multi-electrode continuous flow microbial fuel cell with separator electrode assembly design.* Appl Microbiol Biotechnol, 2012. **93**(5): p. 2241-8.
5. Ren, L., et al., *High current densities enable exoelectrogens to outcompete aerobic heterotrophs for substrate.* Biotechnol Bioeng, 2014. **111**(11): p. 2163-9.
6. Clauwaert, P. and W. Verstraete, *Methanogenesis in membraneless microbial electrolysis cells.* Appl Microbiol Biotechnol, 2009. **82**(5): p. 829-36.
7. Lee, H.-S., et al., *Fate of H2 in an upflow single-chamber microbial electrolysis cell using a metal-catalyst-free cathode.* Environ. Sci. Technol., 2009. **43**(20): p. 7971-7976.
8. Cusick, R.D., et al., *Performance of a pilot-scale continuous flow microbial electrolysis cell fed winery wastewater.* Applied microbiology and biotechnology, 2011. **89**(6): p. 2053-63.

9. Kelly, P.T. and Z. He, *Nutrients removal and recovery in bioelectrochemical systems: a review*. Bioresource Technology, 2014. **153**: p. 351-60.

10. Zhang, Y. and I. Angelidaki, *A new method for in situ nitrate removal from groundwater using submerged microbial desalination-denitrification cell (SMDDC).* Water Res, 2013. **47**(5): p. 1827-36.

11. Kim, B., et al., *Enrichment of microbial community generating electricity using a fuel-cell-type electrochemical cell.* Applied microbiology and biotechnology, 2004. **63**(6): p. 672-681.

12. Sukkasem, C., et al., *Effect of nitrate on the performance of single chamber air cathode microbial fuel cells.* Water Research, 2008. **42**(19): p. 4743-4750.

13. Lovley, D.R., et al., *Geobacter metallireducens gen. nov. sp. nov., a microorganism capable of coupling the complete oxidation of organic compounds to the reduction of iron and other metals.* Archives of microbiology, 1993. **159**(4): p. 336-344.

14. Cruz-Garcia, C., et al., *Respiratory nitrate ammonification by Shewanella oneidensis MR-1*. Journal of Bacteriology, 2007. **189**(2): p. 656-62.

15. Xing, D., et al., *Isolation of the exoelectrogenic denitrifying bacterium Comamonas denitrificans based on dilution to extinction.* Applied microbiology and biotechnology, 2010. **85**(5): p. 1575-87.

16. Greene, A.C., B.K. Patel, and S. Yacob, *Geoalkalibacter subterraneus sp. nov., an anaerobic Fe(III)- and Mn(IV)-reducing bacterium from a petroleum reservoir, and emended descriptions of the family Desulfuromonadaceae and the genus Geoalkalibacter.* Int. J. Syst. Evol. Microbiol., 2009. **59**(Pt 4): p. 781-5.

17. Badalamenti, J.P., R. Krajmalnik-Brown, and C.I. Torres, *Generation of high current densities by pure cultures of anode-respiring Geoalkalibacter spp. under alkaline and saline conditions in microbial electrochemical cells.* MBio, 2013. **4**(3): p. e00144-13.

18. Fu, Q., et al., *A thermophilic gram-negative nitrate-reducing bacterium, Calditerrivibrio nitroreducens, exhibiting electricity generation capability.* Environ. Sci. Technol., 2013. **47**(21): p. 12583-90.

19. Clauwaert, P., et al., *Biological denitrification in microbial fuel cells.* Environ. Sci. Technol., 2007. **41**(9): p. 3354-3360.

20. Virdis, B., et al., *Microbial fuel cells for simultaneous carbon and nitrogen removal.* Water Research, 2008. **42**(12): p. 3013-3024.

21. Virdis, B., et al., *Simultaneous nitrification, denitrification and carbon removal in microbial fuel cells.* Water Research, 2010. **44**(9): p. 2970-80.

22. Zhang, F. and Z. He, *Integrated organic and nitrogen removal with electricity generation in a tubular dual-cathode microbial fuel cell.* Process Biochemistry, 2012. **47**(12): p. 2146-2151.

23. Yan, H., T. Saito, and J.M. Regan, *Nitrogen removal in a single-chamber microbial fuel cell with nitrifying biofilm enriched at the air cathode.* Water Research, 2012. **46**(7): p. 2215-24.

24. Tong, Y. and Z. He, *Current-driven nitrate migration out of groundwater by using a bioelectrochemical system.* RSC Advances, 2014. **4**(20): p. 10290.

25. Yan, H. and J.M. Regan, *Enhanced nitrogen removal in single‐chamber microbial fuel cells with increased gas diffusion areas.* Biotechnology and Bioengineering, 2013. **110**(3): p. 785-791.

26. Tiedje, J.M., *Ecology of denitrification and dissimilatory nitrate reduction to ammonium.* Biology of anaerobic microorganisms, 1988. **717**: p. 179-244.

27. Körner, H. and W.G. Zumft, *Expression of denitrification enzymes in response to the dissolved oxygen level and respiratory substrate in continuous culture of Pseudomonas stutzeri.* Appl. Environ. Microbiol., 1989. **55**(7): p. 1670-1676.

28. Wei, J., et al., *A new insight into potential regulation on growth and power generation of Geobacter sulfurreducens in microbial fuel cells based on energy viewpoint.* Environ. Sci. Technol., 2010. **44**(8): p. 3187-3191.

29. Kiely, P.D., et al., *Anode microbial communities produced by changing from microbial fuel cell to microbial electrolysis cell operation using two different wastewaters.* Bioresour Technol, 2011. **102**(1): p. 388-94.

30. Yates, M.D., et al., *Convergent development of anodic bacterial communities in microbial fuel cells.* ISME J, 2012. **6**(11): p. 2002-13.

31. Vargas, I.T., I.U. Albert, and J.M. Regan, *Spatial distribution of bacterial communities on volumetric and planar anodes in single‐chamber air‐cathode microbial fuel cells.* Biotechnology and Bioengineering, 2013. **110**(11): p. 3059-3062.

32. Zhu, X., et al., *Microbial community composition is unaffected by anode potential.* Environ. Sci. Technol., 2014. **48**(2): p. 1352-8.

33. Inoue, K., et al., *Electricity generation from cattle manure slurry by cassette-electrode microbial fuel cells.* J. Biosci. Bioeng., 2013.

34. Finneran, K.T., M.E. Housewright, and D.R. Lovley, *Multiple influences of nitrate on uranium solubility during bioremediation of uranium ‐ contaminated subsurface sediments.* Environmental Microbiology, 2002. **4**(9): p. 510-516.

35. Gregory, K.B., D.R. Bond, and D.R. Lovley, *Biocathode Geobacter nitrate reduction. Graphite electrodes as electron donors for anaerobic respiration.* Environmental Microbiology, 2004. **6**(6): p. 596-604.

36. Marsili, E., et al., *Microbial biofilm voltammetry: direct electrochemical characterization of catalytic electrode-attached biofilms.* Appl. Environ. Microbiol., 2008. **74**(23): p. 7329-37.

37. Bond, D.R. and D.R. Lovley, *Electricity Production by Geobacter sulfurreducens Attached to Electrodes.* Applied and Environmental Microbiology, 2003. **69**(3): p. 1548-1555.

38. Aklujkar, M., et al., *The genome sequence of Geobacter metallireducens: features of metabolism, physiology and regulation common and dissimilar to Geobacter sulfurreducens.* BMC Microbiol., 2009. **9**: p. 109.

39. Picioreanu, C., et al., *A computational model for biofilm-based microbial fuel cells.* Water Research, 2007. **41**(13): p. 2921-40.

40. Robuschi, L., et al., *Spectroscopic slicing to reveal internal redox gradients in electricity-producing biofilms.* Angew Chem Int Ed Engl, 2013. **52**(3): p. 925-8.

41. Franks, A.E., et al., *Microtoming coupled to microarray analysis to evaluate the spatial metabolic status of Geobacter sulfurreducens biofilms.* ISME J, 2010. **4**(4): p. 509-19.

42. Franks, A.E., *Transcriptional analysis in microbial fuel cells: common pitfalls in global gene expression studies of microbial biofilms.* FEMS microbiology letters, 2010. **307**(2): p. 111-2.

43. Schrott, G.D., et al., *Physiological Stratification in Electricity‐Producing Biofilms of Geobacter sulfurreducens.* ChemSusChem, 2013. **7**(2): p. 598-603.

44. Renslow, R., et al., *Metabolic Spatial Variability in Electrode-Respiring Biofilms.* Energy. Environ. Sci., 2013. **6**(6): p. 1827-1836.

45. Katuri, K.P., et al., *Geobacter sulfurreducens biofilms developed under different growth conditions on glassy carbon electrodes: insights using cyclic voltammetry.* Chemical communications, 2010. **46**(26): p. 4758-4760.

46. Liu, Y., et al., *Linking spectral and electrochemical analysis to monitor c-type cytochrome redox status in living Geobacter sulfurreducens biofilms.* ChemPhysChem, 2011. **12**(12): p. 2235-41.

47. Magnuson, T., et al., *Isolation, characterization and gene sequence analysis of a membrane-associated 89 kDa Fe (III) reducing cytochrome c from Geobacter sulfurreducens.* Biochem. J, 2001. **359**: p. 147-152.

48. Qian, X., et al., *Biochemical characterization of purified OmcS, a c-type cytochrome required for insoluble Fe(III) reduction in Geobacter sulfurreducens.* Biochimica et biophysica acta, 2011. **1807**(4): p. 404-12.

49. Inoue, K., et al., *Purification and characterization of OmcZ, an outer-surface, octaheme c-type cytochrome essential for optimal current production by Geobacter sulfurreducens.* Appl. Environ. Microbiol., 2010. **76**(12): p. 3999-4007.

50. TerAvest , M.A. and L.T. Angenent, *Oxidizing Electrode Potentials Decrease Current Production and Coulombic Efficiency through Cytochrome cInactivation inShewanella oneidensis MR-1.* ChemElectroChem, 2014. **1**(11): p. 2000-2006.

51. Esteve-Nunez, A., C. Nunez, and D.R. Lovley, *Preferential Reduction of Fe(III) over Fumarate by Geobacter sulfurreducens.* Journal of Bacteriology, 2004. **186**(9): p. 2897-2899.

52. Vadivelu, V.M., J. Keller, and Z. Yuan, *Effect of free ammonia and free nitrous acid concentration on the anabolic and catabolic processes of an enriched Nitrosomonas culture.* Biotechnol Bioeng, 2006. **95**(5): p. 830-9.

53. Torres, C.I., A. Kato Marcus, and B.E. Rittmann, *Proton transport inside the biofilm limits electrical current generation by anode‐respiring bacteria.* Biotechnology and bioengineering, 2008. **100**(5): p. 872-881.

54. Marsili, E., J. Sun, and D.R. Bond, *Voltammetry and Growth Physiology of Geobacter sulfurreducens Biofilms as a Function of Growth Stage and Imposed Electrode Potential.* Electroanalysis, 2010. **22**(7-8): p. 865-874.

55. Franks, A.E., et al., *Novel strategy for three-dimensional real-time imaging of microbial fuel cell communities: monitoring the inhibitory effects of proton accumulation within the anode biofilm.* Energy Environ. Sci., 2008. **2**(1): p. 113-119.

56. Vadivelu, V.M., J. Keller, and Z. Yuan, *Effect of free ammonia and free nitrous acid concentration on the anabolic and catabolic processes of an enriched Nitrosomonas culture.* Biotechnology and bioengineering, 2006. **95**(5): p. 830-839.

Chapter 4

Alternative shift between electrode reduction and oxidation in *Geobacter metallireducens* biofilms controlledby electrode potential and co-substrate availability

Abstract

The characterization of metabolic shifts among different electrode-mediated reactions, such as anode reduction and cathode oxidation, is important to understand extracellular electron transfers in natural settings and also to develop stable bioelectrochemical systems (BESs). This chapter presents the investigation of a metabolic shift in anodically-grown *Geobacter metallireducens* biofilms from anode reduction into cathode oxidation. In tests with potentiostatically controlled graphite electrodes, *G. metallireducens* biofilms demonstrated a quick and alternative shift between anode reduction and cathode oxidation as a function of electrode potential and availability of nitrate and acetate. Cathodic electrode oxidation was coupled with nitrate reduction by metabolically active biofilms, with a large cathodic current density of ~ 3.68 A/m^2. The metabolic shift from anode reduction to nitrate reduction took place quicker than the shift from ferric reduction to nitrate reduction. The presence of nitrate-reducing enzyme activity in the anode-reducing biofilm cells in the absence of nitrate was thought to enable such a

rapid metabolic shift to start nitrate reduction. Cyclic voltammetry and the analysis of its first derivative provided insights into electron transfer mechanisms of these biofilms.

4.1. Introduction

The characterization of electrode-mediated microbial reactions has important implications for our understanding of extracellular electron transfers in natural settings, as an analogous metabolism to mineral respiration in subsurface environments, and the development of stable bioelectrochemical systems (BESs) for a variety of potential applications [1]. Electrode-mediated microbial metabolisms are based on extracellular electron transfer between a cell and the solid electrode surface. Mechanistic understandings of these metabolisms have been provided by studies on several model organisms such as *Geobacter sulfurreducens* [2] and *Shewanella oneidensis* [3]. Molecular mechanisms of electrode reduction by these dissimilatory metal-reducing bacteria were investigated relative to knowledge of their insoluble iron oxide reduction mechanisms. For example, outer membrane cytochromes such as OmcS [4] and OmcZ [5] were shown to play important roles in electrode reduction by *G. sulfurreducens*, as well as type IV pili such as pilA, which is essential for optimal current production and development of thick electroactive biofilms [6-8]. In addition, information about locations and roles of these redox-active outer-surface proteins and conductive pili throughout their conductive biofilm matrix [9] [10] have been providing insights into electron transfer to an electrode at the whole biofilm scale [11] [12]. Concerning electrode reduction by *S. oneidensis*, it has been shown that *S. oneidensis* MR-1 uses the Mtr pathway [13] composed of a series of c-type cytochromes located in the cytoplasmic membrane, periplasmic space, and outer

membrane. This involves transferring electrons from the quinone pool in the cytoplasmic membrane to MtrC, located at the outer surface of the outer membrane, to release electrons to extracellular electron acceptors such as insoluble iron and an electrode.

Electrode-mediated respirations couple various redox half-reactions with electrode reduction or oxidation. For example, *Geobacter* spp., which are often dominant taxa in BESs [14-16] and subsurface environments [17, 18], can oxidize organic and inorganic electron donors such as acetate [19], hydrogen [2], lactate [20], ethanol, and aromatic compounds [21] coupled with reduction of an electrode or insoluble iron. Also, *Geobacter* spp. reduce nitrate [22], fumarate [22, 23], and tetrachloroethene [23] with an electrode as the sole electron donor. In addition, studies have reported a wide variety of reactions coupled with electrode reduction and oxidation by various types of microorganisms. Examples include cathode-supported methanogenesis [24-26], acetogenesis [27, 28], uranium (VI) reduction to uranium (IV) [29], oxygen reduction [30], denitrification [31], dechlorination [32], and perchlorate reduction [33]; as well as anode-supported oxidation of organic compounds [1].

In the characterization of this broad array of known electrode-mediated metabolisms, considerably less research has addressed questions about how electrode-associated biofilms select or shift their metabolisms among their options, particularly at a fundamental level with pure cultures. Metabolic shifts among different electrode-mediated reactions, such as electrode reduction and oxidation, are of particular relevance to the development and operation of stable BES processes. For example, alternating anodic-cathodic operation of an electrode catalyzed by mixed-culture biofilms mitigated the pH imbalance often encountered in anodic or cathodic biofilms [34-36]. Also, conversion of

an anode biofilm into a cathode biofilm was reported as a strategy to accelerate the start-up of biocathode processes, which usually require a long time to acclimatize stable cathodic biofilms due to low energy availability and autotrophic cathodic conditions [37].

The engineering merits demonstrated in those studies are contingent upon a biofilm capable of switching its metabolism between electrode reduction and oxidation. Ross et al. [38] showed that the Mtr pathway of *S. oneidensis* MR-1 is functionally reversible and is used for electrode oxidation and reduction. They conducted electrochemical tests of deletion mutants with knocked out gene(s) from the Mtr pathway to show its important role in electrode oxidation. In addition, they found that *Shewanella* biofilm grown anodically on an electrode poised at -360 mV vs. Standard Hydrogen Electrode (SHE) immediately (within a few minutes) switched to electrode oxidation in response to fumarate addition [38]. This result demonstrated a reversible mechanism in extracellular electron transfer between *S. oneidensis* MR-1 cells and an electrode, since the biofilm would have exhibited a lag between electrode reduction and oxidation if they used different unidirectional systems. In contrast to this finding with *Shewanella*, Strycharz et al. [39] showed that the mechanism of electrode oxidation by *G. sulfurreducens* is significantly different from its mechanism of electrode reduction. They compared transcript abundance in electrode-oxidizing biofilms, using a graphite electrode poised at -500 mV vs. Ag/AgCl electrode (-289 mV vs. SHE) coupled with reduction of fumarate to succinate, with transcript abundance in electrode-reducing biofilms, using the same electrode material poised at +300 mV vs. Ag/AgCl (+89 mV vs. SHE) coupled with acetate oxidation. Genes for putative cell to electrode connecting components, which were highly expressed in electrode-reducing biofilms and included outer-surface cytochromes and pili, were not highly

expressed in electrode-oxidizing biofilms. Expression levels of these genes were not higher even compared to the level in biofilms growing on the same electrode material with acetate-fumarate metabolism, but not oxidizing/reducing electrode. In addition, they found that electrode-oxidizing biofilms had greater transcript abundance for a gene (GSU3274) encoding a putative monoheme, c-type cytochrome, and deletion of this gene completely inhibited electrode oxidation but did not impact electrode reduction. Conversely, deletion of genes known to be essential for optimal electrode reduction had no impact on electrode oxidation [12]. These results suggested that, unlike *Shewanella* biofilms, anode-reducing *Geobacter* biofilms most likely have a lag to start electrode oxidation if they prepare significantly different system for electrode oxidation de novo.

Since *Geobacter* is often the dominant taxon in BESs [14-16] and their relative abundance in the electrode biofilm community can correlate with current production, understanding their metabolic shift between electrode reduction and oxidation has implications to BES development. Geelhoed and Stams [40] and Yates et al. [41] demonstrated cathodic hydrogen production by anodically grown *G. sulfurreducens* biofilms, induced by changing poised electrode potential from one favorable for the anodic reaction to one favorable for the cathodic reaction. However, the contribution of a metabolic shift in the biofilm to cathodic proton reduction was likely not significant as the latter study reported that cell debris, and not intact active cells, mainly contributed to cathodic hydrogen evolution [41]. A recent study demonstrated the conversion of *Geobacter*-dominated mixed culture biofilms from acetate-oxidizing anode reduction into nitrate-reducing cathode oxidation [42], suggesting a metabolic shift in the anode-reducing *Geobacter* cells to cathode oxidation. However, given that the anode-to-cathode shift took

about 2 days to record a constant cathodic current, which could allow de novo synthesis of new metabolic machinery as well as a community shift after the cathodic operation, the capability of a metabolic shift of *Geobacter* cells between anode reduction to cathode oxidation remains unclear. It is important to examine the potential occurrence of a metabolic shift with pure culture anode biofilms mainly composed of cells actively reducing the anode without a substantial metabolically inactive fraction, with a focus on the time required to convert the anodic reaction to a cathodic reaction to see if cells construct new metabolic machinery to shift their metabolism. The present study examined the metabolic shift between electrode reduction and oxidation with *G. metallireducens* biofilms. We hypothesized that (1) electrode-reducing *G. metallireducens* biofilms immediately shift their metabolisms between electrode reduction and electrode oxidation based on electrode potential and acetate/nitrate availability, and (2) such immediate metabolic shift is enabled by the preparation of nitrate-reducing machinery under anode-reducing conditions in the absence of nitrate.

4.2. Materials and Methods

4.2.1. Microbial source and culture condition

G. metallireducens GS-15 (ATCC 53774) that had been stored at – 80 ^{O}C was cultured in sterile, anaerobic ATCC medium 1768 with modified concentrations of the following components: ferric citrate (40 mM), acetate (20 mM), and NaH_2PO_4 (1.67mM). Cultures were grown in the dark at 30°C without stirring. Stationary-phase culture was transferred (10 % volume) into the same medium and cultured again under the same conditions. Then stationary-phase culture was anaerobically centrifuged (3500 ×g, 20 mins,

4 ^{O}C), and cell pellets were resuspended in the anaerobic medium described above but omitting ferric citrate and acetate. A 2 mL aliquot of this cell suspension ($O.D._{600}$ = 0.2 - 0.3) was inoculated into each working electrode chamber of electrochemical cells. *G. sulfurreducens* PCA stored at – 80 ^{O}C was cultured with the same procedure as *G. metallireducens* but using modified ATCC medium 1957 containing 30 mM of acetate as electron donor and 50 mM of fumarate as electron acceptor. Purity of *Geobacter* cultures was checked by examining PCR amplicons of the 16S rRNA gene derived from suspended cultures and BES biofilms either by Sanger sequencing or restriction fragment length polymorphism (RFLP) (Appendix B-1).

4.2.2. Electrochemical cell configuration and operation

Dual-chamber, H-type electrochemical cells (Glasstron Inc., Vineland, NJ) were used for the tests, with Nafion 117 cation exchange membrane separating the working electrode chamber and counter electrode chamber. Graphite plates (Isomolded Graphite Plate, GM-10 grade, Graphitestore) cut into 1.0 × 3.0 × 0.3 cm blocks were sanded with 400 and 1500 grit sandpaper and sonicated to remove graphite particles [43]. The graphite plate blocks were then soaked in 1 M HCl overnight for three times to remove possible metal contamination. Cleaned graphite plates were connected to titanium wire and used as working electrodes. The same graphite plate material, cut into 1.0 × 6.0 × 0.3 cm blocks and prepared in the same way, was used as counter electrodes. Reference electrodes (Ag/AgCl, 3 M NaCl, +0.211 V vs SHE, RE-5B, BASi) were inserted into working electrode chambers. All electrochemical cells and media were sterilized and kept anaerobic prior to inoculation by sparging CO_2:N_2 (20 %: 80 %) gas. An aluminum gas bag was connected to each chamber through a sterile 0.2-μm mesh polyethersulfone filter (VWR)

to release pressure imbalance between the two chambers during operation. Acclimatized biofilms were tested in electrochemical analyses in a new batch cycle with freshly replaced media.

Working electrodes were poised at 0 mV vs SHE by a multi-channel potentiostat (VMP3, Bio-Logic), configured with a three electrode connection mode, and served as the sole electron acceptor to acclimatize anodic *G. metallireducens* biofilms. The growth medium described above was used without ferric citrate and with 0.5 mM or 1 mM acetate as the sole electron donor. The BES reactors were operated in a 30 ^{O}C temperature-controlled chamber without stirring in batch operation. After the anodic current production decreased below ~ 50 μA due to acetate depletion, the anodically acclimatized biofilms were subjected to the following tests. (1) To examine the metabolic shift of anodically acclimatized biofilms into a cathodic reaction, working electrode potential was shifted to -250 mV vs SHE to make the electrode a suitable electron donor, and nitrate was spiked as the sole electron acceptor 30 min after changing the potential. Current was monitored as the measure of anodic and cathodic activity. The electron balance was analyzed based on measured circuit-recovered charge compared to the change of electron donor/acceptor compounds in the bulk solution in response to the biofilm environment change from anodic to cathodic condition. (2) To examine the cathodic activity in the presence of an alternative electron donor, the anodically acclimatized biofilms were further incubated at 0 mV vs SHE with additional acetate amendment (10 mM), and after monitoring stable anodic current (~ 5 h) the electrode potential was changed to -150 mV vs SHE and nitrate was spiked 30 min later as an electron acceptor to support electrode oxidation. The electrode poised at -150 mV vs SHE can serve as an electron acceptor for *G. metallireducens* biofilms

using acetate as the electron donor [44], but it was hypothesized to work as an electron donor with nitrate as electron acceptor based on thermodynamic estimation. (3) To examine the shift between anodic and cathodic reactions as a function of poised electrode potential, cyclic voltammetry (CV) was performed to sweep the working electrode potential between -500 mV and +450 mV vs SHE with scan rate of 0.2 mV/sec in the presence of acetate and nitrate. For all three experimental configurations, duplicated biofilms from independent experiments were tested. In addition, abiotic controls without inoculation and killed biofilm control with gamma irradiated biofilms were also tested.

To prepare killed biofilm controls, a set of acclimatized biofilms was subjected to 25 kGy of gamma rays from cobalt-60 with Gammacell 220 at the Gamma irradiation facility at the Breazeale Nuclear Reactor, University Park. The graphite electrodes with acclimatized biofilms were gently transferred from the BES reactor to glass bottles filled with anaerobic 30 mM bicarbonate buffer (pH 7) in the glovebox. The sealed glass bottle was contained in a sealed glass container filled with N_2-sparged water with saturated sodium chloride to avoid oxygen contamination. After the irradiation, which took ~ 6 h, graphite electrodes were returned into sterile BES reactors in the glovebox and subjected to tests. Anodes treated similarly to the killed anodes but left outside of the irradiation reactor at the facility demonstrated comparable results with the active biotic biofilms in the tests of anodic and cathodic conditions, suggesting that the killed control biofilms were inactivated solely by gamma irradiation and not by other effects associated with the irradiation procedure, such as oxygen exposure or temperature change.

4.2.3. Electrochemical analysis

Cyclic voltammetry (CV) was conducted with a scan range between –500 mV and +450 mV vs SHE to characterize biofilms under turnover conditions with amendment of acetate, nitrate, or both; as well as non-turnover conditions in the absence of acetate and nitrate. Working electrode voltage was scanned at a constant speed of 0.2 mV/sec. Abiotic and killed biofilms were tested with CV under the turnover condition. The first derivative of cyclic voltammograms obtained in turnover conditions was calculated to examine different redox peaks of biofilms among different turnover conditions.

4.2.4. Suspended culture test

Washed *G. metallireducens* cells that had been cultured with acetate as electron donor and ferric as electron acceptor (as described in section 4.2.1) were used as inoculum for suspended growth tests using two different growth media with either ferric or nitrate as the sole electron acceptor. Both media were based on anaerobic ATCC medium 1768 but with increased acetate concentration (50 mM) to make electron donor-limited conditions and decreased phosphate concentration (1.67 mM) to avoid formation of iron-phosphorus precipitate, likely vivianite, that was observed in the original phosphate dose (5 mM) and would have introduced artifacts in the iron analysis described below. Decreased phosphorus addition was thought to not limit cell growth, based on the elemental composition of the medium relative to an assumed cell formula of $C_5H_7O_2NP_{0.2}$ as well as similar biomass yields from both phosphorus concentrations in preliminary culture tests. The ferric medium contained 20 mM of ferric citrate as the sole electron acceptor. The nitrate medium contained 10 mM of sodium nitrate as the sole electron acceptor, as well as 10 μM of cysteine as reducing agent to maintain anaerobic conditions over the course of

the experiment. Tests were conducted on 100 mL cultures with initial biomass densities of ~ 0.01 mg-protein/mL in sterilized anaerobic culture bottles sealed with butyl rubber stoppers and aluminum seal. Bottles were incubated at 30 ^{O}C in the dark without agitation, andsamples were collected throughout the batch culture. Duplicated cultures with one abiotic control were tested in each culture condition. Samples were centrifuged (8000 ×g, 5 mins, room temperature) to separate biomass recovered in a pellet and supernatant. Recovered pellet and filtered supernatant was store at -20 ^{O}C to be analyzed later.

4.2.5. Nitrate reductase activity assay

Nitrate-reducing enzyme activity was measured in-vitro using methyl viologen as an artificial electron donor [45, 46] and a procedure previously used for *G. metallireducens* [47-49]. In brief, metabolically active cells were obtained from three different growth conditions. Anode-reducing cells were harvested by scraping biofilm cells from anodes during the peak current of the biofilm acclimatization batch poised at 0 mV vs SHE with 10 mM acetate growth medium. Ferric-reducing cells and nitrate–reducing cells were harvested from suspended cultures (incubated as described in 4.2.4) in late-exponential growth phase by centrifugation (8000 ×g, 20 mins, 4 ^{O}C). Harvested cells were washed with chilled 30 mM bicarbonate buffer (pH 7) and killed/permeabilized with toluene treatment: 0.75 mL of resuspended cells were mixed with 12.5 µL of toluene and subjected to 5 cycles of vortexing for 30 sec followed by 30 sec of rest on ice. A 0.5-mL aliquot of cell lysate (toluene-treated permeabilized cell suspension) was added to the assay mixture with final concentrations of 20 mM nitrate, 10 mM of sodium bicarbonate, 4 mM of methyl viologen, and 20 mM of sodium dithionite in a total volume of 6 mL. The mixture was incubated in the dark at 30°C without agitation, and 0.5 mL samples were collected every

20 mins. Samples were vortexed in a centrifuge tube to stop enzymatic nitrate reduction; sodium dithionite in the mixture was oxidized by air, which would then stop donating electron to methyl viologen, the electron donor for the nitrate reduction reaction. Tubes were then centrifuged (8000 ×g, 5 mins), and the ammonia concentration in the supernatant was measured. In this enzyme assay, nitrite concentrations in the incubated assay mixture samples were below the reliable quantitation level as reported in other studies conducting the methyl viologen assay on *G. metallireducens* [49], and thus ammonia was quantified as the product of the in-vitro nitrate-reducing enzyme reaction. A control assay without nitrate amendment in the assay mixture was conducted to account for ammonia formation that is not derived from nitrate-reducing enzyme activity, such as ammonification of cells. A portion of permeabilized cell sample was used to quantify the protein concentration with the method described in 4.2.6.

4.2.6 Analytical methods

Nitrate, nitrite, and acetate concentrations in anode media were measured with ion chromatography (ICS-1100 with AS-25 anion separation column, Dionex, CA). Ammonia concentration in anode and cathode media was measured with the Salicylate method (Nitrogen-Ammonia Reagent Set, TNT, AmVer (Salicylate), Hach, CO). Cells in biofilms and suspension were solubilized by sodium hydroxide, and the resultant solubilized protein concentration was measured by the modified Lowry method using the DC Protein Assay Kit (Bio-Rad, CA) with Bovine serum albumin fraction V as protein standards. Ferrous and Ferric concentrations in suspended cultures were measured with the Ferrozine assay [50]. Briefly, total soluble iron (the sum of ferrous and ferric) was quantified as ferrous after reducing ferric in the sample with 0.25 M hydroxylamine hydrochloride, and the ferric

concentration was obtained by subtracting the ferrous concentration which was quantified without hydroxylamine treatment.

4.3. Results and Discussion

4.3.1. Rapid shift from electrode reduction to oxidation triggered by electrode potential change and nitrate amendment

Anodically acclimatized *G. metallireducens* biofilms demonstrated a quick shift from anodic electrode reduction into cathodic electrode oxidation in response to change in poised electrode potential and nitrate availability (Figure 4-1). Specifically, a set of biofilms was acclimatized in anodic condition with acetate as electron donor and graphite electrode poised at 0 mV vs SHE as the sole electron acceptor. Under these conditions, the biofilms demonstrated anodic electrode reduction coupled with acetate oxidation. They were then subjected to cathodic conditions by changing the poised electrode potential to -250 mV vs SHE, which was expected to work as an electron donor for the biofilms, and also by spiking nitrate as the electron acceptor 30 minutes after changing the potential. The electrode potential change from 0 mV to -250 mV resulted in a decrease of anodic current from active biofilms to negligible levels (Figure 4-1), as expected by thermodynamics because the poised potential of -250 mV was too low to accept electrons from acetate oxidation. After the 30 mins, electrodes with active biofilms showed cathodic current within a minute of adding a nitrate spike (targeted 5 mM). Cathodic current peaked at ~2.5 mA around 3.5 hour after the nitrate spike, and it decreased to background level over 20 hours of cathodic operation. Negligible current recorded in sodium chloride-spiked biofilms, an abiotic reactor, and a killed biofilm (Figure 4-1) indicated the observed

cathodic current was due to biotic reaction coupled with nitrate amendment. Decreased cathodic current in response to an amendment of malonate, a TCA cycle inhibitor, suggested the potential contribution of TCA cycle activity to cathodic current (Appendix B-2).

The observed peak current corresponded to a current density of ~3.68 A/m^2, based on the geometrical surface area of the graphite electrodes (6.8 cm^2). This observed cathodic current density was 2 orders of magnitude greater than the cathodic current density recorded from anodically-grown, *Geobacter*-dominated mixed culture biofilms subjected to cathodic conditions of an electrode potential poised at -383 mV vs SHE in the presence of nitrate [42]. It was also significantly higher than, the cathodic current density of other biofilms grown under constant electrode potential operation, such as a nitrate-reducing *Thiobacillus denitrificans* biocathode (~0.1 A/m^2) [51], a methanogenic thermophilic mixed culture biocathode (~0.2 A/m^2) [52], and an oxygen-reducing *Acidithiobacillus ferrooxidans* biocathode (~0.01 A/m^2) [53]. However, comparing current density values obtained from different studies is not straightforward as many factors such as electrode materials, surface roughness of the electrode, electrode spacing, and solution composition could influence the results. The observed current density which is in the same order of magnitude for reported anodic current density by mixed culture or *Geobacter* pure cultures biofilms would be fairly large as cathodic current as most of reported cathodic current density were smaller than anode current density.

During the period with cathodic current (17.4 – 34.5 h Figure 4-1A), ~0.8 mM of nitrate (~20 % of amended nitrate) was consumed with the accumulation of 0.68 mM nitrite (~70 % of consumed nitrate) in the biotic treatment (Figure 4-2). The decrease of cathodic

current was likely associated with the observed nitrite accumulation, which could inhibit cell metabolism. Abiotic and killed biofilm reactors did not show significant nitrate consumption nor detectable nitrite accumulation. Also, biotic biofilms subjected to a nitrate spike under open circuit conditions showed nitrate decrease with nitrite accumulation, supported by electrons supplied by the oxidation of acetate remaining in the system after the anodic operation. Electron balance analysis of the cathodic reaction period indicated that the large electron flux coming into the biofilm with electrode oxidation was coupled with nitrate reduction (Figure 4-2). The observed acetate loss also contributed electrons to the measured nitrate reduction in biotic reactors. However, ~2.5 times greater nitrate reduction under the cathodic operation than open circuit operation, which showed comparable acetate loss, as well as cathodic electrode oxidation contributing more than 4 times the electron equivalents potentially supplied by acetate oxidation, indicates the biofilms conducted cathodic electrode oxidation coupled with nitrate reduction.

The electron balance in biotic nitrate-reducing cathodic operation (Biotic NO_3^- in Figure 4-2) was distinct from that reported for a *Geobacter*-dominated mixed culture under nitrate-reducing cathodic conditions. Namely, that study reported that the cathodic current only accounted for ~14 % of the electron equivalents used for nitrate reduction, based on measured concentrations of nitrogen species. Such a small contribution of the cathodic electrode could lead to the hypothesis that some other electron source such as organic compounds stored in the fully grown anode biofilm matrix, was primarily responsible for measured nitrate reduction. In addition, the study assumed complete denitrification to nitrogen gas (i.e. 5 mol electrons per mol nitrogen lost in the system), but dissimilatory nitrite reduction to ammonia (DNRA) might have contributed to nitrite loss in the

Geobacter-dominated biofilm as many *Geobacter* species possess the gene for nitrite ammonification, *nrfAH* [54], but not nitrite reductase in denitrification, *nirS* or *nirK*. An electron balance based on DNRA (i.e. 8 mol electron/mol N lost) would make the contribution of cathodic current even smaller. Some other biocathode studies reported similar trends in electron balance. For example, a study on hydrogen production by biotic and killed biofilms acclimatized in anodic conditions and then converted into cathodic operation demonstrated a greater hydrogen production rate than the cathode-supplied electron flux, and attributed such phenomenon to an alternative electron source such as autolytic cell material or electrode decomposition [41]. By contrast, the electron balance of the nitrate-spiked biocathodes in this study (Biotic NO_3^- in Figure 4-2) showed more cathode-derived electrons than needed for nitrogen reduction as the potential electron sink. The fate of excess cathode-derived electrons not directly accounted for nitrate transformation is unknown, but it is expected to be related to reactions associated with biotic nitrate –reduction because other treatments showed negligible cathodic electrode oxidation. One possibility is the investment of electrons in additional biofilm growth associated with energy derived from cathode oxidation and nitrate reduction and anabolically supported by the presence of acetate. Further study on the electron balance, particularly the fate of excess cathodic electrons, is of interest.

The metabolic shift of anode-reducing biofilms into cathode-oxidizing reactions was also examined in the concurrent presence of high acetate levels and nitrate in another set of experiments (Figure 4-3). The poised potentials of electrodes with anodically grown biofilms was changed from 0 mV to -150 mV vs SHE in the presence of 10 mM acetate as the electron donor. An electrode potential of -150 mV was known to still work as an

electron acceptor, albeit with a lower current than 0 mV, as shown in Figure 3-1 and observed in the first 30 min of these tests. This potential was also hypothesized to work as an electron donor for nitrate reduction based on thermodynamic estimations. Nitrate addition (targeted at 8 mM) 30 min after the potential change resulted in immediate anodic current decrease followed by cathodic current that reached a peak of ~1.2 mA. This observed anodic current decrease followed by cathodic current at a poised potential of -150 mV was distinct from the nitrate-influenced response reported in Chapter 3 for anodes poised at higher electrode potentials that could not serve as an electron donor for nitrate reduction. In those cases, high-level nitrate spikes resulted in anodic current decreases, and the current often converged to zero Such observed continuous change from anodic current into cathodic current illustrated a rapid shift of bulk biofilm metabolism from anode reduction into cathode oxidation.

While a decrease of nitrate and increase of nitrite was observed concurrently with cathodic current, acetate oxidation was the major electron source for nitrate reduction. In fact, acetate loss during the cathodic current period (i.e. from the time of nitrate spike to 17.5 h) was comparable to that in the sodium chloride spiked reactor, and electrons supplied from acetate oxidation to cathode biofilms during that time was approximately 5 times greater than the electrons derived from cathodic current (Appendix B-3). The sole activity of acetate-dependent nitrate reduction, independent from the electrode-mediated reaction, is unclear as a nitrate spike under open circuit condition was not conducted, but cathodic nitrate reduction reaction would largely be influenced by such electrode-independent reactions.

4.3.2. Alternating anodic-cathodic reaction controlled by dynamic electrode potential change and co-substrate availability

The observed quick shift from anode reduction to cathode oxidation induced by changes in poised electrode potential and nitrate amendment prompted interest in examining whether *G. metallireducens* can reversibly shift back from cathode oxidation to anode reduction. To address this question, the electrode potential of biofilm-grown graphite electrodes was swept at a constant rate (0.2 mV/sec) between -500 mV and +450 mV vs SHE in the presence of acetate and nitrate. This cyclic voltammetry test with a slow scan rate had a potential scan range and solution conditions expected to be permissible both for anode reduction and cathode oxidation. *G. metallireducens* biofilms dynamically shifted between anode reduction and cathode oxidation in the presence of nitrate and acetate (Figure 4-4). All 13 potential scan cycles were performed identically as shown in the top part of Figure 4-4A, but each potential scan cycle resulted in a different current response (shown as current versus time plot in panel A, as well as current versus potential plot for selected cycles in panel B), due to changes in solution chemistry and biofilm state over the course of the experiment. Namely, the first four scan cycles showed an anodic current decrease in the anodic potential range due to nitrate versus anode competition induced by the spiked nitrate, as discussed in Chapter 3. In this phase, anodic current decreased even under oxidation scan (time of potential scan from lower to higher potential), as seen in the downward-trending anodic current plateaus in panel A as well as the example of Cycle-4 in panel B. Cathodic nitrate reduction as well as concurrent electrode-independent, acetate-supported nitrate reduction consumed 3 mM of spiked nitrate, and the bulk nitrate concentration was less than 0.1 mM at the end of cycle-5 (15.75 h). Cathodic

current diminished in subsequent cycles due to the low nitrate concentration, and anodic current increased over the following cycles likely due to lowered anode vs nitrate competition as well as biofilm growth. In this phase of anodic biofilm growth, anodic current increased throughout the anodic potential range, even in reduction scans, as seen in upward-trending anodic current plateaus in panel A. After this growth phase, in the final cycles of this experiment, peak anodic current height became symmetrical around the time of scan direction change (panel A) and the biofilms exhibited virtually identical oxidation and reduction scan profiles (panel B). This is possibly due to the biofilm approaching a pseudo-steady state condition. In summary, *G. metallireducens* biofilms reversibly conducted anode reduction and cathode oxidation as a function of electrode potential in the presence of acetate and nitrate.

4.3.3. Metabolic shift from anode reduction to nitrate reduction took place faster than the one from ferric reduction to nitrate reduction

As seen in section 4.3.1 and 4.3.2, *G. metallireducens* quickly shifted from anode reduction to cathodic nitrate reduction in the order of minutes. Also, the metabolic shift from acetate-oxidizing anode reduction to acetate-oxidizing nitrate reduction took place within the order of minutes to an hour as discussed in section 3.4.5. Namely, the anode reduction rate (current) significantly decreased within a minute, and the nitrate concentration decreased within an hour after the nitrate spike. Such quick metabolic shift is distinct from a previous study of this bacterium, which reported “the suspensions of nitrate-grown cells reduced nitrate, but Fe (III)-grown cells did not (data not shown)” [55]. Although this report did not provide further information about a metabolic shift from Fe (III) reduction to nitrate reduction, it is hypothesized that *G. metallireducens* requires a

relatively long time for such a metabolic shift. To test this working hypothesis, ferric-grown cells were transferred into a growth medium with nitrate as the sole electron acceptor, and the growth profile was characterized in batch suspended culture.

Ferric-grown cells transferred into a growth medium with nitrate as the sole electron acceptor took more than 24 hours to start consuming nitrate and increasing biomass, whereas ferric-grown cells transferred into the same ferric medium started to increase biomass without a lag time (Figure 4-5). This suggests that ferric-grown cells requires time to shift their metabolism to nitrate reduction, which supports the above working hypothesis based on the previous report [55], and is distinct from the quick metabolic shift from anode reduction to nitrate reduction.

4.3.4. Preparation of nitrate-reducing enzymes in anode-reducing condition

The quick metabolic shift from anode to nitrate reduction, which was distinct from that for ferric-reducing cells, was thought to be due to better preparation of nitrate-reducing enzymatic machinery by anode-reducing cells relative to ferric-growing cells. Expression of the gene encoding respiratory nitrate reductase that is required for using nitrate as the electron acceptor is regulated by conditions such as presence/absence of nitrate, nitrite, or oxygen [56]. The effect of anode-reducing conditions on preparation of this enzyme is unknown, but it is hypothesized based on the rapid switch from anode to nitrate reduction that cells under anode-reducing growth conditions prepare nitrate-reducing enzymes. To test this hypothesis, the nitrate-reducing enzyme activity of anode-reducing cells was examined.

G. metallireducens biofilm cells growing on a graphite anode electrode as the sole electron acceptor showed significantly higher nitrate-reducing enzyme activity than cells

growing on ferric ion as the sole electron acceptor. Specifically, a toluene-treated permeabilized cell suspension derived from anodic biofilms reducing graphite anodes poised at 0 mV vs SHE in the absence of nitrate and nitrite demonstrated approximately 4-fold greater specific nitrate-reducing enzyme activity relative to cells growing with ferric ion in the absence of nitrate in an in-vitro methyl viologen assay (Figure 4-6). Cells actively reducing nitrate as the electron acceptor showed higher enzyme activity than cells harvested from both non-nitrate growth conditions; ~1.9-fold greater than anode-reducing cells and ~7.4-fold greater than ferric-reducing cells. These results are consistent with the findings of quicker metabolic shift from anode reduction to nitrate reduction than ferric reduction with nitrate reduction, as preparation of active nitrate-reducing enzymes could enable anode-reducing cells to quickly initiate nitrate reduction after the introduction of nitrate as a new electron acceptor.

The result of higher nitrate-reducing enzyme activity by nitrate-reducing cells relative to cells growing without nitrate was reasonable given the nature of prokaryotic membrane-bound respiratory Nar and periplasmic respiratory Nrf, which have their expression induced by nitrate and nitrite [57]. A two-component regulatory system composed of NarX, which is a nitrate/nitrite sensor that responds to both nitrate and nitrite, and NarL, which is the DNA-binding regulator that controls gene expression, is reported to control the expression of the Nar enzyme encoding operon *narGHJI* of certain bacteria such as enterobacteria [56, 58]. Although *narXL* genes or any other genes known to regulate nitrate reductase gene expression have not been annotated for *G. metallireducens*, according to the genome paper [59] and the KEGG pathway map (http://www.genome.jp/kegg-bin/show_pathway?gme02020), it is expected that gene

expression of Nar and Nrf of *G. metallireducens* are induced in the presence of nitrate/nitrite. Also, a previous study that reported nitrate reductase enzyme activity detected in nitrate-growing *G. metallireducens* cells but not in ferric-growing cells [60], as well as another study that discussed nitrate reductase of *G. metallireducens* as a nitrate-induced protein [48], are consistent with such hypothesized regulatory mechanism.

Reports on nitrate reductase enzyme expression, or nitrate reduction potential, of anode-reducing cells were not found in the literature, but the observed significantly higher nitrate-reducing enzyme activity in anode-reducing cells over ferric-reducing cells (Figure 4-6) was possibly due to differential nitrate reductase enzyme expression between anode-reducing and ferric-reducing growth conditions. Findings from one study reported differential nitrate reductase activity of *Geobacter* cells grown under multiple non-nitrate growth conditions [47], which was consistent with the differential enzyme activity observed between anode-reducing cells versus ferric-reducing cells. Stolz et al. conducted the methyl viologen assay with four different electron acceptors, thiosulfate, nitrate, selenite, and fumarate, to examine the activity of reductases for each of these four compounds by the fractionated cell membrane samples of *G. barnesii* strain SeS3 growing with each compound as the sole electron acceptor in each condition. Normalized nitrate reductase activity (100 % with nitrate reductase activity by nitrate-growing cells) of selenite-growing cells (51 %) was higher than ones grown with thiosulfate (8 %) or fumarate (7 %) [47]. This result suggested that nitrate reductase of *Geobacter* species can be differentially expressed under different growth conditions in the absence of nitrate.

It is noted that measuring ammonia production, rather than nitrite production, in this study was because detected nitrite was too low to stably quantify in preliminary tests.

This was consistent with a study that reported a lower apparent K_m for nitrite (10 μM) than for nitrate (32 μM) obtained in methyl viologen based nitrate/nitrite reducing enzyme activity assay of *G. metallireducens* [49], suggesting high nitrite affinity of the enzyme and its rapid reduction to ammonia. The study also reported that nitrite was not detected in the methyl viologen assay with nitrate as the substrate.

To investigate the possibility of differential nitrate reductase gene expression among the growth conditions in this experiment, expression of *narG* of cells harvested from those growth conditions was examined by RT-qPCR with differential CT relative quantification, with *proC* as an endogenous control. The experiment resulted in higher expression of the active *narG* operon in nitrate-reducing cells over ferric-reducing cells, which is consistent with the hypothesis, but conclusive results were not obtained for anode-reducing cells. Further discussion on this gene expression analysis is found in Appendix 4-C.

Taken together, significantly higher in-vitro nitrate-reducing enzyme activity in anode cells over ferric cells suggested the presence of a greater amount of active nitrate-reducing enzyme in anode biofilm cells relative to ferric-growing cells. This possibly enabled quicker metabolic shift from anode reduction to nitrate reduction relative to ferric reduction to nitrate reduction.

4.3.5. Insights in electron transfer mechanism between biofilm cells and electrode

To better characterize electron transfer between an electrode and biofilms cells, anodically acclimatized *G. metallireducens* biofilms under different solution conditions were examined with CV using at potential scan range of -500 mV to +450 mV vs. SHE and a scan rate of 0.2 mV/sec (Figure 4-7). Biofilms in an acetate turnover condition

showed sigmoid-shaped oxidation peak voltammograms without an apparent reduction peak, which is commonly obtained from *Geobacter* electrode biofilms under anodic turnover conditions [61-64]. Biofilms in the presence of both nitrate and acetate induced sigmoidal peaks in both oxidation and reduction current. The peak anodic current was signifcantly lower than the acetate turnover condition, likely due to hampered anode reduction activity by electron acceptor competition against nitrate. A large cathodic current of ~ -1.5 mA, which corresponded to a current density of -2.2 A/m^2, was observed in the presence of ~3 mM nitrate. Biofilms with nitrate showed voltammograms with sigmoidal shaped reduction peaks, suggesting that biofilm cells conducted nitrate-dependent cathodic current production in this turnover condition. In other words, cells continuously re-oxidized the site that had accepted electrons from the electrode by continuous nitrate reduction. Peak cathodic current observed in this condition (0.44 A/m^2) was an order of magnitude smaller than that for the acetate/nitrate condition, but was an order of magnitude greater than the peak current from a *Geobacter*-dominated nitrate-reducing biocathode CV with a scan rate of 1 mV/sec, ~ 0.06 A/m^2 [42]. Biofilms in a non-turnover condition without substrate showed two oxidation peaks with peak potentials around -150 mV and + 100 mV vs SHE, as well as one apparent reduction peak with a peak potential around -200 mV vs SHE. The oxidation peak signal at around +100 mV vs SHE coinsided with the oxidation peak observed in the nitrate turnover voltammogram. Oxidation and reduction peaks in non-turnover cyclic voltammograms likely corresponded to electron transfer components that mediate electron transfer between cells and the electrode surface. Although prior reports of non-turnover CVs of *G. metallireducens* cells were not found, the obtained voltammograms with oxidation peaks at around -150 mV and +100 mV vs SHE were

somewhat similar to reported non-turnover CVs of *G. sulfurreducens* anode biofilms with multiple oxidation peaks at similar potentials [61-66].

The killed biofilm controls showed no sigmoidal catalytic current inr the presence of nitrate and acetate. This suggested that the electrocatalytic signals of nitrate-dependent cathodic current and acetate-dependent anodic current derived from metabolically active cells and not just the biofilm matrix. Killed biofilms did not have an oxidation peak at around -150 mV vs SHE, which was present in living biofilms under non-turnover condition. It could be hypothesized that the oxidation peak is attributed to a specific electron transfer component of the cell that was not functional following by gamma irradiation treatment, but no conclusive finding was drawn from this results. The abiotic control, which was an uninoculated bare graphite electrode in the solution containing growth media with acetate and nitrate, showed no measurable reduction or oxidation peak with in the scan range, suggesting that observed peaks in biotic conditions were not derived from graphite or redox-active components in the growth medium. Overall, CV results suggested that acetate-dependent anodic reduction, anode reduction and cathode oxidation in the presence of both acetate and nitrate, and also nitrate-dependent cathode oxidation were coupled with cellular metabolic activity.

To obtain further insights into the electron transfer mechanism, the first derivatives of cyclic voltammograms obtained under turnover conditions were calculated (Figure 4-8). Interestingly, first derivative CVs of all three turnover conditions had peaks centered within the potential range -140 mV to -160 mV vs SHE. The profiles of nitrate turnover condition replicates were less consistent with each other than those from the other turnover conditions. While a quantitative discussion is not possible given the noise and variance

among replicates, it seems that electron transfer in all three turnover conditions has similar midpoint potentials. With similar signal peak centers in both the acetate-dependent anode reduction and nitrate-dependent cathode oxidation turnover conditions, it is hypothesized that *G. metallireducens* uses the same electron transfer component reversibly as reported in *Shewanella* [38]. This hypothesis is consistent with the quickly reversible metabolic shift demonstrated by *G. metallireducens* biofilms. If cells could reversibly use the same electron transfer machinery for anode reduction and cathode oxidation, they could quickly shift to the cathodic reaction as long as they prepare the machinery to reduce the newly seen electron acceptor, which in this case was nitrate. That is also supported by the in-vitro nitrate-reducing enzyme activity assay.

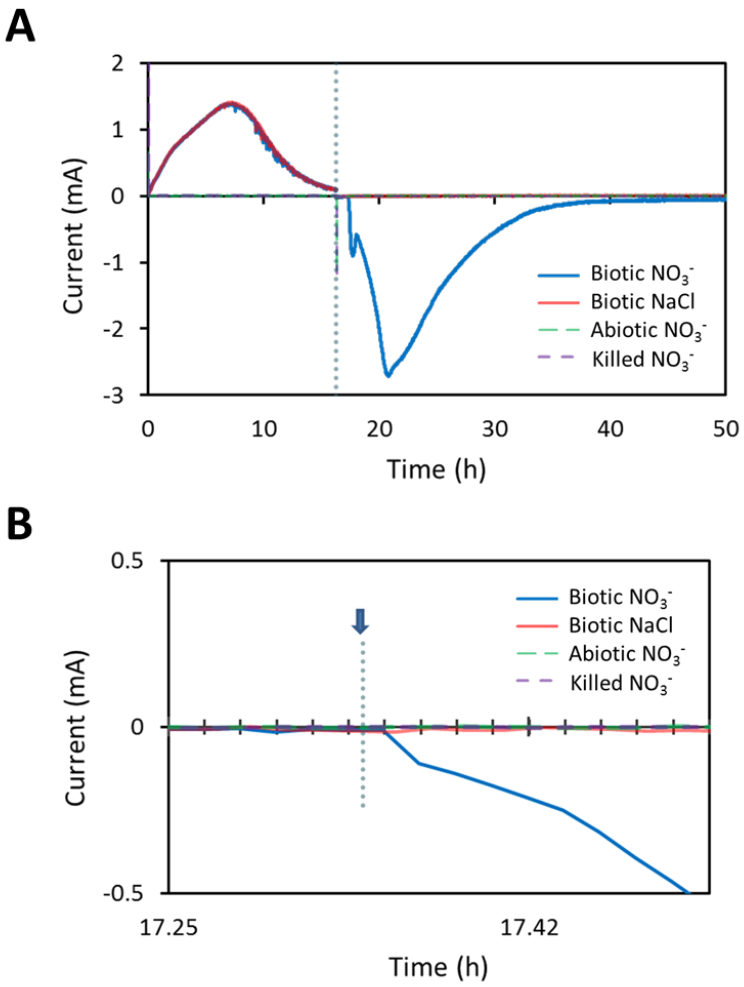

Figure 4-1: Cathodic electrode oxidation by anodically-grown *G. metallireducens* biofilms in response to nitrate amendment under poised electrode potential of -250 mV vs SHE. Anode biofilms were acclimatized with a poised electrode potential of 0 mV vs SHE as the electron acceptor and 0.5 mM of acetate as the electron donor. Growth media in working electrode chambers were replaced with new medium of the same composition, precluding the potential contribution of suspended biomass to anodic and cathodic reactions. The biofilm-grown electrodes were subjected to a second anodic batch cycle with at 0 mV vs SHE with 0.5 mM of acetate (the time 0 of panel A) to demonstrate stable anodic reaction

with 0.5 mM acetate in the replaced medium. Once anodic current decreased, the electrode potential was shifted to -250 mV vs SHE (designated with the vertical dotted line in panel A), and nitrate (targeted 5 mM) was spiked 30 mins after the electrode potential shift. The figure shows results from one of the duplicated experiments with three different control treatments as well as the nitrate-spiked treatment. Biotic NaCl indicates biofilms treated as above except with a 3 mM sodium chloride spike instead of a nitrate spike. Abiotic control indicates a bare graphite electrode without inoculation, and killed control denotes gamma-irradiated biofilm-grown electrodes. Another set of biofilm-grown electrodes (data not shown here, but included in Figure 4-2) were treated identical to the other biotic treatments except the electrode condition was changed to open circuit (no oxidation or reduction of electrode) before the nitrate spike to examine electrode-independent nitrate reduction. Panel B shows the same results but focusing on the period around the nitrate spike event. Each tick mark on the x-axis designates a minute, and the vertical dotted line with an arrow shows the time of the nitrate spike (or chloride spike for control biofilms).

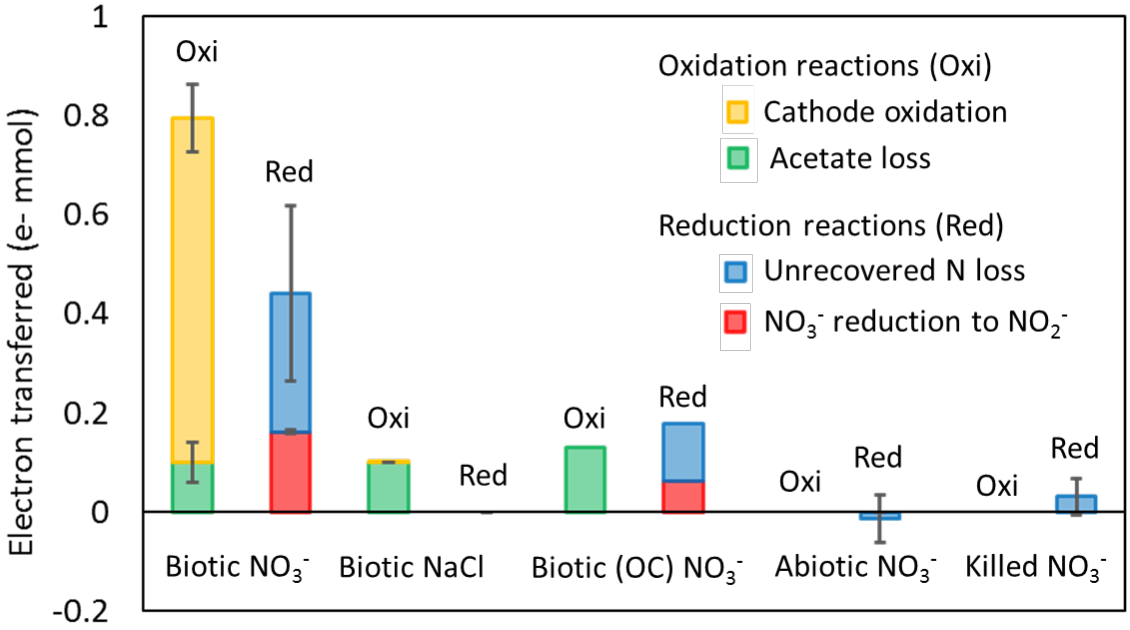

Figure 4-2: Electron balance of working electrode chambers with anodically acclimatized biofilms switched into cathodic conditions. This electron balance was obtained from the experiment shown in Figure 4-1. Three biotic treatments correspond to biofilm-grown electrodes poised at -250 mV vs SHE with nitrate spike (targeted 5 mM), sodium chloride spike, and nitrate spike under open circuit condition. Abiotic and killed treatments were operated as biotic nitrate treatment. Bars designated as Oxi and Red for each treatment show the sum of electrons came into the biofilm-electrode (Oxi) and the one came out from the biofilm-electrode (Red). Electron transferred through biofilm-grown electrodes for 17 hours of operation in cathodic condition after nitrate spike were calculated from following four measured oxidation and reduction reactions. (1) Electrons donated from acetate oxidation was obtained from acetate loss with the assumption of acetate oxidation to carbon dioxide; 8 e^--mol/acetate-mol. Acetate loss observed in biotic samples was derived from

the loss of ~ 0.1 mM acetate that was left in the system after the biofilm acclimatization operation. (2) Electrons donated from electrode oxidation was based on cathodic charge. (3) Electrons consumed for nitrate reduction to nitrite was obtained by change of nitrite concentration in bulk solution between the time of nitrate spike and after 17 hours with the assumption of 2 e^--mol/ NO_2^--mol. (4) Unrecovered nitrogen loss from the system which was obtained by nitrogen balance based on measured nitrate and nitrite concentrations was accounted as electron consumption with the assumption nitrogen reduction to ammonia (dissimilatory nitrate reduction, DNRA) with 8 e^--mol/acetate-mol. As DNRA is two-step reactions of nitrate reduction to nitrite followed by nitrite ammonification, up to 25 % (2 e^- out of 8 e^-) of electrons counted as unrecovered N loss could be attributed to nitrate reduction to nitrite, but missed to account as (3) as it has been further transformed into ammonia at the time of 17 h. Measurement of ammonia concentration was not conducted due to its difficulty with high ammonium background in growth media. Negative mean electron balance in N loss of abiotic treatment was due to inaccurate nitrate quantification in ion chromatography for this experiment which resulted in slightly higher nitrate concentration at the end of 17 hours operation than the one at the start.

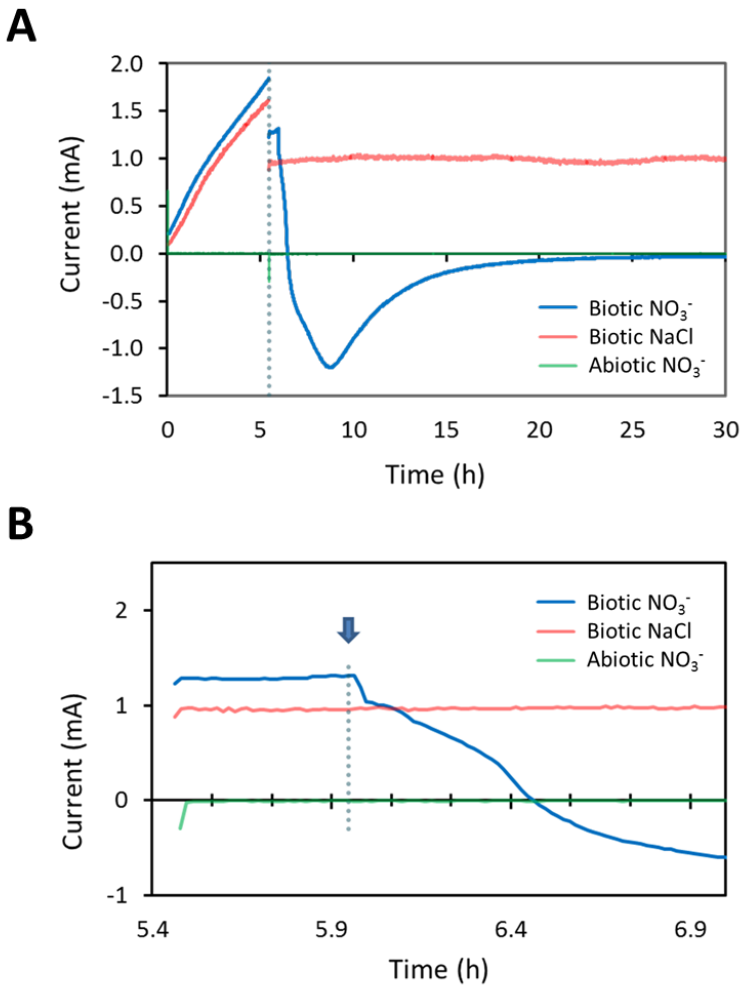

Figure 4-3: Cathodic electrode oxidation by anodically grown *G. metallireducens* biofilms in response to nitrate amendment at a poised electrode potential of -150 mV vs SHE. Anode biofilms were acclimatized with poised electrode potential of 0 mV vs SHE as the electron acceptor and 0.5 mM of acetate as the electron donor. Growth media in working electrode chambers were replaced to new medium containing 10 mM of acetate. The electrodes were poised again at 0 mV vs SHE, for 5 hours starting at time 0 of panel A, and then electrode potential was changed to -150 mV vs SHE (designated with vertical dotted line). After 30 mins operation at the lower electrode potential, nitrate (targeted 8 mM) was spiked to

induce cathodic electrode oxidation coupled with nitrate reduction. The figure shows results from one of the duplicated experiments with two control treatments, Biotic NaCl and Abiotic. Biotic NaCl denotes biofilms treated identical as above expect with addition of an equal molar sodium chloride spike instead of a nitrate spike. Abiotic control was a without inoculation. Panel B shows the same results with magnified scale around the nitrate spike event. The x-axis tick marks designate 10 minute intervals, and the vertical dotted line with an arrow shows the time of nitrate spike (or chloride spike for control biofilms).

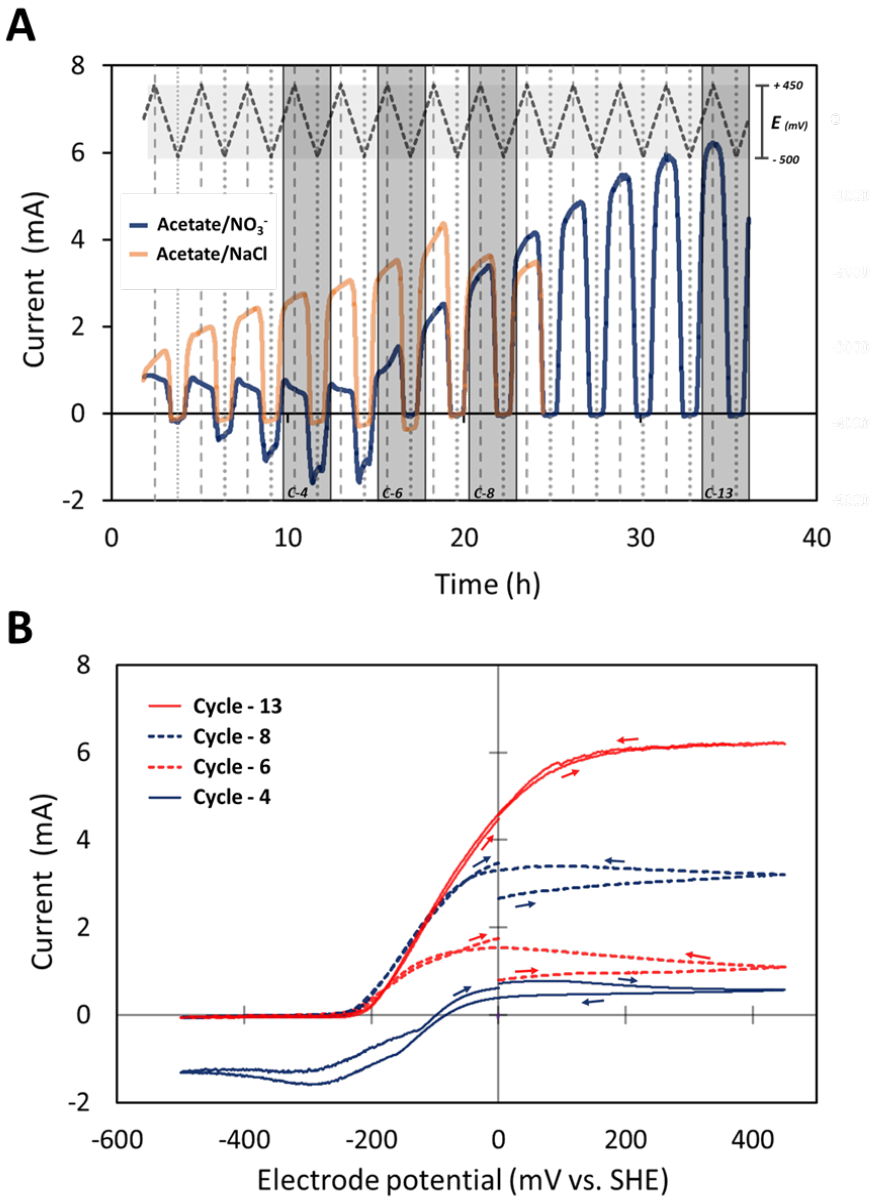

Figure 4-4: Anodic and cathodic current profiles of *G. metallireducens* biofilms in response to cyclic electrode potential sweep between anodic and cathodic potential ranges in the presence/absence of nitrate. **Panel A** shows current profiles of two representative biofilm-grown electrodes under cyclic electrode potential scans between -500 mV and +450 mV vs SHE with steady electrode potential sweep at 0.2 mV/sec. Two biofilms

acclimatized on graphite electrode poised at 0 mV vs SHE as the sole electron acceptor and 0.5 mM of acetate as electron donor were subjected to acetate amendment (targeted 10 mM in the working electrode chamber) at the time of 0 h under the constant poised potential of 0 mV vs SHE. After recording stable anodic current, for 1.75 h, 3 mM of sodium nitrate or sodium chloride were spiked into each reactor, **Acetate/NO_3^-** with blue data line and **Acetate/NaCl** with orange data line, respectively. The cyclic electrode potential sweep cycles were started at 0 mV vs SHE immediately after the nitrate or chloride spikes. The grey dotted line above the current data lines represents electrode potential during the cyclic potential sweep operation. Vertical dotted lines show times at which the potential scan changed between oxidation sweep in which potential changed from low to high direction, and reduction sweep in which potential changed from high to low direction. Measured nitrate concentration at the time 15.75 h, at the end of the 5^{th} sweep cycle, was almost zero (lower than 0.1 mM). **Panel B** shows current profiles of representative potential sweep cycles of an Acetate/NO_3^- electrode as a function of electrode potential. Four cycles shown in this panel correspond the gray cycles shown in Panel A. Arrows shown with each current vs potential line show the direction of the potential sweep during each cycle. All of the cycles start/end at the electrode potential of 0mV vs SHE.

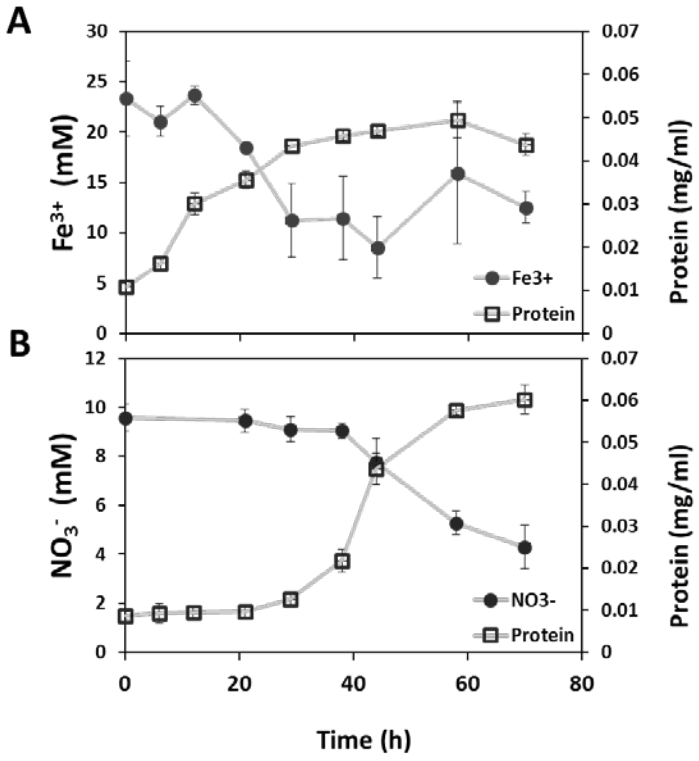

Figure 4-5: Electron acceptor consumption and biomass production of ferric-grown *G. metallireducens* cells in batch suspended cultures with different electron acceptors. **Panel A** shows ferric concentration and protein concentration over the batch culture with a medium containing 20 mM ferric citrate as the sole electron acceptor. **Panel B** shows nitrate concentration and protein concentration profile with a medium containing 10 mM sodium nitrate as the sole electron acceptor. Inoculum of batch cultures was washed cells harvested from cultures growing with ferric citrate as the electron acceptor. Acetate as the electron donor was not limiting (35 mM or higher acetate concentration at 70 h in all tested cultures). Duplicated cultures with one abiotic control were tested in each growth condition. The large deviation and increasing trend after 40 hrs observed in the ferric concentration profile was possibly due to an artifact in the ferric quantification assay, due to ambient oxidation of ferrous in sampled cultures.

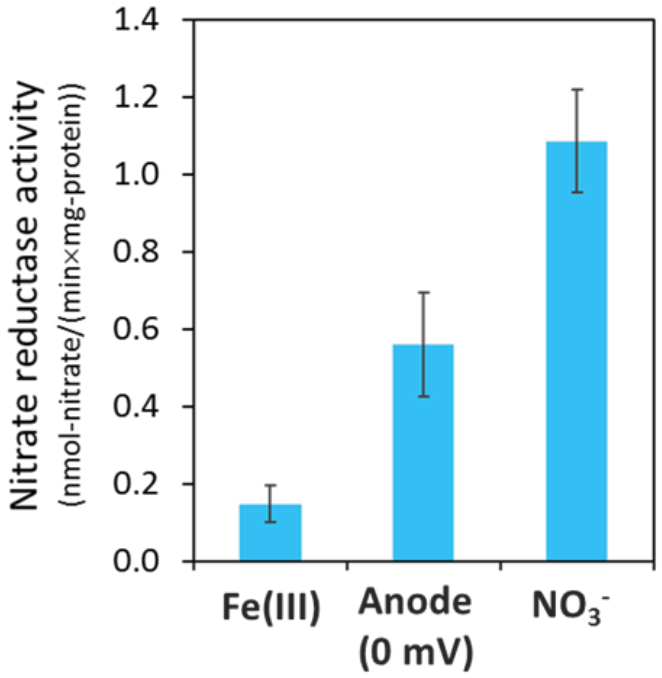

Figure 4-6: Specific in-vitro nitrate-reducing enzyme activity of *G. metallireducens* cells under different growth conditions. In-vitro nitrate reduction rate of toluene-treated permeabilized cell suspensions with methyl viologen as in-vitro cyclic electron donor was obtained by measuring formation of ammonia at multiple assay incubation times, and normalized by the mass of protein in the assay to obtain specific activity. Assay was conducted with duplicated anode biofilms poised at 0 mV vs SHE for anode-reducing growth condition, and triplicated suspended culture cell samples for Fe (III)-reducing and NO_3^--reducing growth conditions.

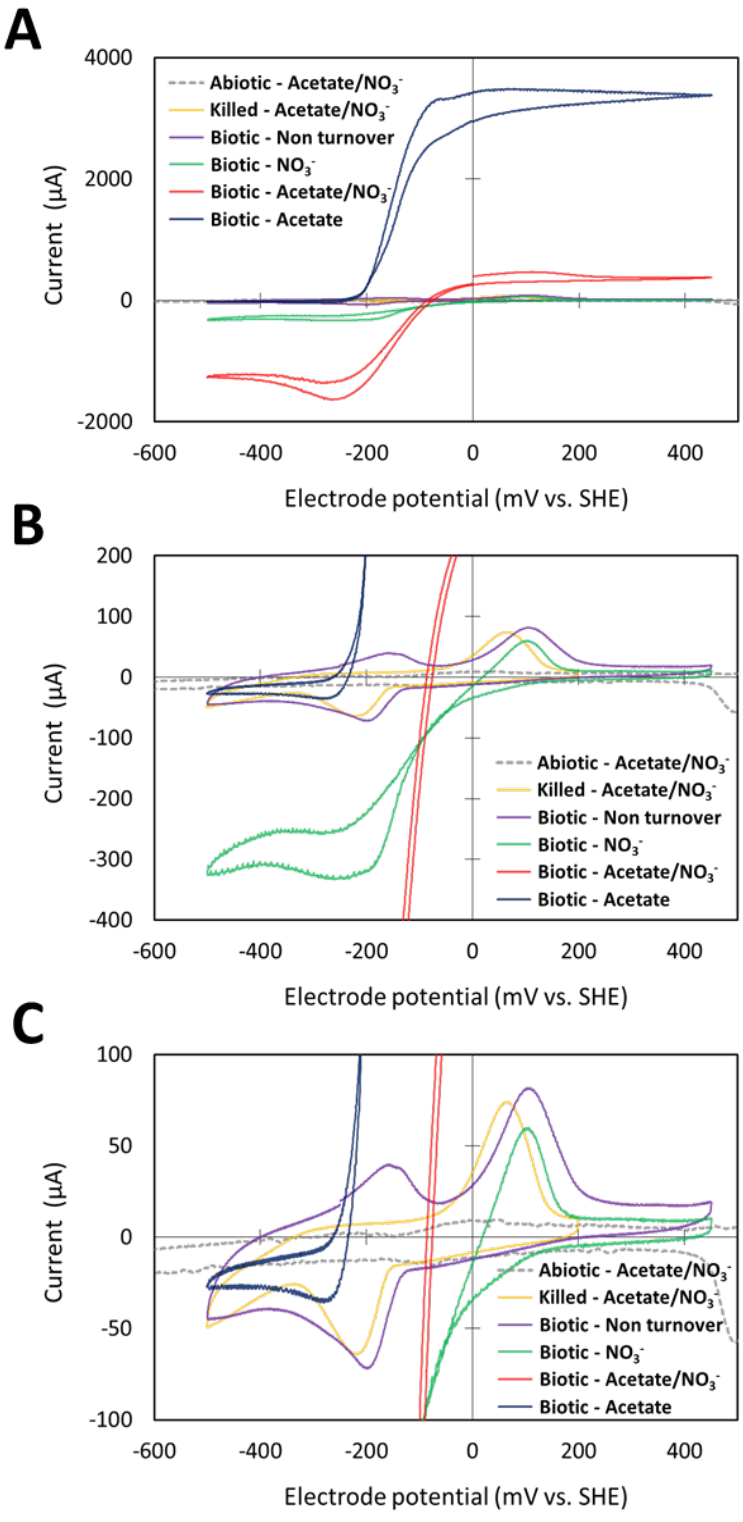
A
4000
2000
0
-2000
Current (µA)
-600
-400
-200
0
200
400
Electrode potential (mV vs. SHE)
Abiotic - Acetate/NO3-
Killed - Acetate/NO3-
Biotic - Non turnover
Biotic - NO3-
Biotic - Acetate/NO3-
Biotic - Acetate
B
200
100
0
-100
-200
-300
-400
Current (µA)
-600
-400
-200
0
200
400
Electrode potential (mV vs. SHE)
Abiotic - Acetate/NO3-
Killed - Acetate/NO3-
Biotic - Non turnover
Biotic - NO3-
Biotic - Acetate/NO3-
Biotic - Acetate
C
100
50
0
-50
-100
Current (µA)
-600
-400
-200
0
200
400
Electrode potential (mV vs. SHE)
Abiotic - Acetate/NO3-
Killed - Acetate/NO3-
Biotic - Non turnover
Biotic - NO3-
Biotic - Acetate/NO3-
Biotic - Acetate

Figure 4-7: Representative cyclic voltammograms of anodically acclimatized *G. metallireducens* biofilms under different conditions. **Panels A-C** shows the same set of voltammograms with different current (y axis) windows. All CVs except abiotic CV were conducted in potential scan window between -500 mV and +450 mV vs. SHE with scan rate of 0.2 mV/sec. Abiotic CV was scaned between -700 mV and +1100 mV with the same scan rate. **Abiotic-Acetate/NO_3^-** (grey dot line) was obtained from CV of uninoculated electrode in the presence of 10 mM acetate and 5 mM nitrate. **Killed-Acetate/NO_3^-** (yellow line) was obtained from CV of gamma-irradiated electrode with anodically-grown biofilm in the presence of 10 mM acetate and 5 mM nitrate. **Biotic-Non turnover** (purple line) was obtained from CV of biofilm-grown electrode in the absence of acetate and nitrate. Small amount of acetate, which was left from biofilm aclimatization operation, was detected from working electrode chamber of replicated reactors with their concentrations less than 0.1 mM. **Biotic-NO_3^-** (green line) was obtained from CV of biofilm-grown electrode that was shifted to cathodic condition with poised electrode potential at -250 mV with 3 mM of nitrate. CV was started after recorded stable cathodic current (after ~5 h of cathodic operation). **Biotic-Acetate/NO_3^-** (red line) was obtained from CV of biofilm-grown electrode in the presence of 10 mM acetate and ~3 mM nitrate. **Biotic-Acetate** (blue line) was obtained from CV of biofilm-grown electrode with 10 mM acetate without nitrate.

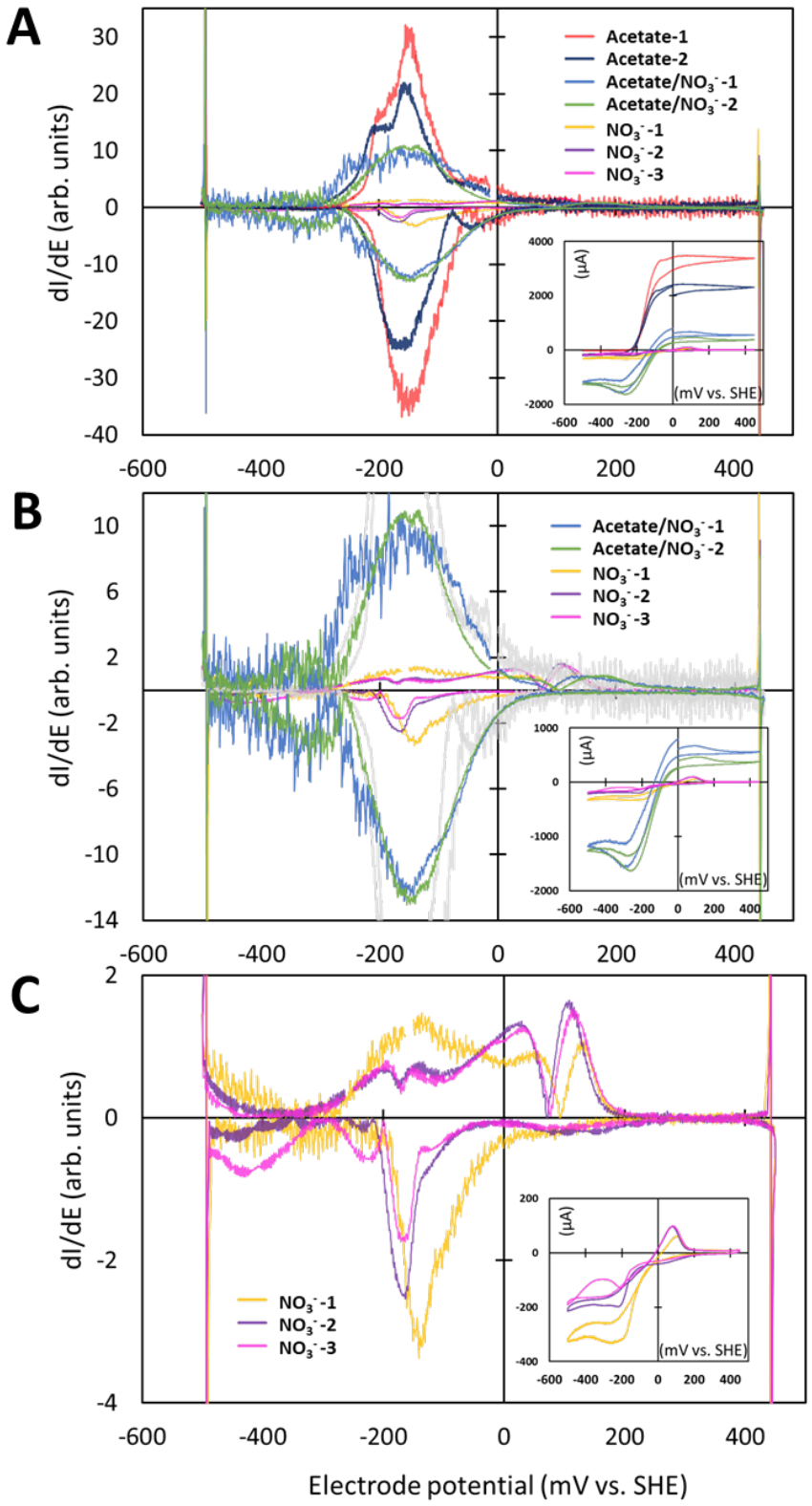
A
B
C
dI/dE (arb. units)
Electrode potential (mV vs. SHE)
Acetate-1
Acetate-2
Acetate/NO3-1
Acetate/NO3-2
NO3-1
NO3-2
NO3-3
(μA)
(mV vs. SHE)

Figure 4-8: First derivative of representative cyclic voltammograms of anodically acclimatized *G. metallireducens* biofilms under different turnover conditions. Plots designated as Acetate, Acetate/NO_3^-, and NO_3^- were calculated from voltammograms under the presence of 10 mM acetate, 10 mM acetate and 3 mM nitrate, and 3 mM nitrate, respectively. Numbers shown with each condition designate the data derived from representative voltamograms obtained from CVs of replicated biofilms. **Panels A-C** first derivative voltammograms with different dI/dE windows. Inset figures in each panel shows cyclic voltammograms that is used to obtain first derivatives shown in each panel.

4.4. Literature Cited

1. Logan, B.E. and K. Rabaey, *Conversion of wastes into bioelectricity and chemicals by using microbial electrochemical technologies.* Science, 2012. **337**(6095): p. 686-690.
2. Caccavo, F., et al., *Geobacter sulfurreducens sp. nov., a hydrogen-and acetate-oxidizing dissimilatory metal-reducing microorganism.* Applied and Environmental Microbiology, 1994. **60**(10): p. 3752-3759.
3. Myers, C.R. and K.H. Nealson, *Bacterial manganese reduction and growth with manganese oxide as the sole electron acceptor.* Science, 1988. **240**.
4. Holmes, D.E., et al., *Microarray and genetic analysis of electron transfer to electrodes in Geobacter sulfurreducens.* Environmental Microbiology, 2006. **8**(10): p. 1805-15.
5. Nevin, K.P., et al., *Anode biofilm transcriptomics reveals outer surface components essential for high density current production in Geobacter sulfurreducens fuel cells.* Plos One, 2009. **4**(5): p. e5628.
6. Reguera, G., et al., *Extracellular electron transfer via microbial nanowires.* Nature, 2005. **435**(7045): p. 1098-1101.
7. Reguera, G., et al., *Biofilm and nanowire production leads to increased current in Geobacter sulfurreducens fuel cells.* Applied and Environmental Microbiology, 2006. **72**(11): p. 7345-7348.
8. Reguera, G., et al., *Possible nonconductive role of Geobacter sulfurreducens pilus nanowires in biofilm formation.* Journal of Bacteriology, 2007. **189**(5): p. 2125-2127.

9. Inoue, K., et al., *Specific localization of the c-type cytochrome OmcZ at the anode surface in current-producing biofilms of Geobacter sulfurreducens.* Environmental microbiology reports, 2011. **3**(2): p. 211-7.

10. Leang, C., et al., *Alignment of the c-type cytochrome OmcS along pili of Geobacter sulfurreducens.* Applied and Environmental Microbiology, 2010. **76**(12): p. 4080-4.

11. Nikhil S. Malvankar, M.V., Kelly P. Nevin, Ashley E. Franks, Ching Leang,, K.I. Byoung-Chan Kim, Tu¨nde Mester, Sean F. Covalla, Jessica P. Johnson,, and M.T.T.a.D.R.L. Vincent M. Rotello, *Tunable metallic-like conductivity in microbial nanowire networks.* NATURE NANOTECHNOLOGY, 2011.

12. Strycharz-Glaven, S.M., et al., *On the electrical conductivity of microbial nanowires and biofilms.* Energy & Environmental Science, 2011. **4**(11): p. 4366.

13. Shi, L., et al., *Respiration of metal (hydr)oxides by Shewanella and Geobacter: a key role for multihaem c-type cytochromes.* Molecular microbiology, 2007. **65**(1): p. 12-20.

14. Kiely, P.D., et al., *Anode microbial communities produced by changing from microbial fuel cell to microbial electrolysis cell operation using two different wastewaters.* Bioresour Technol, 2011. **102**(1): p. 388-94.

15. Yates, M.D., et al., *Convergent development of anodic bacterial communities in microbial fuel cells.* ISME J, 2012. **6**(11): p. 2002-13.

16. Vargas, I.T., I.U. Albert, and J.M. Regan, *Spatial distribution of bacterial communities on volumetric and planar anodes in single‐chamber air‐cathode*

microbial fuel cells. Biotechnology and Bioengineering, 2013. **110**(11): p. 3059-3062.

17. Holmes, D.E., et al., *Enrichment of members of the family Geobacteraceae associated with stimulation of dissimilatory metal reduction in uranium-contaminated aquifer sediments.* Applied and Environmental Microbiology, 2002. **68**(5): p. 2300-2306.
18. Anderson, R.T., et al., *Stimulating the in situ activity of Geobacter species to remove uranium from the groundwater of a uranium-contaminated aquifer.* Applied and environmental microbiology, 2003. **69**(10): p. 5884-5891.
19. Bond, D.R. and D.R. Lovley, *Electricity Production by Geobacter sulfurreducens Attached to Electrodes.* Applied and Environmental Microbiology, 2003. **69**(3): p. 1548-1555.
20. Call, D.F. and B.E. Logan, *Lactate oxidation coupled to iron or electrode reduction by Geobacter sulfurreducens PCA.* Appl Environ Microbiol, 2011. **77**(24): p. 8791-4.
21. Lovley, D.R., et al., *Geobacter metallireducens gen. nov. sp. nov., a microorganism capable of coupling the complete oxidation of organic compounds to the reduction of iron and other metals.* Archives of microbiology, 1993. **159**(4): p. 336-344.
22. Gregory, K.B., D.R. Bond, and D.R. Lovley, *Biocathode Geobacter nitrate reduction. Graphite electrodes as electron donors for anaerobic respiration.* Environmental Microbiology, 2004. **6**(6): p. 596-604.

23. Strycharz, S.M., et al., *Graphite electrode as a sole electron donor for reductive dechlorination of tetrachlorethene by Geobacter lovleyi.* Applied and Environmental Microbiology, 2008. **74**(19): p. 5943-7.

24. Cheng, S., et al., *Direct biological conversion of electrical current into methane by electromethanogenesis.* Environmental Science & Technology, 2009. **43**(10): p. 3953-3958.

25. Siegert, M., et al., *The presence of hydrogenotrophic methanogens in the inoculum improves methane gas production in microbial electrolysis cells.* Frontiers in Microbiology, 2015. **5**.

26. Siegert, M., et al., *MethanobacteriumDominates Biocathodic Archaeal Communities in Methanogenic Microbial Electrolysis Cells.* ACS Sustainable Chemistry & Engineering, 2015. **3**(7): p. 1668-1676.

27. Nevin, K.P., et al., *Microbial electrosynthesis: feeding microbes electricity to convert carbon dioxide and water to multicarbon extracellular organic compounds.* MBio, 2010. **1**(2).

28. Patil, S.A., et al., *Selective Enrichment Establishes a Stable Performing Community for Microbial Electrosynthesis of Acetate from CO2.* Environ Sci Technol, 2015. **49**(14): p. 8833-43.

29. Gregory, K.B. and D.R. Lovley, *Remediation and recovery of uranium from contaminated subsurface environments with electrodes.* Environmental Science & Technology, 2005. **39**(22): p. 8943-8947.

30. Cournet, A., et al., *Electrochemical reduction of oxygen catalyzed by a wide range of bacteria including Gram-positive.* Electrochemistry Communications, 2010. **12**(4): p. 505-508.

31. Clauwaert, P., et al., *Biological denitrification in microbial fuel cells.* Environmental Science & Technology, 2007. **41**(9): p. 3354-3360.

32. Aulenta, F., et al., *Characterization of an electro-active biocathode capable of dechlorinating trichloroethene and cis-dichloroethene to ethene.* Biosens Bioelectron, 2010. **25**(7): p. 1796-802.

33. Thrash, J.C., et al., *Electrochemical stimulation of microbial perchlorate reduction.* Environmental science & technology, 2007. **41**(5): p. 1740-1746.

34. Cheng, K.Y., G. Ho, and R. Cord-Ruwisch, *Anodophilic biofilm catalyzes cathodic oxygen reduction.* Environmental science & technology, 2010. **44**(1): p. 518-525.

35. Cheng, K.Y., M.P. Ginige, and A.H. Kaksonen, *Ano-cathodophilic biofilm catalyzes both anodic carbon oxidation and cathodic denitrification.* Environ Sci Technol, 2012. **46**(18): p. 10372-8.

36. Blanchet, E., et al., *Protons accumulation during anodic phase turned to advantage for oxygen reduction during cathodic phase in reversible bioelectrodes.* Bioresour Technol, 2014. **173**: p. 224-30.

37. Pisciotta, J.M., et al., *Enrichment of microbial electrolysis cell biocathodes from sediment microbial fuel cell bioanodes.* Appl Environ Microbiol, 2012. **78**(15): p. 5212-9.

38. Ross, D.E., et al., *Towards electrosynthesis in Shewanella: energetics of reversing the mtr pathway for reductive metabolism.* Plos One, 2011. **6**(2): p. e16649.

39. Strycharz, S.M., et al., *Gene expression and deletion analysis of mechanisms for electron transfer from electrodes to Geobacter sulfurreducens.* Bioelectrochemistry, 2011. **80**(2): p. 142-50.

40. Geelhoed, J.S. and A.J. Stams, *Electricity-assisted biological hydrogen production from acetate by Geobacter sulfurreducens.* Environmental science & technology, 2011. **45**(2): p. 815-820.

41. Yates, M.D., M. Siegert, and B.E. Logan, *Hydrogen evolution catalyzed by viable and non-viable cells on biocathodes.* International Journal of Hydrogen Energy, 2014. **39**(30): p. 16841-16851.

42. Pous, N., et al., *Bidirectional microbial electron transfer: Switching an acetate oxidizing biofilm to nitrate reducing conditions.* Biosens Bioelectron, 2016. **75**: p. 352-8.

43. Marsili, E., et al., *Microbial biofilm voltammetry: direct electrochemical characterization of catalytic electrode-attached biofilms.* Applied and environmental microbiology, 2008. **74**(23): p. 7329-7337.

44. Kashima, H. and J.M. Regan, *Facultative Nitrate Reduction by Electrode-Respiring Geobacter metallireducens Biofilms as a Competitive Reaction to Electrode Reduction in a Bioelectrochemical System.* Environ Sci Technol, 2015. **49**(5): p. 3195-202.

45. Blümle, S. and W.G. Zumft, *Respiratory nitrate reductase from denitrifying Pseudomonas stutzeri, purification, properties and target of proteolysis.* Biochimica et Biophysica Acta (BBA)-Bioenergetics, 1991. **1057**(1): p. 102-108.

46. Stewart, V. and C.H. MAcGREGOR, *Nitrate reductase in Escherichia coli K-12: involvement of chlC, chlE, and chlG loci.* Journal of Bacteriology, 1982. **151**(2): p. 788-799.

47. Stolz, J.F., et al., *Differential cytochrome content and reductase activity in Geospirillum barnesii strain SeS3.* Archives of microbiology, 1997. **167**(1): p. 1-5.

48. Naik, R.R., M. Francisco M, and J.F. Stolz, *Evidence for a novel nitrate reductase in the dissimilatory iron-reducing bacterium< i> Geobacter metallireducens</i>.* FEMS microbiology letters, 1993. **106**(1): p. 53-58.

49. Murillo, F.M., et al., *A heme-C-containing enzyme complex that exhibits nitrate and nitrite reductase activity from the dissimilatory iron-reducing bacterium Geobacter metallireducens.* Archives of microbiology, 1999. **172**(5): p. 313-320.

50. Lovley, D.R. and E.J. Phillips, *Availability of ferric iron for microbial reduction in bottom sediments of the freshwater tidal Potomac River.* Applied and Environmental Microbiology, 1986. **52**(4): p. 751-757.

51. Yu, L., et al., *Direct uptake of electrode electrons for autotrophic denitrification by Thiobacillus denitrificans.* Electrochemistry Communications, 2015. **60**: p. 126-130.

52. Fu, Q., et al., *Bioelectrochemical Analyses of the Development of a Thermophilic Biocathode Catalyzing Electromethanogenesis.* Environ Sci Technol, 2015.

53. Ishii, T., et al., *From chemolithoautotrophs to electrolithoautotrophs: CO2 fixation by Fe(II)-oxidizing bacteria coupled with direct uptake of electrons from solid electron sources.* Frontiers in Microbiology, 2015. **6**.

54. Welsh, A., et al., *Refined NrfA phylogeny improves PCR-based nrfA gene detection.* Applied and Environmental Microbiology, 2014. **80**(7): p. 2110-9.

55. Finneran, K.T., M.E. Housewright, and D.R. Lovley, *Multiple influences of nitrate on uranium solubility during bioremediation of uranium ‐ contaminated subsurface sediments.* Environmental Microbiology, 2002. **4**(9): p. 510-516.

56. Stewart, V., *Regulation of nitrate and nitrite reductase synthesis in enterobacteria.* Antonie van Leeuwenhoek, 1994. **66**(1-3): p. 37-45.

57. Moreno-Vivián, C., et al., *Prokaryotic nitrate reduction: molecular properties and functional distinction among bacterial nitrate reductases.* Journal of bacteriology, 1999. **181**(21): p. 6573-6584.

58. Nohno, T., et al., *The narX and narL genes encoding the nitrate-sensing regulators of Escherichia coli are homologous to a family of prokaryotic two-component regulatory genes.* Nucleic acids research, 1989. **17**(8): p. 2947-2957.

59. Aklujkar, M., et al., *The genome sequence of Geobacter metallireducens: features of metabolism, physiology and regulation common and dissimilar to Geobacter sulfurreducens.* BMC microbiology, 2009. **9**: p. 109.

60. Gorby, Y.A. and D.R. Lovley, *Electron transport in the dissimilatory iron reducer, GS-15.* Applied and Environmental Microbiology, 1991. **57**(3): p. 867-870.

61. Harnisch, F. and S. Freguia, *A basic tutorial on cyclic voltammetry for the investigation of electroactive microbial biofilms.* Chemistry, an Asian journal, 2012. **7**(3): p. 466-75.

62. Peng, L., et al., *Using Acetate and Formate as the Substrates for Geobacter sulfurreducens Exoelectrogenesis Resulted in Different Half-saturation Potentials.* Electrochemistry, 2015. **83**(8): p. 600-604.

63. Marsili, E., et al., *Microbial biofilm voltammetry: direct electrochemical characterization of catalytic electrode-attached biofilms.* Applied and Environmental Microbiology, 2008. **74**(23): p. 7329-37.

64. Marsili, E., J. Sun, and D.R. Bond, *Voltammetry and Growth Physiology of Geobacter sulfurreducens Biofilms as a Function of Growth Stage and Imposed Electrode Potential.* Electroanalysis, 2010. **22**(7-8): p. 865-874.

65. Zhu, X., M.D. Yates, and B.E. Logan, *Set potential regulation reveals additional oxidation peaks of Geobacter sulfurreducens anodic biofilms.* Electrochemistry Communications, 2012. **22**: p. 116-119.

66. Fricke, K., F. Harnisch, and U. Schröder, *On the use of cyclic voltammetry for the study of anodic electron transfer in microbial fuel cells.* Energy & Environmental Science, 2008. **1**(1): p. 144.

Chapter 5

Study on expression and diversity of *nrfA*, molecular marker of dissimilatorynitrate reduction to ammonium, in wastewater activated sludge

Abstract

Dissimilatory nitrate reduction to ammonium (DNRA) in biological wastewater treatment systems is poorly understood despite its potential impacts on system performance. This study reports differential expression and diversity of *nrfA*, a key marker gene for DNRA, in activated sludge from a full-scale domestic wastewater treatment plant designed for enhanced biological phosphorus removal (EBPR). Expression of *nrfA*, which encodes the penta-heme nitrite reductase NrfA catalyzing the nitrite ammonification step of DNRA, was observed in anaerobic and anoxic sludge, but not in aerobic sludge samples. The expression of *nrfA* under anaerobic and anoxic conditions suggests an overlooked potential for DNRA activity to occur in biological wastewater treatment systems. Some retrieved *nrfA* sequences were related to sequences associated with anammox activity, and the *nrfA* diversity in this wastewater treatment system differed from that observed in soil systems. Retrieved *nrfA* sequences both in genomic DNA and transcript samples were dominated by sequences associated with *Actinobacteria*, which are often abundant in

EBPR processes. This report encourages further studies in different types of wastewater treatment systems and with chemical tracer analyses to obtain comprehensive understanding of DNRA in this context.

Part of materials presented in this chapter was submitted as:

Kashima, H., Bruns, M. A., Regan, J. M., Detection of *nrfA* genes and transcripts, molecular markers of dissimilatory nitrate reduction to ammonium, in wastewater activated sludge. Submitted.

5.1. Introduction

Nitrogen management imposes high economic and environmental costs on human society. Industrial nitrogen fixation via the Haber-Bosch process consumes a considerable percentage of the world's natural gas production, and nitrogen removal from wastewater requires significant money and energy inputs to mitigate the negative impacts of anthropogenic nitrogen on the environment [1]. Our mechanistic understanding of the nitrogen cycle has been dramatically transformed by recent discoveries of novel microbial nitrogen transformations, such as anaerobic ammonia oxidation (anammox) [2], nitrifier denitrification [3], and complete nitrification by a single microorganism [4, 5]. These new insights can lead to improved predictive models and management processes for nitrogen and the associated carbon cycle.

One poorly understood microbial nitrogen transformation is dissimilatory nitrate reduction to ammonium (DNRA) [6]. DNRA is the two-step sequential reduction of nitrate

into ammonium, in which nitrate is first reduced to nitrite by nitrate reductase, a reaction that also occurs during denitrification. The second step, respiratory nitrite ammonification, is distinct from other nitrate transformation reactions such as denitrification or anammox, because it produces ammonium rather than gaseous end products. DNRA has been conventionally presumed to have a minor contribution to nitrate transformation relative to denitrification in anoxic environments [7]. However, a laboratory study demonstrating comparable or an even higher actual energy yield of DNRA to denitrification [8] challenges that presumption. Many recent studies of DNRA in soil [9], sediment [10], estuary [11, 12], and ocean [13] ecosystems indicate a greater role of DNRA in the nitrogen cycle of such systems.

Despite such findings in natural systems, DNRA has been largely overlooked in wastewater treatment systems, even though many systems remove nitrate through biological denitrification processes under conditions permissible for DNRA. For example, the data from a metatranscriptomic analysis of activated sludge showed expression of a DNRA-related gene at levels comparable to nitrification and denitrification genes, but no mention of DNRA was made in the text [14]. The occurrence of DNRA during biological wastewater treatment would have impacts on system performance. For example, DNRA (8 electron transfer reaction) requires 60 % more reducing equivalents than denitrification (5 electron transfer reaction), which would be provided by the oxidation of biochemical oxygen demand (BOD) in wastewater or supplemental electron donors. Also, whereas denitrification removes aqueous nitrogen to the gas phase as dinitrogen, the formation of ammonium by DNRA would result in additional oxygen demand for nitrification or elevated effluent ammonia concentrations. In addition, DNRA could impact emissions of

nitrous oxide, a strong greenhouse gas [15] associated with denitrification processes. Some studies suggested a potential contribution of DNRA to explain increased ammonium levels in denitrifying reactors [16, 17], biofilters [18, 19], and a bioelectrochemical system (BES) [20], but none of these studies investigated direct evidence of DNRA activity. The investigation of DNRA through chemical monitoring is confounded by interconnected nitrogen transformations (e.g., ammonium release associated with biomass decay). While the use of isotope-labeled nitrogen compounds would resolve this problem, this is not feasible in full-scale wastewater treatment systems.

The pentaheme cytochrome C nitrite reductase NrfA, which catalyzes respiratory nitrite ammonification, is unique to DNRA. Therefore, *nrfA* was reported to be a useful molecular marker to assess diversity and activity of microbial populations associated with DNRA [12, 21-23], as genes *nirK* and *nirS* that encode nitrite reductases have been extensively used as molecular markers to characterize denitrification [24]. A recent metagenomic study of anammox communities in two wastewater-treating bioreactors reported an abundance of *nrfA*, indicating DNRA functional capability and suggesting the need for further RNA-based studies to demonstrate actual activity [25]. In the present study, amplicons of *nrfA* genes and transcripts were sequenced to investigate the relative abundance and activity of potential DNRA populations in activated sludge of a full-scale biological wastewater treatment process. We hypothesized that *nrfA* diversity in wastewater treatment processes is different from soil systems and *nrfA* is differentially expressed in different biochemical environments in activated sludge.

5.2. Materials and Methods

5.2.1. Activated Sludge Sample Collection from a Wastewater Treatment Plant

Activated sludge samples were collected from the University Area Joint Authority (UAJA) Plant (State College, PA, USA) on September 10, 2014. The UAJA Plant treats approximately 2.13×10^4 m^3 per day of municipal wastewater from several townships in the State College, PA area and employs the modified University of Cape Town (UCT) process [26] to promote enhanced biological phosphorus removal (EBPR). This design includes three zones with distinct biochemical conditions, and a grab sample was collected from each of these zones (Figure C-1). The anaerobic zone receives primary clarifier effluent and recycled mixed liquor from the end of the downstream anoxic zone, and is designed to select for polyphosphate-accumulating organisms (PAOs) based on their ability to accumulate BOD intracellularly as polyhydroxyalkanoate (PHA) inclusions. The subsequent anoxic zone receives effluent from the anaerobic zone and recycle flow from the downstream aerobic zone (which contains nitrate), and is designed primarily for nitrogen removal via denitrification. The UAJA adds supplemental electron donor to the anoxic zone to improve this denitrification, but other sources of electron donor can include residual BOD not removed by PAO in the anaerobic zone and PHAs in systems that have denitrifying PAO (i.e., DPAO). Finally, an aerobic zone is designed for PHA oxidation by PAOs and nitrification, which is the source of the nitrate that gets recycled to the upstream anoxic zone. The biochemical conditions of the anoxic and aerobic zones (i.e., dissolved oxygen (DO) and nitrate concentration) are monitored continuously (with probe measurements recorded every minute) by the UAJA and were provided for the month of

September 2014 (Table 5-1). The UAJA does not monitor these parameters in the anaerobic zone.

5.2.2. Nucleic Acid Isolation from Activated Sludge Samples and cDNA synthesis

Activated sludge samples were immediately treated with RNAlater Stabilization Solution (Life Technologies) to stabilize nucleic acids in the sample. The DNA and RNA from these samples were co-isolated with PowerMicrobiome RNA Isolation Kit (MO BIO) with several modifications from the manufacturer's instructions. Briefly, activated sludge samples were centrifuged at 5000 × g for 20 min at 4 °C, and 0.1-g pellet fractions of the samples were washed with sterile chilled phosphate buffered saline. An Omni Bead Ruptor 12 Homogenizer (OMNI International) was used for mechanical bead beating with two cycles at 5 m/s for 30 s and 30 seconds of rest time between cycles to avoid heat generation. Isolated nucleic acids were used directly as genomic DNA templates. To prepare the RNA samples, a fraction of isolated nucleic acid samples was treated with TURBO DNase (Life Technologies) to remove DNA and purified with the RNeasy Mini Kit (Qiagen) according to the manufacturer's RNA Cleanup protocol. Quality and quantity of nucleic acid samples were measured with a NanoDrop 2000c Spectrophotometer (Thermo Scientific) and gel electrophoresis. First-strand complementary DNAs (cDNAs) were synthesized from the RNA samples with GoScript Reverse Transcription System (Promega) based on manufacturer's instructions. The cDNA synthesis reaction without reverse transcriptase was also conducted to make Reverse Transcription (RT) controls for examination of residual genomic DNA contamination in the RNA sample.

5.2.3. PCR Amplification of *nrfA* Fragment and Sequencing

Fragments of *nrfA* sequence in DNA, cDNA, and negative PCR control samples were amplified with PCR using the primer set nrfAF2aw (5'-CAR TGY CAY GTB GAR TA-3') and nrfAR1 (5'-TWN GGC ATR TGR CAR TC-3') [23] and the following PCR conditions, which were slightly modified from the method previously reported [23]. Specifically, PCR was conducted by using *Taq* PCR Master Mix Kit (Qiagen) with final concentrations of 0.8 mM each primer, 2.5 mM $MgCl_2$, and ~ 1.6 ng/µL template DNA, with thermal cycling conditions of initial denaturation step at 94 °C for 5 min; 35 cycles of denaturation at 94 °C for 30 s, annealing at 45 °C for 30 s, and extension at 72 °C for 20 s; and a final extension step at 72 °C for 10 min. PCR amplicons were visualized with 2.0 % agarose gel electrophoresis. PCR amplification of *nrfA* fragments was conducted in triplicate and the amplicons were pooled into one sample [23] and purified with the QIAquick PCR Purification Kit (Qiagen). These amplicon samples were then sequenced by paired-end sequencing with Illumina MiSeq with tagged Illumina sequencing primers, F- TCGTCGGCAGCGTCAGATGTGTATAAGAGACAG and R-GTCTCGTGGGCTCGGAGATGTGTATAAGAGACAG.

5.2.4. *nrfA* Sequence Analysis

Raw DNA sequences were subjected to denoising, which involved operational taxonomic unit (OTU) selection at 4 % divergence clustering [27] followed by singleton removal, chimera removal, and base-correction [28]. The reads were then deconvoluted to the FASTA data. After the samples were grouped, a second OTU selection at 3 % divergence was performed via the UPARSE OTU selection algorithm [29]. The centroid OTU sequences were translated and subjected to USEARCH global alignment algorithm [27] against a NrfA amino acid database (just over 4000 NrfA amino acid sequences

including environmental clones from the GenBank protein database) with a 70 % matching criterion to identify their taxonomy. Out of the 710 OTUs generated from DNA sequences, 152 OTU sequences did not meet this 70 % amino acid matching criterion. The DNA sequences of such OTU sequences were subjected to blastX, from which 46 *nrfA*-like OTU sequences were added to the *nrfA* OTU sequence pool based on two criteria: an amplicon size > 160 bp without PCR primer sequences, and blast hit with NrfA or other cytochrome C proteins (Expect value less than 1e-19, determined arbitrarily based on the dataset) without a frameshift. Summary results of the analysis of OTUs that were not identified as *nrfA* OTUs in taxonomic identification via USEARCH global alignment algorithm was shown in Figure C-2. The *nrfA* OTU sequences (604 OTUs) were translated, and 514 amino acid OTUs were obtained by merging identically translated OTUs.

Sequences representing OTUs accounting for greater than 1 % of any sample (21 OTUs) were used to construct a phylogenetic tree and relative abundance heat map. The amino acid sequences of these OTUs, and 55 truncated NrfA sequences from the NCBI database, were aligned using MUSCLE [30]. Bayesian phylogenetic analysis [31] of the alignment was conducted by MrBayes version 3.2 [32] assuming WAG amino acid substitution model [33] with gamma distribution of rates across sites, which showed the lowest BIC and AIC scores for the alignment data set among 48 models through the amino acid substitution model selection package in MEGA5 [34]. Metropolis-coupled Markov chain Monte Carlo (MCMCMC) analysis was conducted with 2 independent runs, 2 million generations, 4 Markov chains with a 0.15 temperature difference constant, and sampling every 1000 generations. Octaheme nitrite reductase (ONR) of *Thioalkalivibrio nitratireducens* was used as outgroup [23, 35]. The consensus tree was constructed after

discarding of 25 % of trees as burn-in. The abundance of OTUs in each sample was illustrated with a heat map, and similarity among samples with respect to OTU composition was illustrated with a dendrogram representing the average linkage hierarchical clustering with Manhattan distance metric constructed using R version 3.1.2. The phylogenetic tree and the heat map were integrated and displayed with Interactive Tree Of Life [36].

5.2.5. Nucleotide Sequence Accession Numbers

Raw sequences of *nrfA* fragments obtained in this study were deposited in the Sequence Read Archive database under the BioProject with accession number PRJNA298591. Representative *nrfA* OTU sequences constituting 21 amino acid-based OTUs that accounted for greater than 1 % of any sample were deposited in the GenBank with accession numbers KT954280 to KT954346.

5.3. Results

5.3.1. Differential *nrfA* Expression in Wastewater Activated Sludge

PCR amplicons of the expected *nrfA* fragment length (approximately 250 bp) were detected in genomic DNA samples from all three distinct biochemical conditions (i.e. anaerobic, anoxic, and aerobic zones). This was expected, as some bacteria commonly found in wastewater treatment systems are known to possess the metabolic potential for nitrite ammonification [23]. By contrast, PCR amplicons of *nrfA* derived from the cDNA preparations were only detected in samples from the anaerobic and anoxic zones, but not the aerobic zone, suggesting *nrfA* was only expressed under anaerobic and anoxic conditions (Figure 5-1). This is consistent with our knowledge of DNRA physiology and also the regulatory system of dissimilatory nitrate and nitrite reduction [37]. The

biochemical data from the time of sampling confirmed that the zones conformed to the expected conditions for a modified UCT design: the anoxic zone had moderate nitrate, and the aerobic zone had relatively high DO and nitrate (Table 5-1). Negative PCR results from the RT-control templates showed that DNase treatment was effective and the positive signals in anaerobic and anoxic cDNA preparations were not due to genomic DNA contamination. Faint amplicon bands of approximately 350 bp were detected in genomic DNA samples from the anaerobic and aerobic zones. These were possibly derived from other multi-heme containing sequences, since this PCR primer set was designed to target heme-binding motifs and could amplify other multiple heme-binding motifs such as other multi-heme cytochromes.

5.3.2. Diversity of *nrfA* Gene and its Transcripts in Activated Sludge in Different Biochemical Conditions

Diverse *nrfA* gene sequences and transcripts were retrieved from the activated sludge samples, with abundances of each OTU varying across samples. Modest differences were observed among DNA samples from different zones, while more pronounced differences were seen between DNA and cDNA samples (Figure 5-2). Many OTUs were closely related to soil *nrfA* clone sequences but distant from *nrfA* sequences of known isolates, suggesting bacterial communities with diverse *nrfA* in wastewater activated sludge which have not yet been characterized well. Two conspicuous OTUs, 1019 and 1040, were abundant in genomic DNA and cDNA preparations across all three conditions. *Austwickia chelonae*, in the class of *Actinobacteria*, was the top protein blast match of OTU 1040. Closely related NrfA sequences to OTU 1019 were also in the class of *Actinobacteria* and included *Actinomyces israelii*, *Propionibacterium propionicum*, and *Arcanobacterium*

haemolyticum. *Actinobacteria* have often been found in activated sludge of EBPR processes [38], such as the UAJA plant sampled in this study. Five OTUs (23, 367, 655, 1031, and 1047) showed higher relative abundance in cDNA samples over genomic DNA samples, suggesting that members of these OTUs actively expressed *nrfA* gene in these activated sludges under anoxic and anaerobic conditions. By contrast, several other OTUs (1028, 1032, 1049, and 1050) exhibited an appreciably higher relative abundance in genomic DNA over cDNA, indicating populations possessing but not actively expressing *nrfA*. Some OTUs were related to *nrfA* sequences derived from anammox bioreactors. OTU 1001 was distant from soil clones but closely related to *nrfA* clones ANASD5, ANASE3, and ANADB07, retrieved from an anammox community using a different forward PCR primer [21]. The top blast hit of OTUs 655 and 1027 was the *nrfA* sequence of *Candidatus* Brocadia fulgida (KKO19962), which was retrieved from metagenomic analysis of an anammox bioreactor enrichment culture.

The centroid sequences representing all 21 OTUs contained a conserved KXQH/KXRH motif that was suggested as a diagnostic feature of all pentaheme NrfA proteins [23]. Specifically, OTUs 1011, 1012, and 1013 had KMQH while all other OTUs had KAQH sequence (Figure 5-3). The highest protein blast hits of the former three OTU sequences were uncultured soil *nrfA* clones UCA5 and UCE2 from Welsh et al. (2014), which had KMQH (UCA5) and KIQH (UCE2) sequences. Those two soil clone sequences were classified in clade L, in which many database sequences possessed a variable amino acid in the X position of the KXQH/KXRH motif. By contrast, the highest blast hits of other OTUs were soil clone sequences classified into clades J, K, and M [23], which had A in the X position of the motif.

The *nrfA* PCR amplicon sequences from this study included some non-*nrfA* sequences that were removed from the *nrfA* OTU pool through blastX search following UPARSE OTU selection. Collectively, these 106 OTUs corresponded to 0.05, 0.06, 0.44, 2.38, and 5.89 % of total sequence reads in DNA anaerobic, DNA anoxic, DNA aerobic, cDNA anaerobic, and cDNA anoxic samples, respectively. These non-*nrfA* sequences included OTUs closely related to other multiheme cytochrome sequences, such as hexa-heme cytochrome of *Zixibacteria* spp. and C554 cytochrome of *Geobacter lovleyi*, as well as other gene sequences. Some of those OTU sequences exhibited signatures of a frameshift mutation in blastX search. Also, OTUs with a NrfA blastX hit derived from a different reading frame were presumed to not contribute to nitrite ammonification and were removed from the *nrfA* OTU pool. Whereas faint DNA bands with approximate fragment size of 350 bp were observed in genomic DNA samples from the anaerobic and aerobic zones (Figure 5-1), sequences corresponding to this length were not retrieved. After denoising and chimera removal processes, centroid OTU sequences longer than 300 bps (including primer sequences), all of which were non-*nrfA* sequences, only accounted for 0.15 % or less of sequences for each sample. This suggested that sequences corresponding to the 350 bp bands were not successfully sequenced with MiSeq or were discarded in denoise-chimera removal processes.

In addition to above analysis of UAJA activated sludge samples, another grab sample was obtained from anoxic denitrification tank in the biological nitrogen removal process in The Pennsylvania State University Wastewater Treatment Plant (PSU plant) University Park, PA. The PSU plant employs trickling filter [26] followed by activated sludge based nitrification and denitrification processes which is different from the UAJA

plant (Figure C-1). Preliminary clone library analysis of cDNA preparation derived from activated sludge sample from anoxic tank of PSU plant yielded *nrfA* sequences with signature KXQH/KXRH motif in translated amino acid sequences. In phylogenetic analysis of these PSU clone sequences and clone sequences derived from cDNA preparations of UAJA anoxic and anaerobic samples, clone sequences retrieved from PSU sample were placed in different phylogenetic positions from ones retrieved from UAJA samples (Figure C-3). These results suggested that bacterial population possess *nrfA* are exist in different types of wastewater treatment processes but the phylogenetic diversity is of *nrfA* is different among different process types.

5.4. Discussion

Results demonstrated that activated sludge of biological wastewater treatment processes can harbor bacterial communities with diverse *nrfA*, of which a significant portion of phylotypes has yet to be better characterized. Many *nrfA* OTUs detected in the activated sludge were closely related to soil *nrfA* clones, but some conspicuous OTUs were distant from soil clones and similar to clones retrieved from anammox communities or *Actinobacteria*.

Several OTUs with high abundance across the samples were classified as *Actinobacteria*, which have been detected previously in wastewater activated sludge. High abundances of *Actinobacteria* representatives are also often found in EBPR processes, such as the wastewater treatment plant surveyed in this study [39, 40]. Alternating exposure of the microbial community to aerobic and anaerobic conditions, which occurs in the UAJA plant as a modified UCT process, was suggested as a reason that the slow-growing

actinobacterium *Microthrix parvicella* could have a selective advantage and thrive in EBPR processes [41]. Members of the *Actinobacteria* taxon were also suggested as major polyphosphate -accumulating organisms (PAOs) in some full-scale EBPR plants [42, 43].

The predominance of *Actinobacteria*-like *nrfA* gene and transcript sequences leads to a hypothesis that DNRA is associated with EBPR. PAOs couple the energy yield from respiration with the uptake of phosphate and the formation of intracellular poly-phosphate granules. While oxygen typically serves as the terminal electron acceptor in EBPR systems, nitrate and nitrite can also be suitable electron acceptors for denitrifying PAOs under anoxic conditions [39, 44]. Studies on nitrate and nitrite-reducing PAOs have extensively investigated denitrification as the mechanism and associated nitrous oxide emission from the process [45, 46], but the potential contribution of DNRA has not been reported. While the somewhat limited *nrfA* database does not specifically intersect with known PAOs, some *Actinobacteria* such as *Tetrasphaera japonica* isolated from activated sludge [47, 48] and *Microlunatus phosphovorus* [49-51] are known PAO and also possess the cytoplasmic nitrite reductase NirBD. While nitrite ammonification by cytoplasmic NirBD is not coupled with proton motive force generation and therefore does not compose a respiratory chain, this nitrite reduction was reported to be used as a dissimilatory process, in addition to assimilatory cytoplasmic ammonium production, as a sink for excess reducing equivalents to regenerate NAD+. This cytoplasmic nitrite reduction is also a detoxifying process to treat accumulated nitrite in a nitrate-respiring cell [37, 52]. For example, *Tetrasphaera japonica*, an intracellular poly-phosphate storage confirmed *Actinobacteria* species isolated from activated sludge [47, 48] and *Microlunatus phosphovorus*, a bacterium conducts nitrate reduction, and phosphorus uptake associated with glucose

fermentation [49-51] contains *nirBD* encoding NirBD as well as denitrifying *nirK* on their genome. The expression of *Actinobacteria*-like *nrfA* in an EBPR full-scale wastewater treatment processes and nitrite ammonifying genes, *nrfA* and *nirBD*, on genome of PAO or related *Actinobacteria* suggested potential contribution of DNRA in anaerobic metabolism of phosphate accumulating *Actinobacteria*. Phosphate uptake coupled with nitrite ammonification in DNRA does not favorable for nitrogen removal strategy but potentially a better pathway for phosphate uptake than denitrification particularly under anoxic nitrate/nitrite limiting conditions since it drives a 60 % greater electron transfer as per nitrite. Further study is encouraged to investigate metabolic link between DNRA and phosphate uptake of PAOs and its impact on phosphorus and nitrogen cycles.

It was interesting to see *nrfA* OTUs expressed in anaerobic and anoxic conditions that are similar to *nrfA* sequences retrieved from anammox systems. DNRA has been reported in anammox conditions [21, 53] and was suggested to provide ammonia for anammox [54]. A recent metagenomic study reported higher abundance of *nrfA* relative to the NO-producing nitrite reductases *nirK* and *nirS* associated with denitrification in anammox communities [25]. Further study is needed to investigate the role of bacterial populations possessing *nrfA* related to the sequences retrieved from anammox systems in activated sludge.

DNRA could also be important in other wastewater treatment processes such as BESs [55], as many metal/sulfate-reducing bacteria with electrogenic or electrotrophic activity such as *Geobacter metallireducens* [56], *Shewanella oneidensis* [57], and *Desulfobulbaceae* [58, 59] have potential to conduct DNRA. Studies of integrated nitrogen removal in BESs [60, 61] have been primarily focused on denitrification as the nitrate

reduction mechanism, but the potential contribution of DNRA has not been investigated. In addition, DNRA could act as a competitive side reaction to desired BES processes. For example, facultative DNRA could disrupt anode reduction [62]. Alternatively, cathode-derived electrons could be directed to DNRA instead of reductive dechlorination with bacteria capable of DNRA such as *Anaeromyxobacter dehalogenans* [63, 64].

Preliminary clone library analysis examined phylogenetic placements of *nrfA* sequences derived from the UAJA plant and the PSU plant suggested that bacterial population possess *nrfA* are exist in different types of wastewater treatment processes but the phylogenetic diversity is of *nrfA* is different among different process types. Further study is needed to characterize bacterial communities across different types of biological wastewater treatment processes.

The *nrfA* sequences retrieved in this study broaden the representation of diversity in the rather limited *nrfA* database, which is primarily comprised of pure culture and soil-derived sequences. This study also extends the database to include *nrfA* genes expressed under different biochemical conditions. Some non-*nrfA* sequences were retrieved, which is not surprising since the *nrfA* PCR primers hybridize to heme-binding motifs and could also amplify non-*nrfA* sequences with these heme-binding motifs in environmental nucleic acid samples. Those non-*nrfA* sequences were sorted out from *nrfA*-like sequences through NrfA database match, size segregation, blastX, and the signature KXQH/KXRH motif. These findings suggest uncharacterized diverse bacterial populations that possess and express *nrfA*. This study encourages further research targeting *nrfA* in different types of activated sludge designs, a quantitative assessment of *nrfA* genes and transcripts relative to other nitrate-reducing pathways [11], and laboratory-based isotope labeled tracer analyses

to obtain a comprehensive understanding of DNRA in biological wastewater treatment systems.

5.5. Acknowledgement

This study was supported by the Penn State Institutes of Energy and the Environment (PSIEE) 2015/2016 Seed Grant Program and the USDA National Institute of Food and Agriculture, Hatch Project 1003346. I thank Art Brant and Tom Willson, from the University Area Joint Authority Plant, for providing operational data and assisting with activated sludge sampling.

Table 5-1. Biochemical conditions measured in activated sludge during the sampling month [a]

	Dissolved oxygen (mg O_2/L)	Nitrate (mg NO_3^--N/L)
Anoxic zone	Not measured	2.67 ± 3.32 [b]
Aerobic zone	2.98 ± 0.27	9.36 ± 3.41 [c]

[a] Averaged dissolved oxygen and nitrate concentration of activated sludge monitored continuously and recorded every minute in anoxic and aerobic zones of September 2014 shown with ± SD. Dissolved oxygen and nitrate concentration were not monitored in anaerobic zone.

[b] Probe was located near the middle of the anoxic zone. The averaged nitrate concentration is typical for this section of the plant, but large SD was due to a one-week perturbation in performance during this month as a result of variable loading. Such perturbations occur in this plant several times a year.

[c] Probe was located near the end of the aerobic zone.

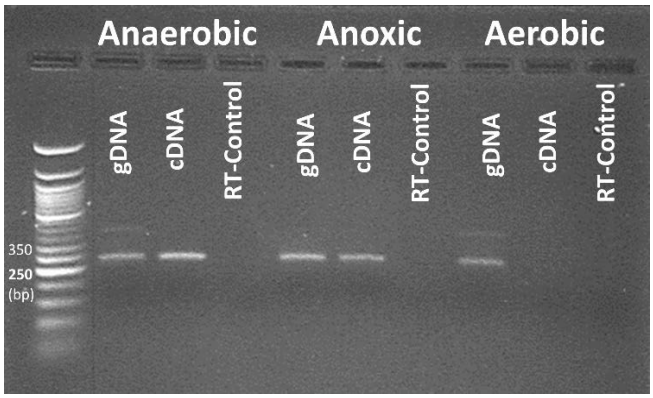

Figure 5-1: Agarose gel of PCR products amplified with *nrfA* primers (nrfAF2aw and nrfAR1 for expected length of approximately 250 bp). Nucleic acids were isolated from activated sludge samples collected from the anaerobic, anoxic, and aerobic zones of the UAJA plant. Lanes designated as gDNA and cDNA were loaded with PCR products from isolated genomic DNA and cDNA preparations, respectively. RT-controls to test for gDNA contamination were cDNA preparations without reverse transcriptase treatment.

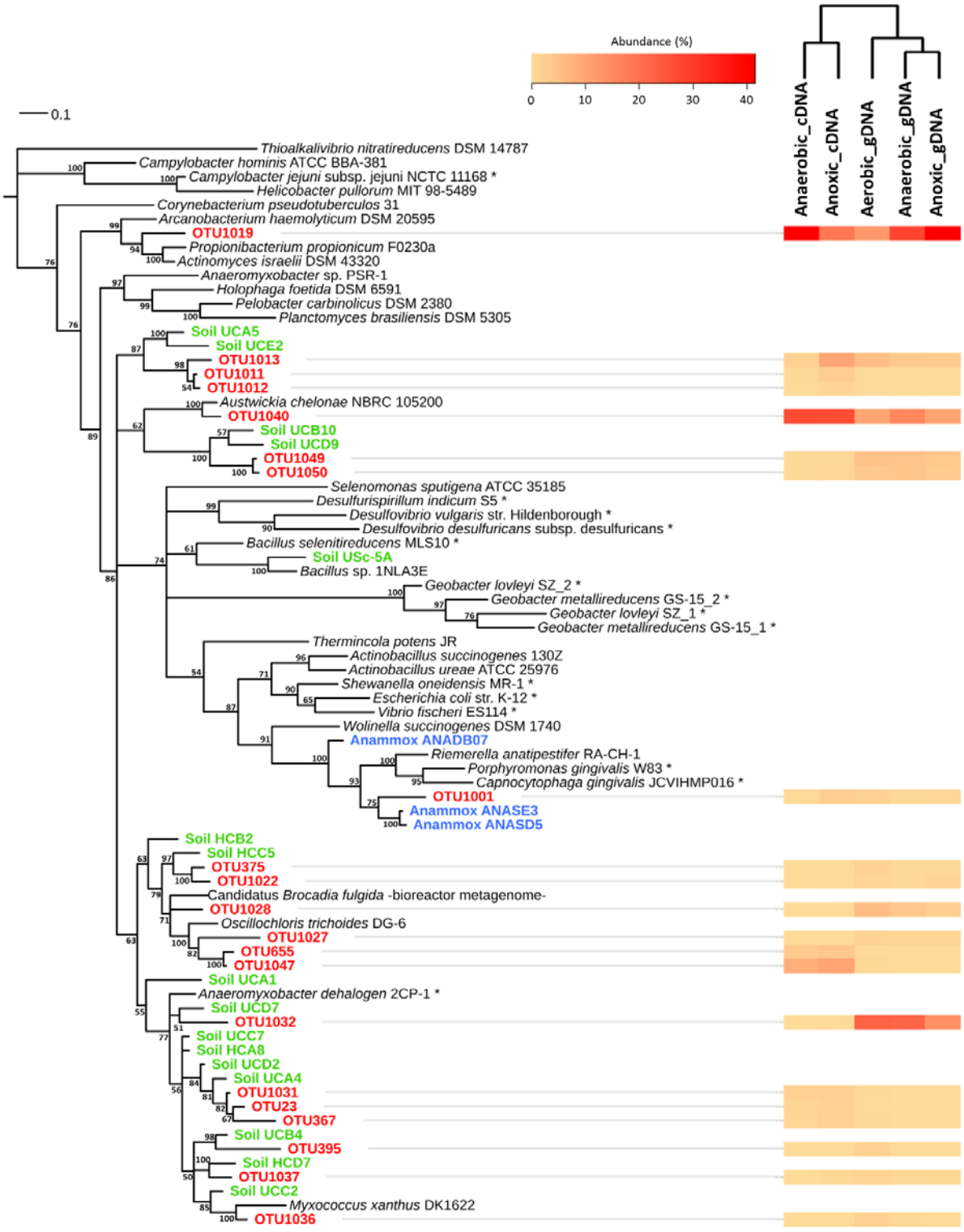
Abundance (%)
0
10
20
30
40
0.1
Anaerobic_cDNA
Anoxic_cDNA
Aerobic_gDNA
Anaerobic_gDNA
Anoxic_gDNA
Thioalkalivibrio nitratireducens DSM 14787
Campylobacter hominis ATCC BBA-381
Campylobacter jejuni subsp. jejuni NCTC 11168 *
Helicobacter pullorum MIT 98-5489
Corynebacterium pseudotuberculos 31
Arcanobacterium haemolyticum DSM 20595
OTU1019
Propionibacterium propionicum F0230a
Actinomyces israelii DSM 43320
Anaeromyxobacter sp. PSR-1
Holophaga foetida DSM 6591
Pelobacter carbinolicus DSM 2380
Planctomyces brasiliensis DSM 5305
Soil UCA5
Soil UCE2
OTU1013
OTU1011
OTU1012
Austwickia chelonae NBRC 105200
OTU1040
Soil UCB10
Soil UCD9
OTU1049
OTU1050
Selenomonas sputigena ATCC 35185
Desulfurispirillum indicum S5 *
Desulfovibrio vulgaris str. Hildenborough *
Desulfovibrio desulfuricans subsp. desulfuricans *
Bacillus selenitireducens MLS10 *
Soil USc-5A
Bacillus sp. 1NLA3E
Geobacter lovleyi SZ_2 *
Geobacter metallireducens GS-15_2 *
Geobacter lovleyi SZ_1 *
Geobacter metallireducens GS-15_1 *
Thermincola potens JR
Actinobacillus succinogenes 130Z
Actinobacillus ureae ATCC 25976
Shewanella oneidensis MR-1 *
Escherichia coli str. K-12 *
Vibrio fischeri ES114 *
Wolinella succinogenes DSM 1740
Anammox ANADB07
Riemerella anatipestifer RA-CH-1
Porphyromonas gingivalis W83 *
Capnocytophaga gingivalis JCVIHMP016 *
OTU1001
Anammox ANASE3
Anammox ANASD5
Soil HCB2
Soil HCC5
OTU375
OTU1022
Candidatus Brocadia fulgida -bioreactor metagenome-
OTU1028
Oscillochloris trichoides DG-6
OTU1027
OTU655
OTU1047
Soil UCA1
Anaeromyxobacter dehalogen 2CP-1 *
Soil UCD7
OTU1032
Soil UCC7
Soil HCA8
Soil UCD2
Soil UCA4
OTU1031
OTU23
OTU367
Soil UCB4
OTU395
Soil HCD7
OTU1037
Soil UCC2
Myxococcus xanthus DK1622
OTU1036

Figure 5-2: Bayesian phylogenetic tree based on analysis of amino acid sequences encoded by *nrfA* fragment between the nrfAF2AW/nrfAR1 PCR primer set target sites. The tree includes 21 representative *nrfA* OTU sequences retrieved in this study, and 55 *nrfA* sequences from pure cultures and uncultured clones. Octaheme nitrite reductase (ONR) of *Thioalkalivibrio nitratireducens* was used as outgroup. Numbers designate posterior probabilities of each node. Taxa with an asterisk, *, have been demonstrated to conduct nitrite ammonification. Groups of taxa are indicated by colors as follows: OTUs retrieved from this study (red), uncultured soil clones (green) from Welsh et al. (2014) [23], and uncultured anammox reactor clones (blue) from Mohan et al. (2004) [21]. The heat map on the right illustrates relative abundance of OTUs in each sample with percent abundance shown in the color key as a linear color progression. Similarity among samples with respect to OTU composition was illustrated with a dendrogram representing the average linkage hierarchical clustering with Manhattan distance metric.

```
                1                  10                  20                  30                  40                  50                  60                  68
OTU23     HFKG-PEKRLVYPWAKGLKVENILAYYDGAKFKDWTHADTGALTLKAQHPEFELWNQG-IHARSGVACA
OTU367    HFKG-PEKRLTYPWSKGLKVEDIMAYYDEIKFKDWTHAESGAETLKAQHPEFELWNQG-IHARAGVSCA
OTU375    YFKG-EGKLLTYPWHKGVKAEQIESYYDEVGWKDWQHTDSGAPVLKAQHPEFEMWSQG-IHARSGVSCA
OTU395    YFKG-PDKQLTFPWHNGLKADQILSYYQENKHKDWVHKETSAPVLKAQHPEFEMFNQG-THARAGVSCV
OTU655    RFKG-DEKLLTYPWQNGLKMEEAEAYYDEIGFKDWTHKDSGATVLKAQHPEFEMWSQG-IHAASGVTCA
OTU1001   YFKGKEEEKYLTFPWDKGFTVEDIEQYYDSVKHVDFVNTLSRTPIVKAQHPDFELFKAG-IHSERGLSC-
OTU1011   YFKG-DNKVLTFPWEQGLSIDNIEAYYNKYGFKDWDHAESGAPMLKMQHPEFEMYSSG-IHAQSGVACA
OTU1012   YFKG-DNKVLTFPWEQGLSIDNIEVYYNKYGFKDWDHAESGAPMLKMQHPEFEMYSSG-IHAQSGVACA
OTU1013   YFQG-DNKVLTFPWAEGLSIDNIETYYNSYGFKDWDHAESGAPMLKMQHPEYEMYSSG-IHAQSGVACA
OTU1019   YFAG-DAKTLTFPWDKGLTVTNALDYYDQVGFTDFTHTLTGAKALKAQHPDFETWSQG-IHAANGVTCA
OTU1022   YFKG-EGKLLTYPWQKGLKADQIETYYDEVGWKDWVHADSGAPVLKAQHPEFEMWSQG-IHARSGVSCA
OTU1027   YFKG-DAKLVVFPWQNGLKMEQIESYYDTAAFKDFVHKDSGANVLKAQHPEFETWSQG-VHAQSGVSCA
OTU1028   YFKG-DGKLLTYPWFNGLKVEQIEKYYDEQGFSDWTHADSGAKVIKAQHPEFETWSQG-IHARSGVACA
OTU1031   YFKG-PEKRLVYPWAKGLKVENILAYYDEAKFKDWTHADTGALTLKAQHPEFELWNQG-IHARSGVSCA
OTU1032   YFKG-PEKRLTFPWANGLRADEILAYYEQTGFKDWTHADTGASTLKAQHPEFELWSQG-VHARSGVSCA
OTU1036   YFKG-PEKRLVYPWAKGMKIDEIMAYYEENGHKDWTHAETGASVLKAQHPEFELYNQG-IHARSGVACA
OTU1037   YFKG-TEKRLVYPWANGVKVEEILAYYDEVKHKDWVHAESGAPTLKAQHPEFELWNQG-IHARSGVACA
OTU1040   YFKG-DAKTLTFPWDKGSKATDALAYYDEVGFKDWQHKITNAPALKAQHPEFETWQQG-VHYRAGVSCA
OTU1047   HFKG-DEKLLTYPWQNGLKMEEAEAYYDEIGFKDWTHKDSGATVLKAQHPEFEMWSQG-IHAASGVACA
OTU1049   YFKG-DGKYLTFPWEQGTRIQDIVAYYNEVGFKDWEYPDTGIAMLKAQHPEYELFSAGSTHYAAGVSCA
OTU1050   YFKG-DGKYLTFPWEQGTRIQEIVAYYNEVGFKDWEYPDTGIAMLKAQHPEYELFSAGSTHYAAGVSCA
                                                                                  Δ Δ Δ Δ
```

Figure 5-3: Alignment of amino acid sequences derived from 21 representative *nrfA* OTU sequences retrieved in this study. Partial *nrfA* sequences between the third and the fourth heme-binding motif sites of NrfA (upstream of position 1 and downstream of position 68, respectively) were obtained by the nrfAF2AW/nrfAR1 PCR primer set. Open triangles indicate the conserved KXQH/KXRH motif that was suggested as a diagnostic feature of all pentaheme NrfA proteins [23]. Amino acid residues conserved across all 21 OTU sequences are shaded in gray.

5.6. Literature Cited

1. McCarty, P.L., J. Bae, and J. Kim, *Domestic wastewater treatment as a net energy producer--can this be achieved?* Environmental Science & Technology, 2011. **45**(17): p. 7100-6.
2. Strous, M., et al., *Missing lithotroph identified as new planctomycete.* Nature, 1999. **400**(6743): p. 446-449.
3. Wrage, N., et al., *Role of nitrifier denitrification in the production of nitrous oxide.* Soil Biology and Biochemistry, 2001. **33**(12): p. 1723-1732.
4. van Kessel, M.A., et al., *Complete nitrification by a single microorganism.* Nature, 2015. **528**(7583): p. 555-9.
5. Daims, H., et al., *Complete nitrification by Nitrospira bacteria.* Nature, 2015. **528**(7583): p. 504-9.
6. Tiedje, J.M., *Ecology of denitrification and dissimilatory nitrate reduction to ammonium.* Biology of anaerobic microorganisms, 1988. **717**: p. 179-244.
7. Cole, J., *Physiology, biochemistry and genetics of nitrate dissimilation to ammonia*, in *Denitrification in soil and sediment*. 1990, Springer. p. 57-76.
8. Strohm, T.O., et al., *Growth yields in bacterial denitrification and nitrate ammonification.* Appl Environ Microbiol, 2007. **73**(5): p. 1420-4.
9. Rutting, T., et al., *Assessment of the importance of dissimilatory nitrate reduction to ammonium for the terrestrial nitrogen cycle.* Biogeosciences, 2011. **8**(7): p. 1779-1791.
10. Nizzoli, D., et al., *Effect of organic enrichment and thermal regime on denitrification and dissimilatory nitrate reduction to ammonium (DNRA) in*

hypolimnetic sediments of two lowland lakes. Water Research, 2010. **44**(9): p. 2715-2724.

11. Smith, C.J., et al., *Seasonal variation in denitrification and dissimilatory nitrate reduction to ammonia process rates and corresponding key functional genes along an estuarine nitrate gradient.* Front Microbiol, 2015. **6**: p. 542.
12. Decleyre, H., et al., *Dissimilatory nitrogen reduction in intertidal sediments of a temperate estuary: small scale heterogeneity and novel nitrate-to-ammonium reducers.* Front Microbiol, 2015. **6**: p. 1124.
13. Lam, P., et al., *Revising the nitrogen cycle in the Peruvian oxygen minimum zone.* Proceedings of the National Academy of Sciences, 2009. **106**(12): p. 4752-4757.
14. Yu, K. and T. Zhang, *Metagenomic and metatranscriptomic analysis of microbial community structure and gene expression of activated sludge.* PLoS One, 2012. **7**(5): p. e38183.
15. Canfield, D.E., A.N. Glazer, and P.G. Falkowski, *The evolution and future of Earth's nitrogen cycle.* science, 2010. **330**(6001): p. 192-196.
16. Shen, Z., Y. Zhou, and J. Wang, *Comparison of denitrification performance and microbial diversity using starch/polylactic acid blends and ethanol as electron donor for nitrate removal.* Bioresource Technology, 2013. **131**: p. 33-39.
17. Wu, W., F. Yang, and L. Yang, *Biological denitrification with a novel biodegradable polymer as carbon source and biofilm carrier.* Bioresource technology, 2012. **118**: p. 136-140.

18. McCarthy, M.J. and W.S. Gardner, *An application of membrane inlet mass spectrometry to measure denitrification in a recirculating mariculture system.* Aquaculture, 2003. **218**(1): p. 341-355.

19. Rodriguez-Caballero, A., et al., *Treatment of high ethanol concentration wastewater by biological sand filters: enhanced COD removal and bacterial community dynamics.* Journal of environmental management, 2012. **109**: p. 54-60.

20. Huang, B., et al., *The effect of C/N ratio on nitrogen removal in a bioelectrochemical system.* Bioresource technology, 2013. **132**: p. 91-98.

21. Mohan, S.B., et al., *Detection and widespread distribution of the nrfA gene encoding nitrite reduction to ammonia, a short circuit in the biological nitrogen cycle that competes with denitrification.* Fems Microbiology Ecology, 2004. **49**(3): p. 433-43.

22. Smith, C.J., et al., *Diversity and abundance of nitrate reductase genes (narG and napA), nitrite reductase genes (nirS and nrfA), and their transcripts in estuarine sediments.* Applied and Environmental Microbiology, 2007. **73**(11): p. 3612-22.

23. Welsh, A., et al., *Refined NrfA phylogeny improves PCR-based nrfA gene detection.* Applied and Environmental Microbiology, 2014.

24. Braker, G., et al., *Nitrite Reductase Genes (nirK and nirS) as Functional Markers To Investigate Diversity of Denitrifying Bacteria in Pacific Northwest Marine Sediment Communities.* Applied and Environmental Microbiology, 2000. **66**(5): p. 2096-2104.

25. Guo, J., et al., *Metagenomic analysis of anammox communities in three different microbial aggregates.* Environmental microbiology, 2015.

26. Grady Jr, C.L., et al., *Biological wastewater treatment*. 2011: CRC Press.

27. Edgar, R.C., *Search and clustering orders of magnitude faster than BLAST*. Bioinformatics, 2010. **26**(19): p. 2460-2461.

28. Edgar, R.C., et al., *UCHIME improves sensitivity and speed of chimera detection.* Bioinformatics, 2011. **27**(16): p. 2194-2200.

29. Edgar, R.C., *UPARSE: highly accurate OTU sequences from microbial amplicon reads.* Nature methods, 2013. **10**(10): p. 996-998.

30. Edgar, R.C., *MUSCLE: multiple sequence alignment with high accuracy and high throughput.* Nucleic acids research, 2004. **32**(5): p. 1792-1797.

31. Huelsenbeck, J.P., et al., *Bayesian inference of phylogeny and its impact on evolutionary biology.* science, 2001. **294**(5550): p. 2310-2314.

32. Ronquist, F. and J.P. Huelsenbeck, *MrBayes 3: Bayesian phylogenetic inference under mixed models.* Bioinformatics, 2003. **19**(12): p. 1572-1574.

33. Whelan, S. and N. Goldman, *A general empirical model of protein evolution derived from multiple protein families using a maximum-likelihood approach.* Molecular biology and evolution, 2001. **18**(5): p. 691-699.

34. Tamura, K., et al., *MEGA5: molecular evolutionary genetics analysis using maximum likelihood, evolutionary distance, and maximum parsimony methods.* Molecular biology and evolution, 2011. **28**(10): p. 2731-2739.

35. Klotz, M.G., et al., *Evolution of an octahaem cytochrome c protein family that is key to aerobic and anaerobic ammonia oxidation by bacteria.* Environ Microbiol, 2008. **10**(11): p. 3150-63.

36. Letunic, I. and P. Bork, *Interactive Tree Of Life v2: online annotation and display of phylogenetic trees made easy.* Nucleic Acids Res, 2011. **39**(Web Server issue): p. W475-8.

37. Moreno-Vivián, C., et al., *Prokaryotic nitrate reduction: molecular properties and functional distinction among bacterial nitrate reductases.* Journal of bacteriology, 1999. **181**(21): p. 6573-6584.

38. Seviour, R.J., et al., *Ecophysiology of the Actinobacteria in activated sludge systems.* Antonie van Leeuwenhoek, 2008. **94**(1): p. 21-33.

39. Oehmen, A., et al., *Advances in enhanced biological phosphorus removal: from micro to macro scale.* Water research, 2007. **41**(11): p. 2271-2300.

40. Seviour, R.J., T. Mino, and M. Onuki, *The microbiology of biological phosphorus removal in activated sludge systems.* FEMS Microbiology Reviews, 2003. **27**(1): p. 99-127.

41. Andreasen, K. and P.H. Nielsen, *Growth of Microthrix parvicella in nutrient removal activated sludge plants: studies of in situ physiology.* Water Research, 2000. **34**(5): p. 1559-1569.

42. Kong, Y., J.L. Nielsen, and P.H. Nielsen, *Identity and ecophysiology of uncultured actinobacterial polyphosphate-accumulating organisms in full-scale enhanced biological phosphorus removal plants.* Appl Environ Microbiol, 2005. **71**(7): p. 4076-85.

43. Beer, M., et al., *Which are the polyphosphate accumulating organisms in full‐scale activated sludge enhanced biological phosphate removal systems in Australia?* Journal of applied microbiology, 2006. **100**(2): p. 233-243.

44. Meinhold, J., E. Arnold, and S. Isaacs, *Effect of nitrite on anoxic phosphate uptake in biological phosphorus removal activated sludge.* Water Research, 1999. **33**(8): p. 1871-1883.

45. Pan, Y., et al., *Electron competition among nitrogen oxides reduction during methanol-utilizing denitrification in wastewater treatment.* Water research, 2013. **47**(10): p. 3273-3281.

46. Wei, Y., et al., *The effect of poly-β-hydroxyalkanoates degradation rate on nitrous oxide production in a denitrifying phosphorus removal system.* Bioresource technology, 2014. **170**: p. 175-182.

47. Maszenan, A., et al., *Three isolates of novel polyphosphate-accumulating gram-positive cocci, obtained from activated sludge, belong to a new genus, Tetrasphaera gen. nov., and description of two new species, Tetrasphaera japonica sp. nov. and Tetrasphaera australiensis sp. nov.* International journal of systematic and evolutionary microbiology, 2000. **50**(2): p. 593-603.

48. Kristiansen, R., et al., *A metabolic model for members of the genus Tetrasphaera involved in enhanced biological phosphorus removal.* ISME J, 2013. **7**(3): p. 543-54.

49. Nakamura, K., et al., *Microlunatus phosphovorus gen. nov., sp. nov., a new gram-positive polyphosphate-accumulating bacterium isolated from activated sludge.* International journal of systematic bacteriology, 1995. **45**(1): p. 17-22.

50. Santos, M.M., et al., *Glucose metabolism and kinetics of phosphorus removal by the fermentative bacterium Microlunatus phosphovorus.* Applied and environmental microbiology, 1999. **65**(9): p. 3920-3928.

51. Kawakoshi, A., et al., *Deciphering the genome of polyphosphate accumulating actinobacterium Microlunatus phosphovorus.* DNA research, 2012: p. dss020.

52. Stewart, V., *Regulation of nitrate and nitrite reductase synthesis in enterobacteria.* Antonie van Leeuwenhoek, 1994. **66**(1-3): p. 37-45.

53. Jensen, M.M., et al., *Intensive nitrogen loss over the Omani Shelf due to anammox coupled with dissimilatory nitrite reduction to ammonium.* Isme Journal, 2011. **5**(10): p. 1660-1670.

54. Jasper, J.T., et al., *Nitrate removal in shallow, open-water treatment wetlands.* Environmental science & technology, 2014. **48**(19): p. 11512-11520.

55. Logan, B.E. and K. Rabaey, *Conversion of wastes into bioelectricity and chemicals by using microbial electrochemical technologies.* Science, 2012. **337**(6095): p. 686-690.

56. Aklujkar, M., et al., *The genome sequence of Geobacter metallireducens: features of metabolism, physiology and regulation common and dissimilar to Geobacter sulfurreducens.* BMC Microbiol., 2009. **9**: p. 109.

57. Cruz-Garcia, C., et al., *Respiratory nitrate ammonification by Shewanella oneidensis MR-1.* Journal of Bacteriology, 2007. **189**(2): p. 656-62.

58. Pfeffer, C., et al., *Filamentous bacteria transport electrons over centimetre distances.* Nature, 2012. **491**(7423): p. 218-221.

59. Ishii, S., et al., *A novel metatranscriptomic approach to identify gene expression dynamics during extracellular electron transfer.* Nature communications, 2013. **4**: p. 1601.

60. Virdis, B., et al., *Simultaneous nitrification, denitrification and carbon removal in microbial fuel cells.* Water Research, 2010. **44**(9): p. 2970-80.

61. Kelly, P.T. and Z. He, *Nutrients removal and recovery in bioelectrochemical systems: a review.* Bioresource Technology, 2014. **153**: p. 351-60.

62. Kashima, H. and J.M. Regan, *Facultative Nitrate Reduction by Electrode-Respiring Geobacter metallireducens Biofilms as a Competitive Reaction to Electrode Reduction in a Bioelectrochemical System.* Environ Sci Technol, 2015. **49**(5): p. 3195-202.

63. Strycharz, S.M., et al., *Reductive dechlorination of 2-chlorophenol by Anaeromyxobacter dehalogenans with an electrode serving as the electron donor.* Environ Microbiol Rep, 2010. **2**(2): p. 289-94.

64. Sanford, R.A., J.R. Cole, and J.M. Tiedje, *Characterization and description of Anaeromyxobacter dehalogenans gen. nov., sp. nov., an aryl-halorespiring facultative anaerobic myxobacterium.* Applied and Environmental Microbiology, 2002. **68**(2): p. 893-900.

Appendix A

Supporting Information for Chapter 3

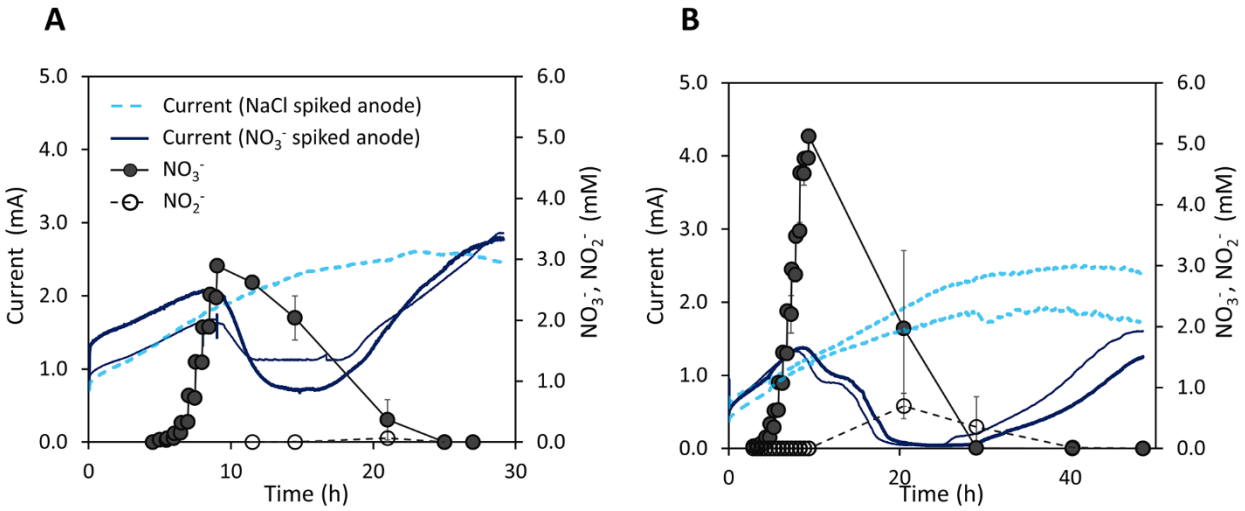

Figure A-1: Current, nitrate, and nitrite profiles in a gradual nitrate spike test of *G. metallireducens* biofilms acclimatized on anodes poised at 0 mV with one batch cycle of 10 mM acetate (0.26 mg-protein/cm^2) (Panel A) and two consecutive batch cycles of 10 mM acetate (0.52 mg-protein/cm^2) (Panel B). Nitrate and nitrite data points are means of duplicates. Error bars designate one standard deviation.

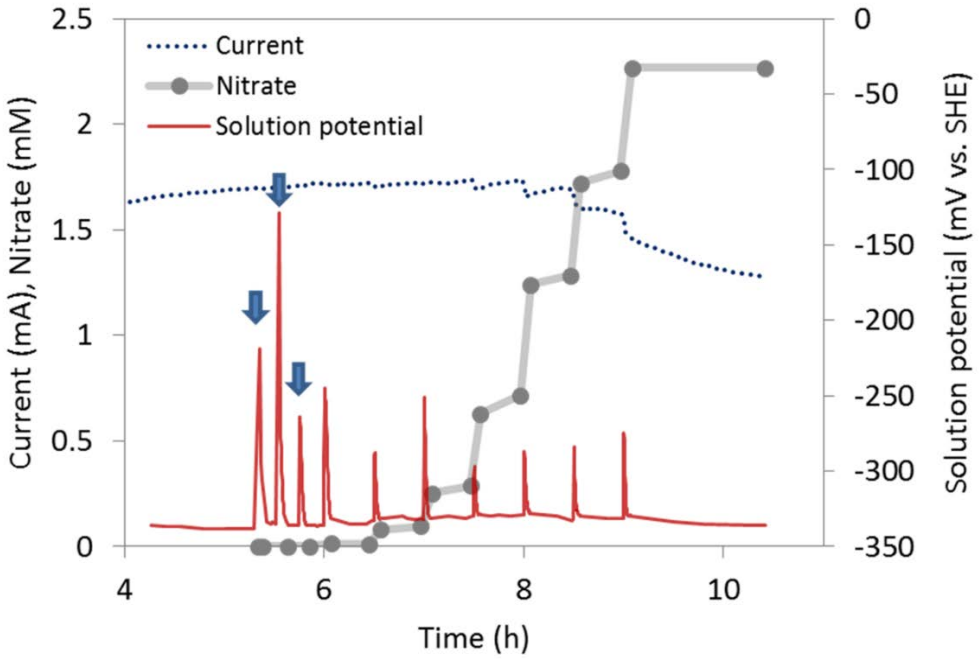

Figure A-2: Current and solution redox potential profile in response to sodium chloride and nitrate spikes. Arrows represent times of sodium chloride spikes. Redox potential of bulk anode chamber solution was measured by a redox electrode (InLab Redox Micro, Mettler Toledo) inserted to the anode chamber. The biofilm was acclimatized on an anode poised at 0 mV with a single batch cycle of 10 mM acetate as the electron donor.

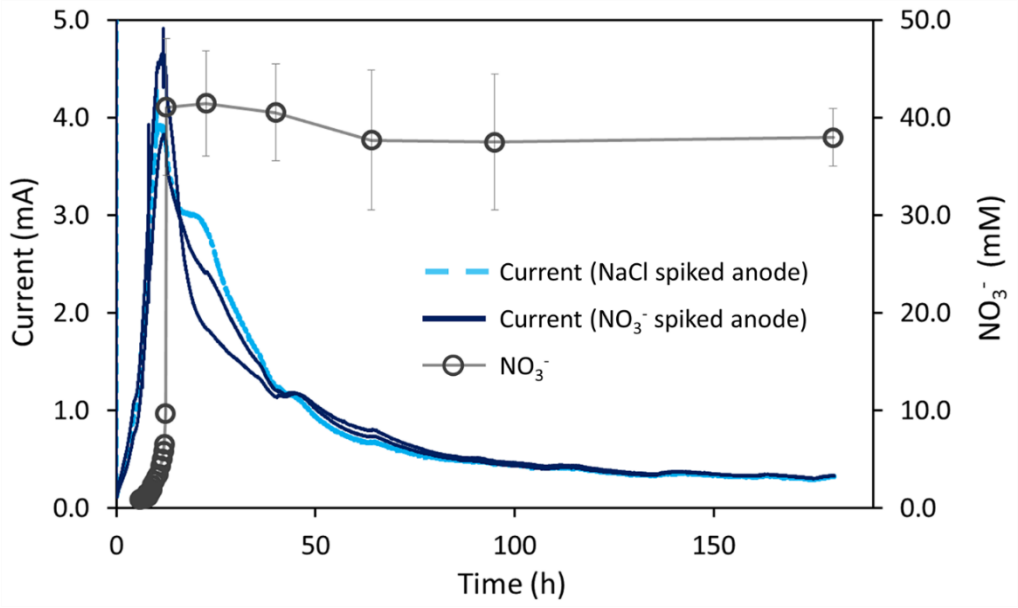

Figure A-3: Current production of *G. sulfurreducens* acclimatized on anodes poised at 0 mV with 0.5 mM acetate in response to gradual spikes of nitrate and chloride. Nitrate data points are means of duplicates. Error bars designate one standard deviation. Chloride spike concentrations were calculated to be equivalent to the nitrate spikes, but they were not measured.

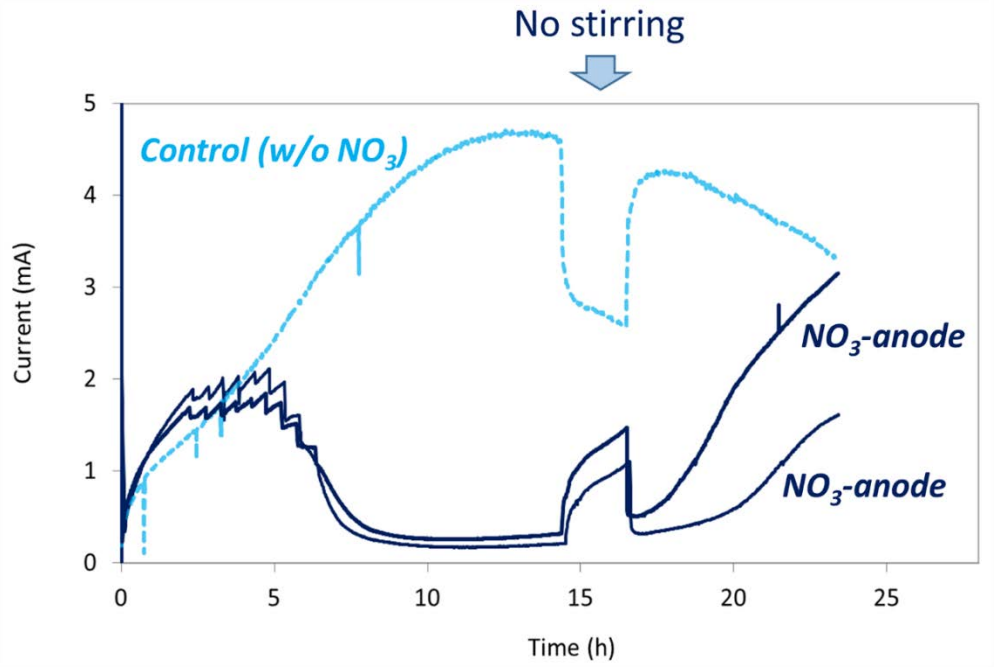

Figure A-4: Effects of intermittent mixing of bulk solution on *G. metallireducens* biofilms subjected to gradual nitrate spikes (NO_3-anode) and chloride spikes (Control (w/o NO_3)). Biofilms were acclimatized on anodes poised at 0 mV with 0.5 mM acetate prior to the shown batch cycle with 10 mM acetate. Stirring at 180 rpm was paused to see the effects of substrate diffusion into and out of anode biofilms. Decreased current of biofilms w/o nitrate during no-stir operation was attributed to decreased acetate and proton transport between bulk liquid and cells in the anode biofilm. By contrast, increased current of nitrate-influenced biofilms during no-stir operation was due to the net effect of decreased acetate and proton transport, which decreases the anode reduction activity of cells in the biofilm, and decreased nitrate transport into the biofilm, which decreased nitrate reduction activity of cells in the biofilm. The bulk acetate concentrations of all anodes was > 8 mM at 20 hours.

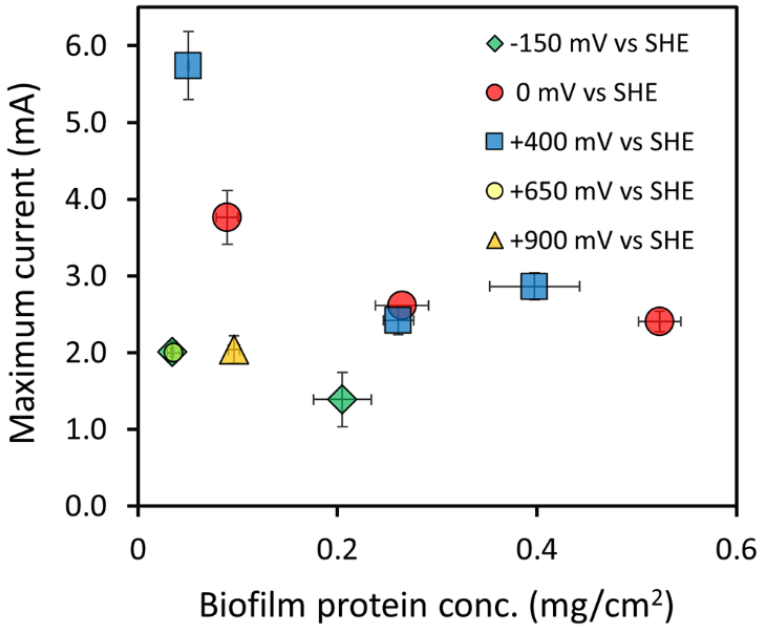

Figure A-5: Maximum current of nitrate-free control biofilms with different biofilm protein concentrations at different anode potentials. Each data point corresponds to a sodium chloride-spiked control from the gradual nitrate spike tests summarized in Figure 2. For each data point, biofilm protein concentration was obtained from two anodes sacrificed for protein analysis at the first nitrate spike (mean, ±S.D.), and maximum current was obtained by duplicate anodes (mean, ±S.D.) or a single anode.

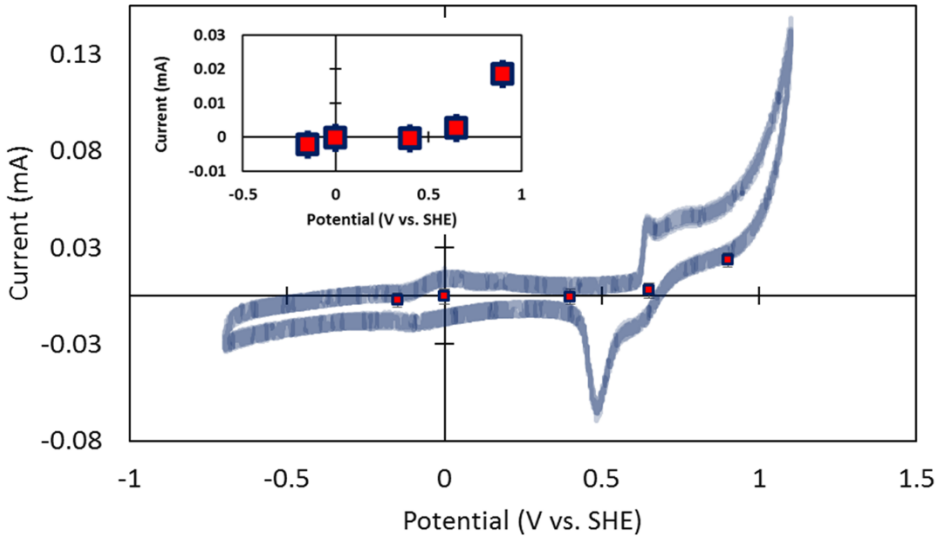

Figure A-6: Abiotic current level across the tested anode potential range, with three representative abiotic CV cycles at a scan rate of 0.2 mV/s as well as averaged abiotic current levels at each poised anode potential (square symbols). Error bars show standard deviation.

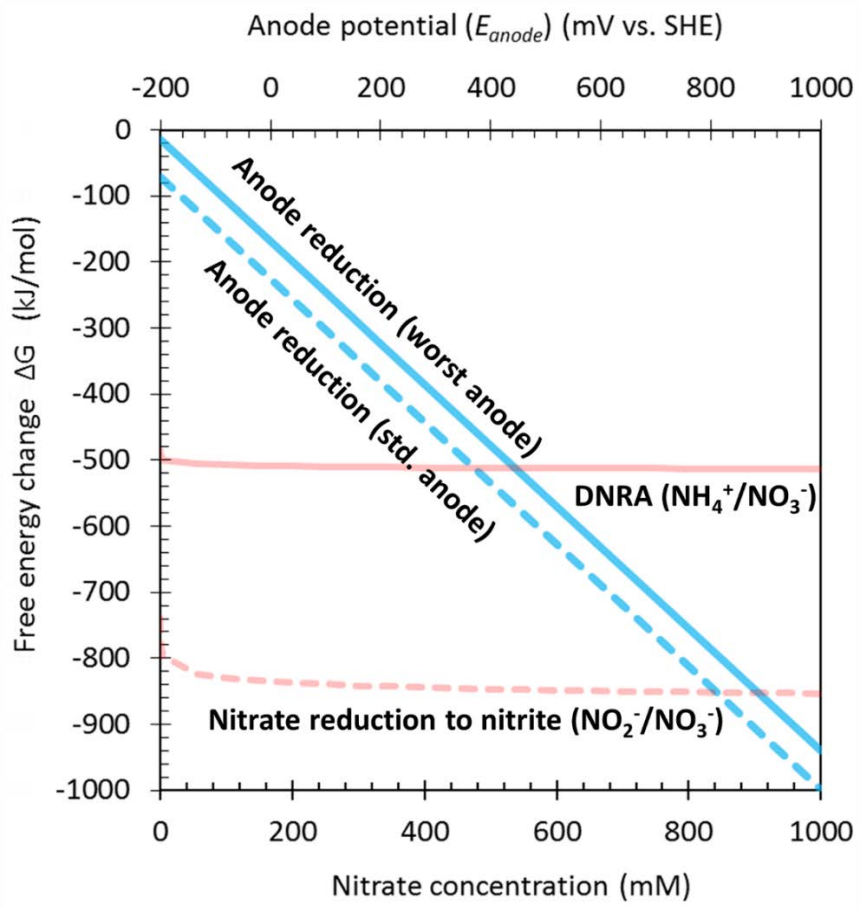

Figure A-7: Thermodynamic potential energy gain of anode respiration at different anode potentials and nitrate respirations at different nitrate concentrations.

The following balanced reactions were used to describe the system: (eq. S1) complete dissimilatory nitrate reduction to ammonia (DNRA), which is conducted by many metal reducers including known exoelectrogens [1]; (eq. S2) nitrate reduction to nitrite, which is the first step of both DNRA and sequential denitrification and thought to be the most energy harvesting step [2]; and (eq. S3) anode reduction coupled with acetate oxidation to carbon dioxide.

$$NO_3^- + 2H^+ + CH_3COO^- = NH_4^+ + CO_2 + HCO_3^- \qquad (1)$$

$$4NO_3^- + CH_3COO^- = 4NO_2^- + CO_2 + HCO_3^- + 2H_2O \quad (2)$$

$$CO_2 + HCO_3^- + 8H^+ + 8e^- = CH_3COO^- + 3H_2O \quad (3)$$

Assuming standard biological conditions (303 K, 1 atm, pH 7.0) in the presence of 10 mM acetate as the model electron donor, the Gibbs free energy change (ΔG_{rxn}; kJ/mol) of the nitrate reduction reactions were calculated by (eq. S4). Based on the Nernst equation, the free energy change by anode reduction was calculated by (eq. S5) for standard biological conditions (pH 7.0) and 10 mM acetate, and a worst-case anode condition represented by an acidified, electron donor-depleted anode (pH 6.0, 0.1 mM acetate) [3].

$$\Delta G_{DNRA\,or\,{NO_2}/{NO_3}} = \Delta G^{\circ} + RT \times LnQ \quad (4)$$

$$\Delta G_{anodereduction} = -nF\left(E_{anode} - Eco_{2}/_{Acetate}\right) \text{ where } Eco_{2}/_{Acetate} = E^{0\prime} + {RT}/_{nF} \times LnQ \quad (5)$$

where ΔG^0 is the Gibbs free energy of reaction under standard condition (kJ/mol), R is the ideal gas constant, Q is the equilibrium constant, F is the Faraday constant, E_{anode} is the anode potential (mV vs. SHE), and $E_{CO2/acetate}$ is the redox potential of the CO_2/acetate redox couple under given condition (mV vs. SHE). Gibbs free energy of formations were obtained from Rittmann and McCarty [4].

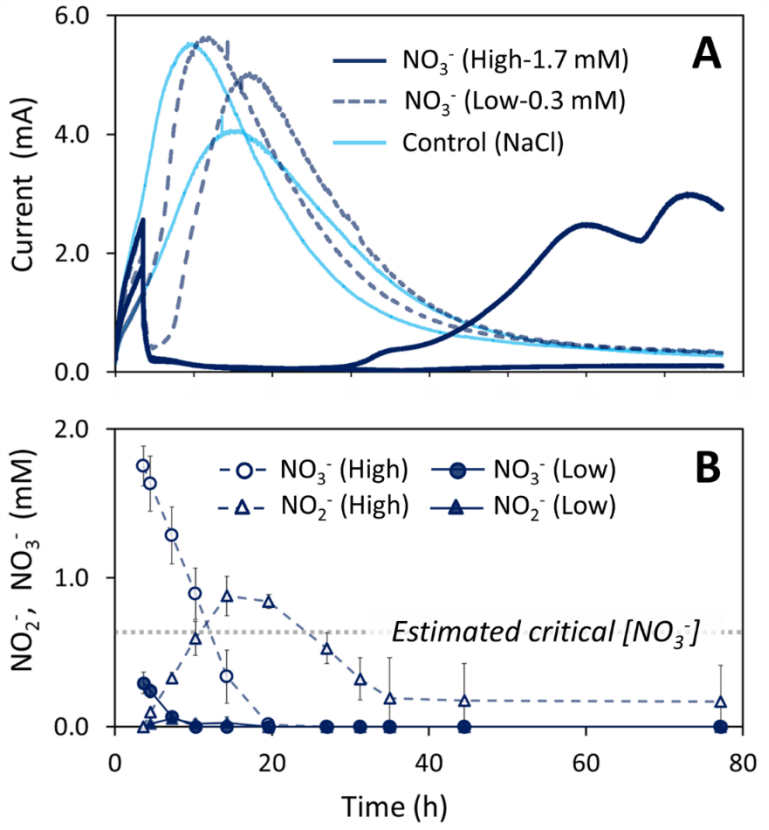

Figure A-8: Current, nitrate, and nitrite profiles of anode-reducing biofilms in response to exposure to various levels of nitrate. Biofilms acclimatized on anodes poised at 0 mV (protein concentration: 0.08 ± 0.02 mg-protein/cm^2, estimated critical nitrate concentration: 0.63 mM) were subjected to various levels of nitrate: High condition (target 1.7 mM, more than two times higher than the critical level), Low condition (0.3 mM), and No nitrate control (target 1.7 mM sodium chloride). Each condition was tested in duplicate.

Appendix A-9:

Additional discussion about decreased anode reduction rate in response to nitrate addition

Summary

Additional discussion about different nitrate induced effects on anode-reducing biofilms were made by using the bulk biofilm electron flux, a proposed measure to analyze nitrate effects. Although the quantitative validity of the discussion is rather limited due to lack of enough experimental support, analysis based on the bulk biofilm electron flux showed its potential to illustrate three different nitrate-induced effects: metabolic shift of anode-reducing cells to nitrate/nitrite reduction, nitrite/free nitrous acid (FNA) inhibition of cell metabolisms, and contribution from previously inactive cells to nitrate reduction.

Experiments in chapter 3 showed that anode-reducing biofilms of *Geobacter metallireducens*, an exoelectrogenic nitrate reducer, grown on potentiostatically poised graphite electrodes facultatively reduced nitrate. The observed bulk shift from current production, in other words anode reduction, to nitrate reduction was attributed to be a composite effects of metabolic shift of anode-reducing cells to nitrate/nitrite reduction, nitrite/free nitrous acid (FNA) inhibition of cell metabolisms, and contribution from previously inactive cells to nitrate reduction. This appendix would further discuss potential contribution of above factors by using the bulk biofilm electron flux, a hypothetical measure of biofilm's bulk metabolic activity defined as the sum of electron flux into two metabolisms, anode reduction and nitrate reduction. Here, I make following two

assumptions to develop the discussion: (1) anode reduction and nitrate reduction were the major catabolic reactions in tested anode biofilms and most of the electron flux were distributed into those two pathways, and (2) biofilm cells conduct both metabolisms with approximately similar electron flux under optimal environmental conditions. The first assumption is thought to be reasonable for tested anode biofilms as electron balance of anode biofilms were close to 100 % by adding up electron distribution into anode and nitrate reduction, and biomass synthesis (Figure 3-5). I acknowledge that the later assumption is not validated with experimental evidence and thus the quantitative validity of following discussion is rather limited, but I would value the discussion as it briefly explain the experimental data and could help future research of biofilms' metabolic competitions to design experiments focused on bulk electron flux of biofilms.

The effects of nitrate described above, metabolic shift of anode-reducing cells to nitrate/nitrite reduction, nitrite/FNA inhibition of cell metabolisms, and contribution from previously inactive cells to nitrate reduction, are thought to differentially alter the bulk electron flux of nitrate spiked biofilms relative to their sodium chloride spiked control biofilms. First, under the assumption of approximately similar electron flux on both metabolisms, the complete metabolic shift of anode-reducing cells to nitrate/nitrite reduction would not greatly change bulk electron flux of biofilm. For example, a cell actively reduced anode is responsible for the approximately similar electron flux to actively reduce nitrate after the metabolic shift without inhibition. Second, nitrite/FNA inhibition of cell metabolisms would decrease the total electron flux of the biofilm as such inhibition decreases both of electrode reduction and nitrate reduction as nitrite/FNA above toxic level inhibits not only metabolism using nitrate/nitrate as electron acceptors but also various

other bacterial cell metabolisms [5]. Such nitrite/FNA inhibition is expected to occur under the presence of nitrate in high concentration which cause rapid nitrite/FNA formation results in accumulation of nitrite/FNA in toxic level. Third, contribution from previously inactive cells to nitrate reduction would increase the bulk electron flux of a biofilm. This is expected to only happen to thick biofilms which contains metabolically inactive cells as stratified biochemical condition within a thick biofilm could result in a fraction of the biofilm unfavorable for anode reduction metabolism.

Effects of nitrate on thin anode-reducing biofilms (protein concentration ca. 0.08-0.09 mg/cm^2), which were estimated to be composed of up to few cell layers based on areal protein density of monolayer anode biofilms [6], were a composite of the metabolic shift and nitrite/FNA inhibition likely dependent on spiked nitrate concentration. These thin biofilms were presumed to be composed entirely of active anode-reducing cells as there is no significant stratification in biochemical conditions which could result in stratified metabolic activity across the biofilm cross section [7, 8]. The bulk biofilm electron flux, sum of electron flux of anode reduction and nitrate reduction, of anode-reducing biofilms after nitrate spike with critical level (Figure A-9-1), or lower than critical level (Figure A-9-2) were not significantly different from ones of sodium chloride spiked control biofilms during the period of initial sudden current decrease in response to nitrate spike (Figure 3-1 and Figure A-8). This is consistent with the expectation of metabolic shift effect of similar bulk electron flux to no nitrate control biofilms. The bulk electron flux of these nitrate spiked biofilms exceeded the one of control biofilm 10 hours or more after the nitrate spike due to increased nitrate reduction electron flux possibly by increased biofilm and suspended biomass.

Thin anode-reducing biofilms exposed to high level of nitrate, more than two times higher than critical level, showed lower bulk electron flux relative to control biofilms (Figure A-9-2). This is attributed mainly to decreased bulk metabolic activity by nitrite inhibition derived from rapid nitrite accumulation observed in the experiment. Metabolic inhibition was mainly caused by nitrite, but not FNA, as pH of the entire thin biofilms without pH stratification was maintained about neutral range at which nitrate is dominant species over FNA. One of duplicated high nitrate spiked biofilms did not recover the current production till the end of the batch with nitrite accumulation even under the presence of excess electron donor (Figure A-8) further suggested nitrite inhibition.

Effects of nitrate spike on bulk electron flux of thick anode-reducing biofilms were different from ones on thin anode-reducing biofilms. Anode-reducing biofilms exposed to critical level of nitrate with gradual nitrate spike tests showed significantly higher bulk electron flux relative to their control biofilms (Figure A-9-3). This is likely due to increased bulk metabolic activity relative to no-nitrate control biofilms by contribution from previously inactive cells to nitrate reduction. Such thick biofilms were presumably composed of significant fraction of inactive cells suggested by lower specific current density (current normalized by aerial protein concentration) of such thick biofilms over thin biofilms (Figure A-5). Other studies also reported spatially heterogeneous metabolic activity of anode-reducing biofilms [9-11] which was likely derived from stratified biochemical condition across the biofilm cross section [12]. Higher bulk electron flux of nitrate spiked biofilms than control biofilms observed in thick anode-reducing biofilms, but not in thin anode-reducing biofilms, were consistent with the expected effect of nitrate reduction by such inactive biofilm cell fraction.

The bulk electron flux profiles obtained from a set of thick anode-reducing biofilms (protein concentration of 0.49 mg-protein/cm^2-anode) further demonstrated expected effects of nitrate reduction by previously inactive cells. In tested thick anode-reducing biofilms, effect of nitrite/FNA inhibition which lower the electron flux was likely dissipated by the counter effect of the nitrate reduction by previously inactive cells which press up the electron flux. In fact, the bulk electron flux of biofilms exposed to high level of nitrate, more than twice as high as the critical level, was higher than no-nitrate control or ones exposed to lower levels of nitrate at least for 20 hours in response to nitrate spike event (Figure A-9-4). These high nitrate exposed biofilms showed almost zero bulk electron flux at later period of the batch likely due to severe metabolic inhibition by nitrite/FNA derived from significant nitrite accumulation during the period of high electron flux. The contrastive two profiles of bulk electron flux serially observed in the same set of biofilms illustrated different effects of nitrate on anode biofilms.

As discussed above, three different nitrate induced effects on anode-reducing biofilms were consistent with expected trends in the bulk biofilm electron flux even though the quantitative validity is rather limited due to lack of enough experimental results in this study to validate a key assumption for the discussion. However, the above discussion demonstrates the potential for analyzing different nitrate effects on anode-reducing biofilm systems by focusing on the bulk biofilm electron flux.

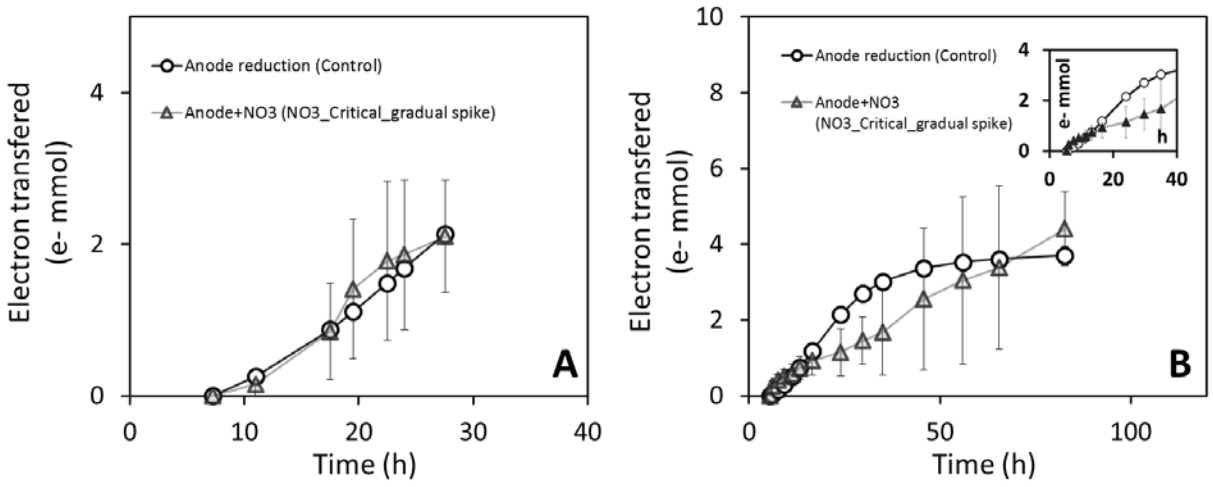

Figure. A-9-1: Time-series cumulative bulk electron flux, sum of electrons distributed into anode reduction and nitrate reduction of Thin anode biofilms that were acclimated with growth medium with 0.5 mM acetate as electron donor. Panel A was calculated from gradual nitrate spike test summarized in Figure 3-1. Panel B was calculated from different independent gradual nitarte spike test of other set of 0.5 mM acetate-medium acclimatized biofilms. The inset figure shows datapoints for initial 40 hours of the batch operation.

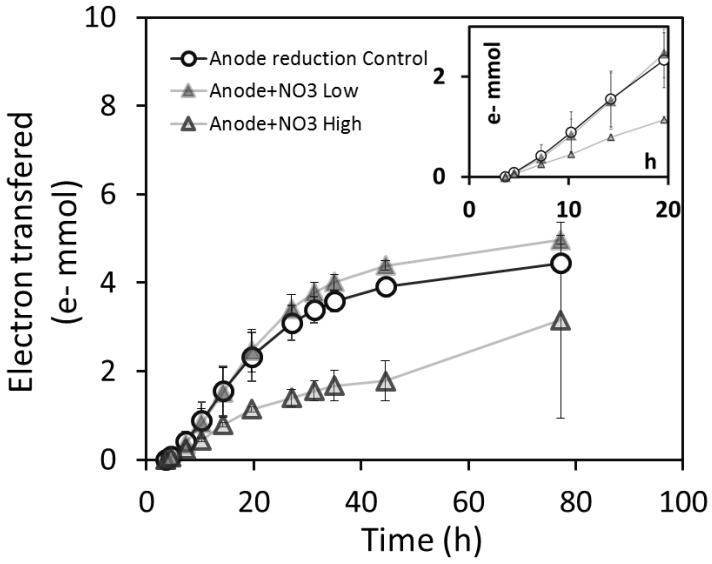

Figure A-9-2: Time-series cumulative bulk electron flux, sum of electrons distributed into anode reduction and nitrate reduction of Thin anode biofilms (acclimated with growth medium with 0.5 mM acetate as electron donor) subjected to nitrate spike lower and higher than critical level, which were calculated from the dataset of nitrite spike test summarized in Figure A-8. The inset figure shows datapoints for initial 20 hours of the batch operation.

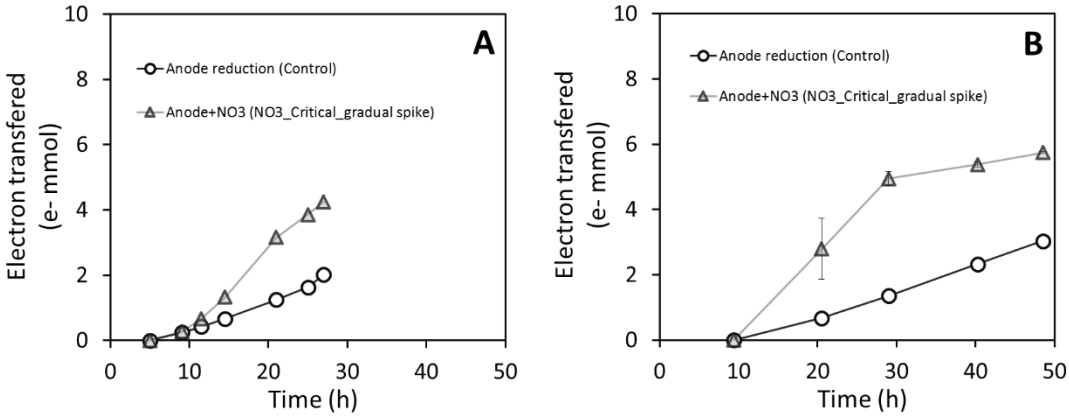

Figure A-9-3: Time-series cumulative bulk electron flux of anode biofilms that were acclimated with growth medium with 10 mM acetate as electron donor (Panel A) and ones acclimated with two batch cycles with growth medium contains 10 mM acetate (Panel B). These electron flux profiles were calculated from gradual nitrate spike tests summarized in Figure A-1.

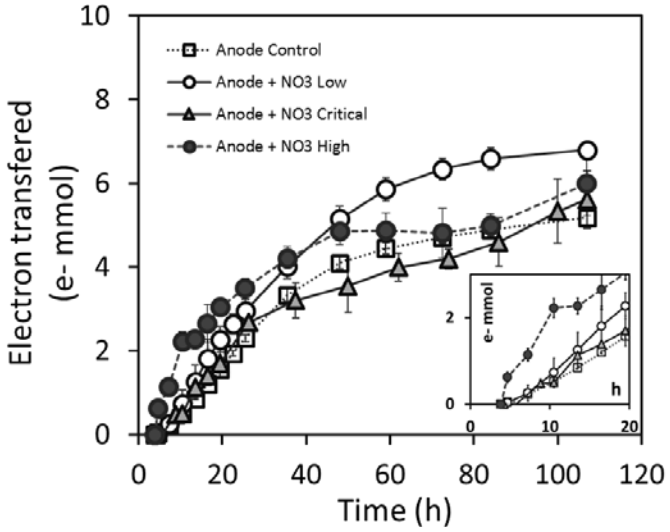

Figure A-9-4: Time-series cumulative bulk electron flux of anode biofilms exposed to different levels of nitrate, which were calculated from the dataset of nitrite spike test summarized in Figure 3-3. The inset figure shows datapoints for initial 20 hours of the batch operation.

Literature Cited

1. Tiedje, J.M., *Ecology of denitrification and dissimilatory nitrate reduction to ammonium.* Biology of anaerobic microorganisms, 1988. **717**: p. 179-244.
2. Kraft, B., M. Strous, and H.E. Tegetmeyer, *Microbial nitrate respiration - Genes, enzymes and environmental distribution.* Journal of Biotechnology, 2011. **155**(1): p. 104-117.
3. Picioreanu, C., et al., *A computational model for biofilm-based microbial fuel cells.* Water Research, 2007. **41**(13): p. 2921-40.
4. Rittmann, B.E. and P.L. McCarty, *Environmental Biotechnology: Principles and Applications.* McGRAW-HILL INTERNATIONAL EDITIONS Biological Sciences Series, 2001.
5. Vadivelu, V.M., J. Keller, and Z. Yuan, *Effect of free ammonia and free nitrous acid concentration on the anabolic and catabolic processes of an enriched Nitrosomonas culture.* Biotechnol Bioeng, 2006. **95**(5): p. 830-9.
6. Marsili, E., J. Sun, and D.R. Bond, *Voltammetry and Growth Physiology of Geobacter sulfurreducens Biofilms as a Function of Growth Stage and Imposed Electrode Potential.* Electroanalysis, 2010. **22**(7-8): p. 865-874.
7. Franks, A.E., et al., *Microtoming coupled to microarray analysis to evaluate the spatial metabolic status of Geobacter sulfurreducens biofilms.* ISME J, 2010. **4**(4): p. 509-19.
8. Franks, A.E., *Transcriptional analysis in microbial fuel cells: common pitfalls in global gene expression studies of microbial biofilms.* FEMS microbiology letters, 2010. **307**(2): p. 111-2.

9. Schrott, G.D., et al., *Physiological Stratification in Electricity‐Producing Biofilms of Geobacter sulfurreducens.* ChemSusChem, 2013. **7**(2): p. 598-603.

10. Renslow, R., et al., *Metabolic Spatial Variability in Electrode-Respiring Biofilms.* Energy. Environ. Sci., 2013. **6**(6): p. 1827-1836.

11. Sun, D., et al., *Temporal-spatial changes in viabilities and electrochemical properties of anode biofilms.* Environ Sci Technol, 2015. **49**(8): p. 5227-35.

12. Franks, A.E., et al., *Novel strategy for three-dimensional real-time imaging of microbial fuel cell communities: monitoring the inhibitory effects of proton accumulation within the anode biofilm.* Energy Environ. Sci., 2008. **2**(1): p. 113-119.

Appendix B

Supporting Information for Chapter 4

Appendix B-1:

Restriction fragment length polymorphism (RFLP) to examine purity of *Geobacter* cultures

Purity of *Geobacter* cultures used in this study was examined by analysis of PCR amplified 16S rRNA gene fragments. In brief, genomic DNA was isolated from cultures of interest, stock cultures and BES biofilms after tests, by commercial DNA isolation kits such as PowerSoil DNA isolation kit (MOBIO) and DNeasy Blood & Tissue Kit (QIAGEN). Mixing cells directly into PCR reaction without DNA isolation, like colony PCR, was also conducted by shaking a sterile pipette tip touched on centrifuged culture cell pellet in the PCR reaction mixture. A fragment of bacterial 16S rRNA gene was amplified PCR primer set of 341F (5'-CCT ACG GGA GGC AGC AG-3') and 1492R (5'-CGGTTACCTTGTTACGACTT-3') with PCR condition of initial denaturation step at 94 °C for 5 min, followed by 30 cycles of denaturation at 94 °C for 45 s, annealing at 55 °C for 30 s, and extension at 72 °C for 95 s, and final extension step at 72 °C for 10 min with HotStarTaq Master Mix Kit (QIAGEN) with manufacturer's instructions. PCR amplicon samples were subjected to Sanger sequencing at Penn State Genomics Core Facility with PCR primers as the sequencing primer, or Restriction fragment length polymorphism (RFLP) as follows. PCR amplicon without any purification step was digested by *Alu*I (R0137S, NEB), which cleaves 5'--- AG CT---3', with digestion reaction at 37 ^{o}C for 2

hours with manufacturer's instructions. Digested PCR amplicons was visualized with 2 % agarose gel electrophoresis with TBE buffer stained by SYBR safe DNA gel stain (ThermoFisher Scientific).

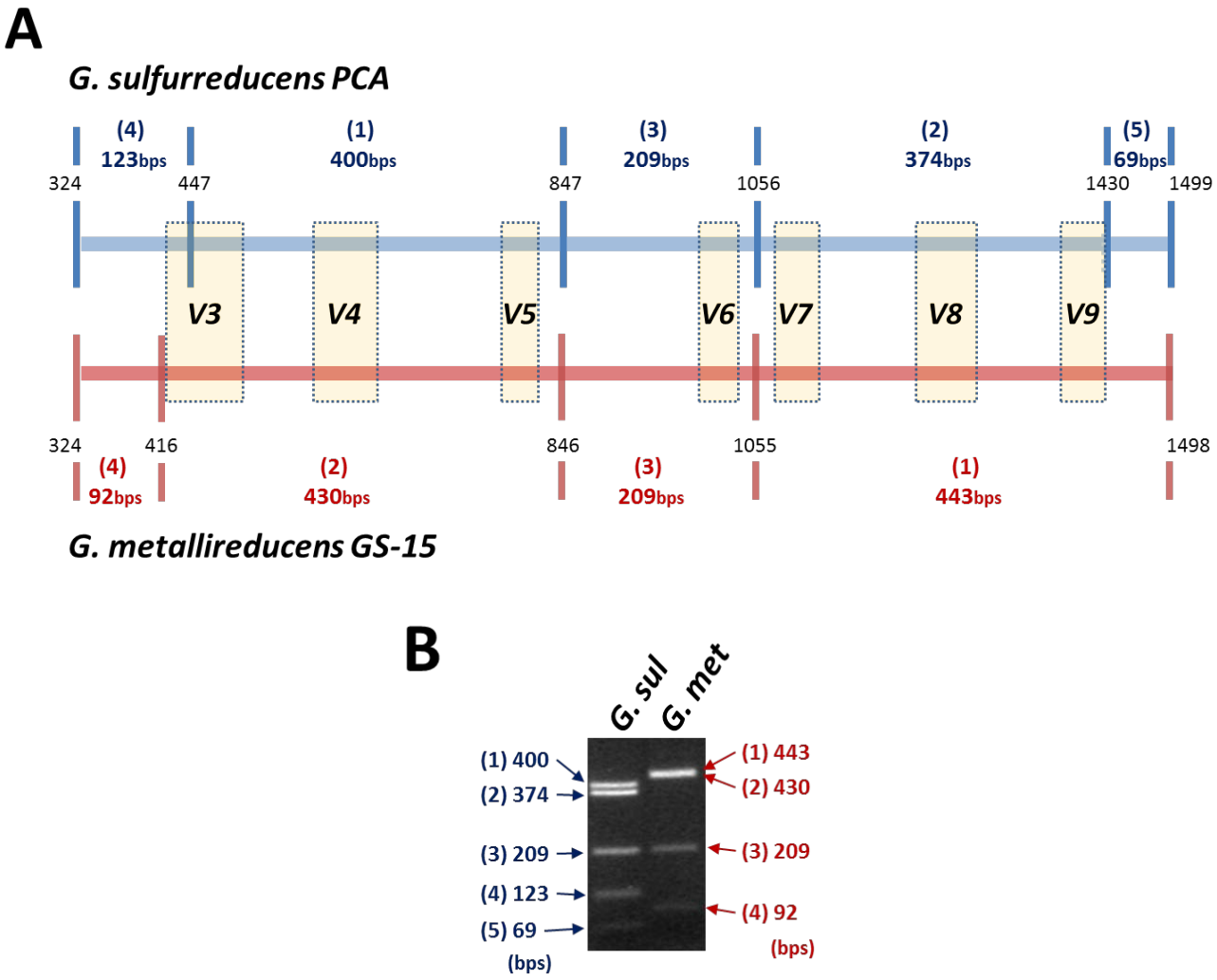

Figure B-1-1: *Alu*I restriction digestion fragment profiles of *Geobacter* 16S rRNA gene PCR amplicons. Panel A shows *Alu*I restriction digestion map of 16S rRNA gene sequences of *G.sulfurreducens* PCA [1] and *G. metallireducens* GS-15 [2] which are

PCR-amplified by Bacterial 16S rRNA gene primers (341F/1492R). V3-V9 represent variable regions within PCR amplicons [3]. Panel B shows actual RFLP profiles of *AluI* digested PCR amplicons derived from isolated DNA samples from laboratory cultures of *G.sulfurreducens* PCA and *G. metallireducens* GS-15.

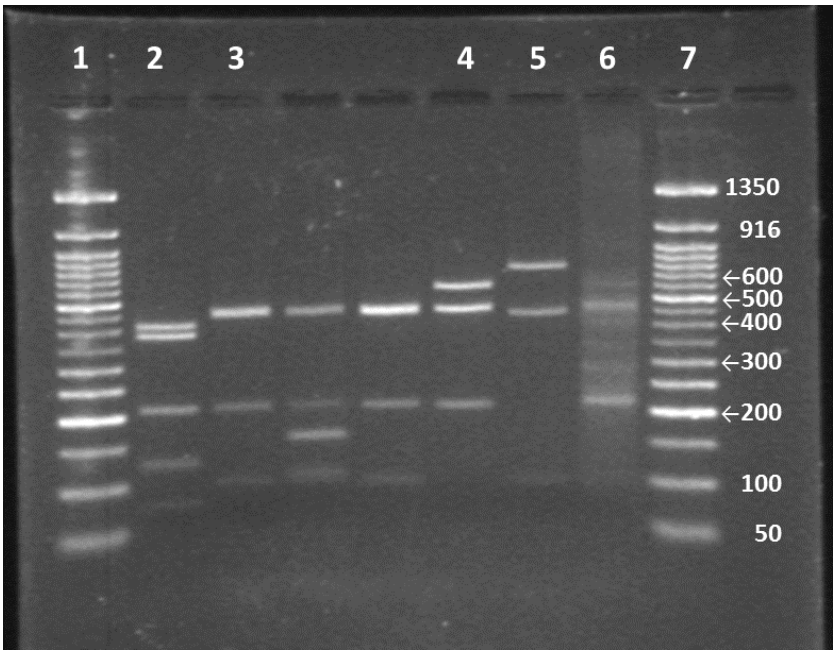

Figure B-1-2: Representative RFLPs of 16S rRNA gene PCR amplicons of laboratory cultures and mixed culture sample. Agarose gel picture (2.0 % agarose concentration, TBE buffer) of *AluI* digested PCR amplicons amplified with bacterial 16S rRNA gene primers (341F/1492R). Lanes 1 and 7 show Molecular size marker (50 bp DNA Ladder, NEB). Lanes 2-7 contained digested PCR amplicons derived from isolated DNA of following culture/samples, 2: *G.sulfurreducens* PCA, 3: *G. metallireducens* GS-15, 4: *Comamonas denitrificans* 110, 5: *Paracoccus denitrificans* PS-1, 6: total isolated DNA from activated sludge from anoxic zone of the University Area Joint Authority plant.

Appendix B-2: Effects of TCA cycle inhibitor on nitrate dependent cathodic current production

In order to examine the potential contribution of TCA cycle, reported as a major catabolic pathway [4], on cathodic current, malonate, a competitive inhibitor of succinate dehydrogenase in TCA cycle which decreased current production of anodic *Shewanella* biofilms [5], was spiked in a cathodic BES chamber. Anodic *G. metallireducens* biofilms were acclimatized with 0.5 mM acetate and graphite electrode poised at 0 mV vs SHE. After andic current production decreased ~ 50 μA, electrode potential was shifted to -250 mV vs SHE and 2 mM of sodium nitrate was spiked to induce nitrate-dependent cathodic electrode oxidation. During increase of cathodic current, malonate (targeted 20 mM) was spiked to working electrode chamber.

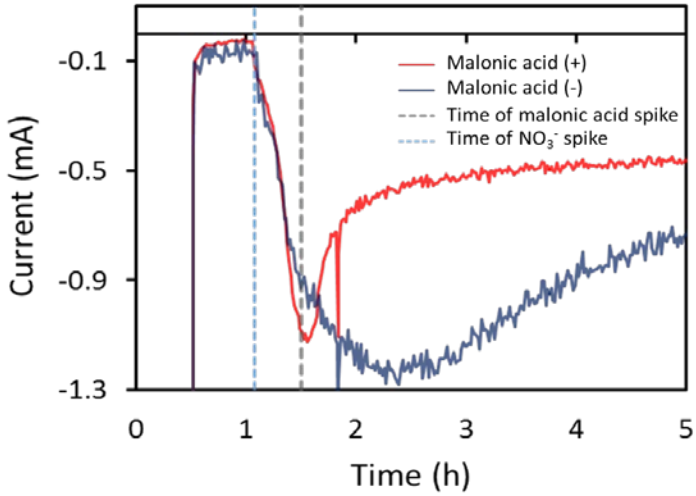

Figure B-2: Cathodic current decrease in response to malonate (20 mM) spike. Cathodic current monitored in *G. metallireducens* biofilm on graphite electrode poised at-250 mV vs SHE decreased after malonate spike (targeted 20 mM) relative to sodium chloride-spiked biofilm run in parallel.

Appendix B-3:

Electron balance during cathodic operation with -150 mV vs SHE with nitrate/acetate

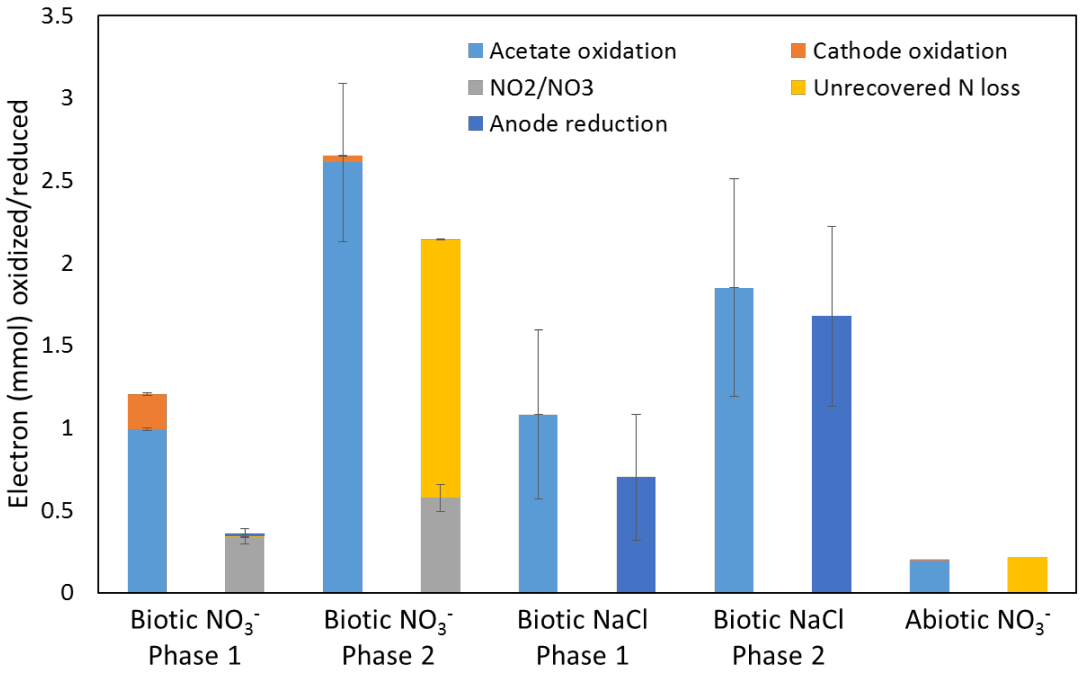

Figure B-3: Electron balance of working electrode chambers with anodically acclimatized biofilms switched into cathodic conditions with -150 mV vs SHE with nitrate/acetate. Electron balance for Biotic NO_3^- and Biotic NaCl (refer to Figure 4-3) during cathodic operations was separated into two time phases. Phase 1 represents time at which significant cathodic current was monitored in Biotic NO_3^- reactors, time at nitrate spike to 17.5 h. Phase 2 represents duration after the cathodic current diminished, 17.5 h to 59 h.

Appendix B-4: *narG* expression analysis with qPCR

Relative expression of two *narG* genes on *G. metallireducens* genome [2] of different cultures was measured by RT-qPCR via differential CT relative quantification with *proC* as endogenous control [6], with following PCR primer sets.

***narG*-1:**
Forward (5'-TGGCAGTACGACAAGGTGGTG-3'), Reverse (5'- CGTCGAACTGGGGATAGTCGT-3')
***narG*-2:**
Forward (5'-ATGGATCAAGGAGTTGACGGA-3'), Reverse (5'-CACGTAGACCAGCCACGAA-3')
***proC*:**
Forward (5'- CCTCGATGCCGTTGATGGAT-3'), Reverse (5'- CCGTGAAGCCCCAGGTATTT-3')

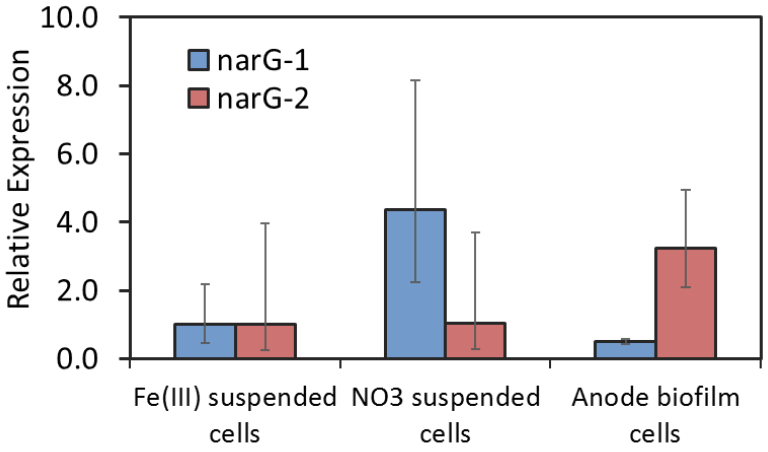

Figure B-4: Relative expression of two *narG* genes of ferric-reducing cultures, nitrate-reducing cultures and anode-reducing cultures. Relative expression was normalized by ones of ferric-reducing cultures. Results shows duplicated biological tests each has three technical replicates.

Literature Cited

1. Methe, B., et al., *Genome of Geobacter sulfurreducens: metal reduction in subsurface environments.* Science, 2003. **302**(5652): p. 1967-1969.

2. Aklujkar, M., et al., *The genome sequence of Geobacter metallireducens: features of metabolism, physiology and regulation common and dissimilar to Geobacter sulfurreducens.* BMC microbiology, 2009. **9**: p. 109.

3. Neefs, J.-M., et al., *Compilation of small ribosomal subunit RNA structures.* Nucleic Acids Research, 1993. **21**(13): p. 3025-3049.

4. Sun, J., et al., *Genome-scale constraint-based modeling of Geobacter metallireducens.* BMC Syst Biol, 2009. **3**: p. 15.

5. Matsuda, S., et al., *Electrochemical Gating of Tricarboxylic Acid Cycle in Electricity-Producing Bacterial Cells of Shewanella.* Plos One, 2013. **8**(8): p. e72901.

6. Holmes, D.E., et al., Potential for quantifying expression of the Geobacteraceae citrate synthase gene to assess the activity of Geobacteraceae in the subsurface and on current-harvesting electrodes. Applied and Environmental Microbiology, 2005. 71(11): p. 6870-7.

Appendix C

Supporting Information for Chapter 5

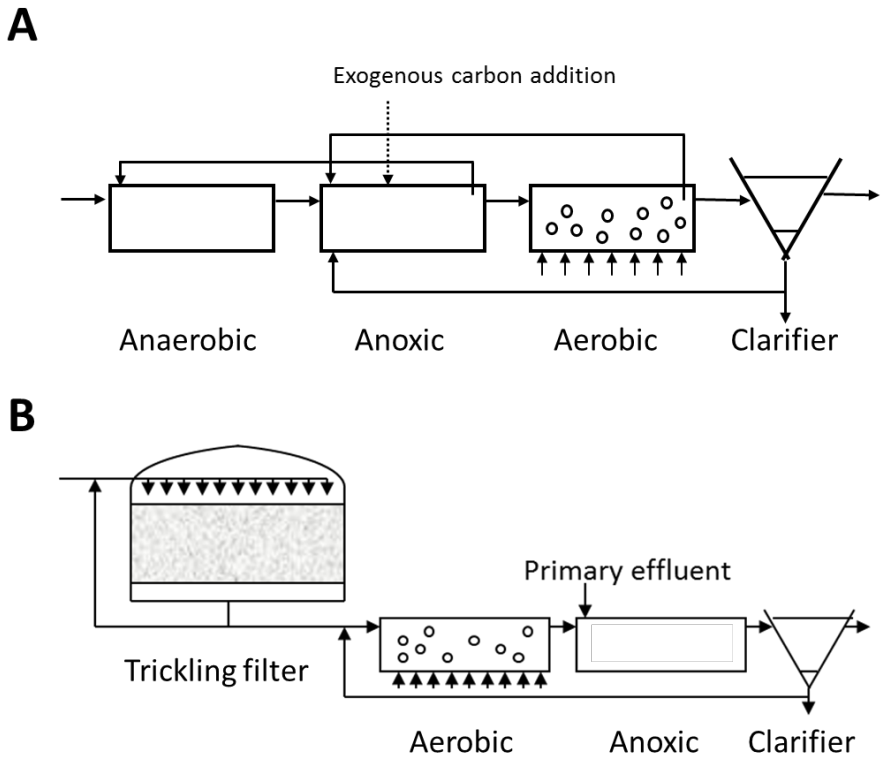

Figure C-1: Schematics of biological nitrogen removal processes where activated sludge was sampled. **A**: University of Cape Town (UCT) activated sludge process [1] at the University Area Joint Authority (UAJA) Plant (State College, PA, USA). The process includes three zones with distinct biochemical conditions followed by clarifier with internal recycle flows. **B**: The Pennsylvania State University (PSU) Wastewater Treatment Plant. The process is composed of trickling filter followed by activated sludge nitrification and denitrification processes.

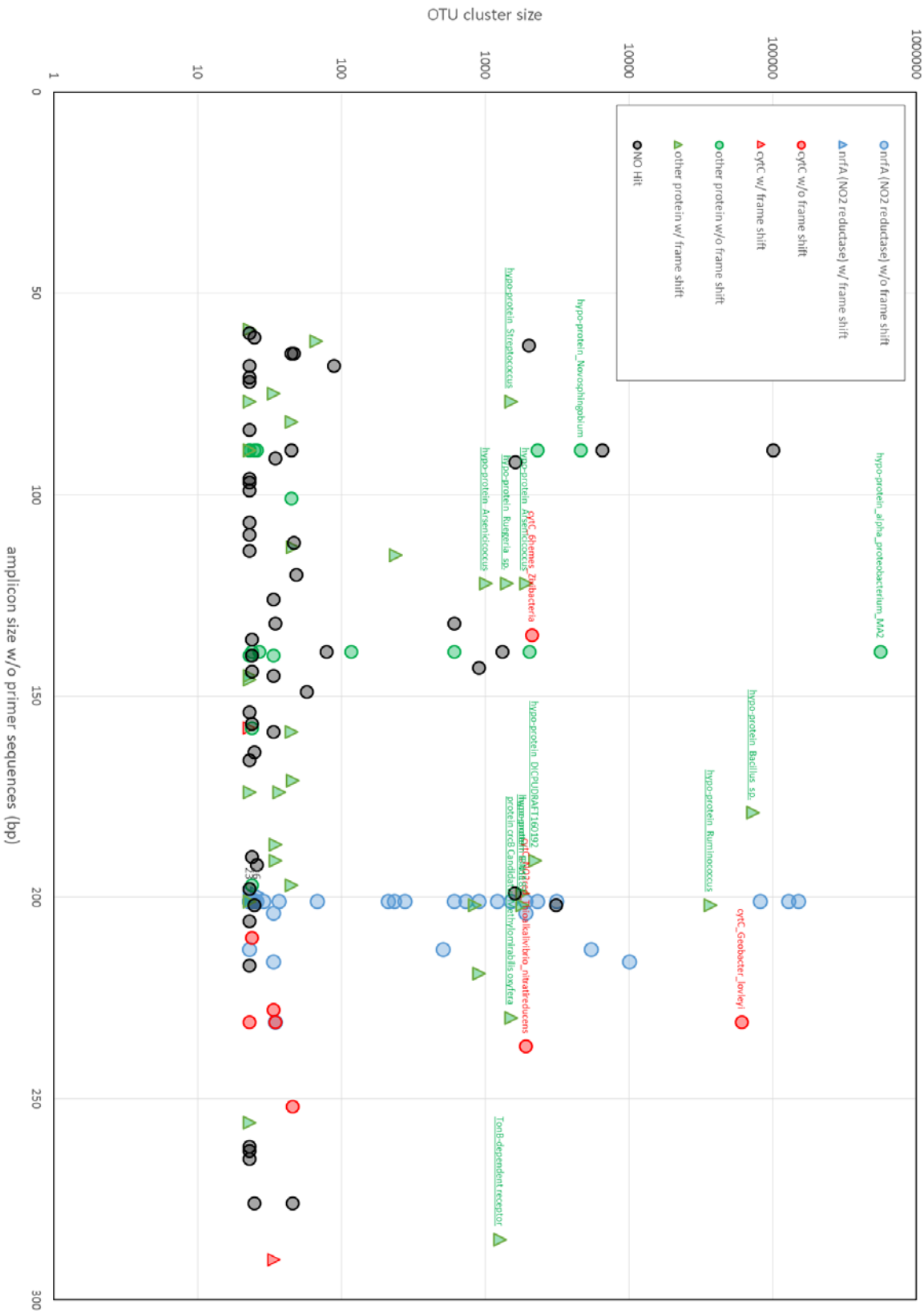
OTU cluster size
1000000
100000
10000
1000
100
10
1
0
50
100
150
200
250
300
amplicon size w/o primer sequences (bp)
nrfA (NO2 reductase) w/o frame shift
nrfA (NO2 reductase) w/ frame shift
cytC w/o frame shift
cytC w/ frame shift
other protein w/o frame shift
other protein w/ frame shift
NO Hit
hypo-protein_alpha_proteobacterium_MA2
hypo-protein_Novosphingobium
hypo-protein_Streptococcus
hypo-protein_Arsenicicoccus
hypo-protein_Ruegeria sp.
cytC_Geobacter_bonleyi
hypo-protein_Bacillus sp.
hypo-protein_Ruminococcus
TonB-dependent receptor

Figure C-2: Analysis of OTUs that were not identified as a *nrfA* OTU. The 152 OTUs (out of 710 OTUs generated from DNA sequences) that did not meet 70 % amino acid matching criterion in initial taxonomic identification against NrfA amino acid database (just over 4000 NrfA amino acid sequences including environmental clones from the GenBank protein database) via USEARCH global alignment algorithm [2]. Blue, red, and green symbols represent OTUs with centroid OTU sequences hit with NrfA (or cytochrome c-552), other cytochrome C proteins, and other proteins in blastx search. Circle and triangle symbols represent OTUs had highest hit with the first reading frame, the reading frame based on primer binding sites, and with different, second or third, reading frames. Black-circle symbol represent OTUs did not have any hit in non-redundant protein sequences database in blastx search with its default cutoff criteria. Attributions of some of highest blastx hit were shown next to the OTU.

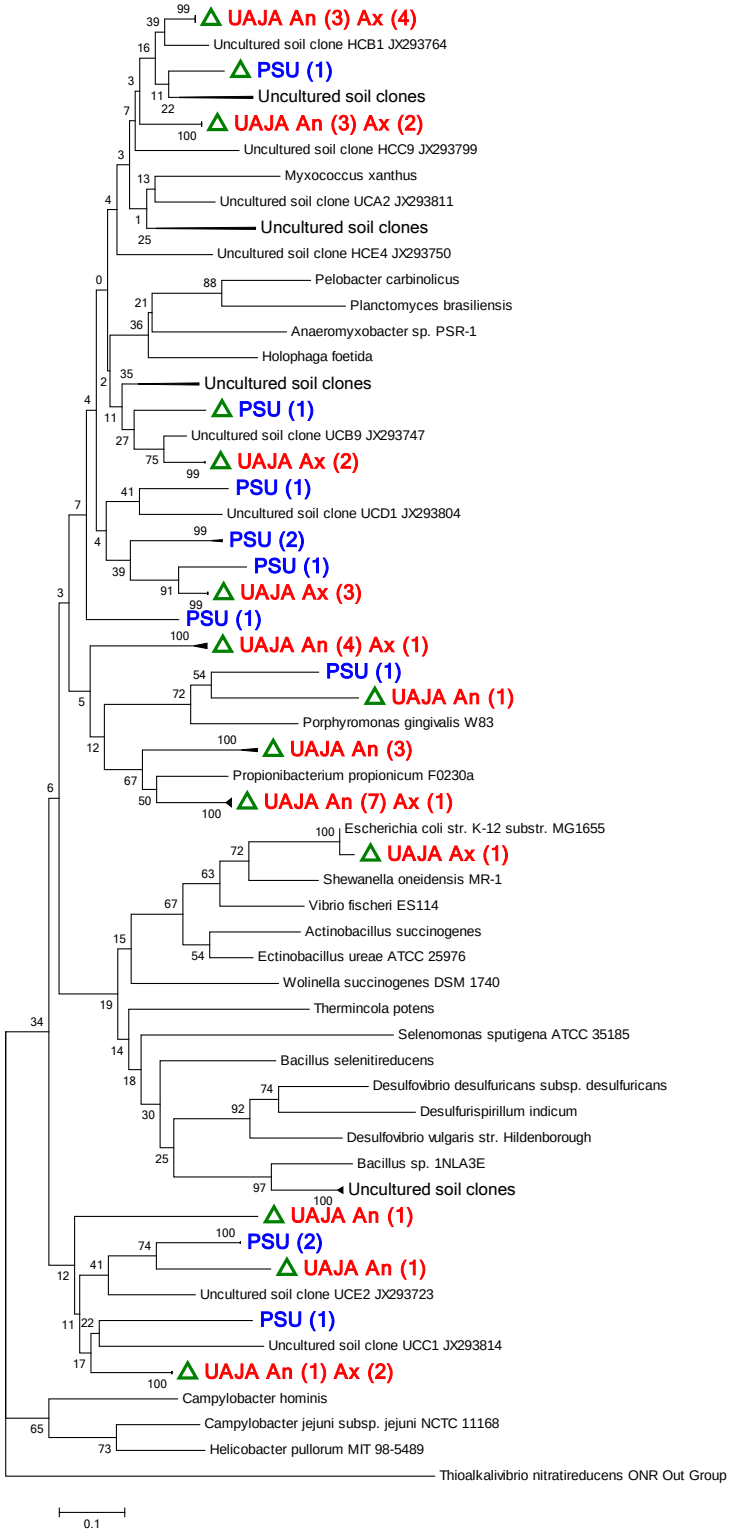
UAJA An (3) Ax (4)
Uncultured soil clone HCB1 JX293764
PSU (1)
Uncultured soil clones
UAJA An (3) Ax (2)
Uncultured soil clone HCC9 JX293799
Myxococcus xanthus
Uncultured soil clone UCA2 JX293811
Uncultured soil clones
Uncultured soil clone HCE4 JX293750
Pelobacter carbinolicus
Planctomyces brasiliensis
Anaeromyxobacter sp. PSR-1
Holophaga foetida
Uncultured soil clones
PSU (1)
Uncultured soil clone UCB9 JX293747
UAJA Ax (2)
PSU (1)
Uncultured soil clone UCD1 JX293804
PSU (2)
PSU (1)
UAJA Ax (3)
PSU (1)
UAJA An (4) Ax (1)
PSU (1)
UAJA An (1)
Porphyromonas gingivalis W83
UAJA An (3)
Propionibacterium propionicum F0230a
UAJA An (7) Ax (1)
Escherichia coli str. K-12 substr. MG1655
UAJA Ax (1)
Shewanella oneidensis MR-1
Vibrio fischeri ES114
Actinobacillus succinogenes
Ectinobacillus ureae ATCC 25976
Wolinella succinogenes DSM 1740
Thermincola potens
Selenomonas sputigena ATCC 35185
Bacillus selenitireducens
Desulfovibrio desulfuricans subsp. desulfuricans
Desulfurispirillum indicum
Desulfovibrio vulgaris str. Hildenborough
Bacillus sp. 1NLA3E
Uncultured soil clones
UAJA An (1)
PSU (2)
UAJA An (1)
Uncultured soil clone UCE2 JX293723
PSU (1)
Uncultured soil clone UCC1 JX293814
UAJA An (1) Ax (2)
Campylobacter hominis
Campylobacter jejuni subsp. jejuni NCTC 11168
Helicobacter pullorum MIT 98-5489
Thioalkalivibrio nitratireducens ONR Out Group
0.1

Figure C-3: Neighbor-joining phylogenetic tree of *nrfA* amino acid sequences encoded by *nrfA* fragment between the nrfAF2AW/nrfAR1 PCR primer set target sites [3]. The tree includes *nrfA* clone sequences from PCR amplicons from cDNA preparations derived from anoxic tank of the PSU plant (shown with blue), anoxic and anaerobic zones of UAJA plant (shown with red) obtained in this study, as well as *nrfA* amino acid sequences of uncultured soil clones obtained by Welsh et al. [3], and of pure cultures. Octaheme nitrite reductase (ONR) of *Thioalkalivibrio nitratireducens* was used as outgroup. Numbers on node designates bootstrap values. Two different sampling locations in the UAJA plant, anoxic zone and anaerobic zone, were designated as Ax and An. Numbers in parentheses represent the number of clones in the clade. The green triangle designate clades that the same *nrfA* amino acid sequence was retrieved in Illumina Miseq analysis.

Literature Cited

1. Grady Jr, C.L., et al., *Biological wastewater treatment*. 2011: CRC Press.
2. Edgar, R.C., *Search and clustering orders of magnitude faster than BLAST*. Bioinformatics, 2010. **26**(19): p. 2460-2461.
3. Welsh, A., et al., *Refined NrfA phylogeny improves PCR-based nrfA gene detection.* Applied and Environmental Microbiology, 2014. **80**(7): p. 2110-9.

VITA

Hiroyuki Kashima

EDUCATION

Ph.D. in Environmental Engineering,

The Pennsylvania State University, University Park, 2016.

M.S. in Environmental and Agricultural Engineering,

Tokyo University of Agriculture and Technology, 2009.

B.S. in Environmental and Agricultural Engineering,

Tokyo University of Agriculture and Technology, 2007.

PUBLICATIONS

Rezaei, F., Joh, L. D., **Kashima, H.,** Reddy, A. P., & VanderGheynst, J. S. (2011). Selection of Conditions for Cellulase and Xylanase Extraction from Switchgrass Colonized by *Acidothermus cellulolyticus*. *Applied Biochemistry and Biotechnology*, 164(6), 793-803.

Zhang, L., Zhu, X., **Kashima, H.,** Li, J., Ye, D. D., Liao, Q., & Regan, J. M. (2015). Anolyte Recirculation Effects in Buffered and Unbuffered Single-Chamber Air-Cathode Microbial Fuel Cells. *Bioresource Technology*, 179, 26-34.

Kashima, H., & Regan, J. M. (2015). Facultative Nitrate Reduction by Electrode-Respiring *Geobacter metallireducens* Biofilms as a Competitive Reaction to Electrode Reduction in a Bioelectrochemical System. *Environmental Science & Technology*, 49(5), 3195-3202.

Liu, J., Hou, H., Chen, X., Bazan, G., **Kashima, H.,** & Logan, B. E. (2015). Conjugated Oligoelectrolyte Represses Hydrogen Oxidation by *Geobacter sulfurreducens* in Microbial Electrolysis Cells. *Bioelectrochemistry*. 106, 379-382.

Ou, S., **Kashima, H.,** Aaron, D. S., Regan, J. M., & Mench, M. M. Multi-Variable Mathematical Models for the Air-Cathode Microbial Fuel Cell System. *Journal of Power Sources*. Accepted.

Kashima, H., Bruns, M. A., Regan, J. M. Detection of *nrfA* genes and transcripts, molecular markers of dissimilatory nitrate reduction to ammonium, in wastewater activated sludge. (in review)